JRC Scientific and Technical Reports

01 APRIL 2007 SOLOMON ISLAND TSUNAMI: CASE STUDY TO VALIDATE JRC TSUNAMI CODES

Natalia Zamora[1]
Giovanni Franchello[2]
Alessandro Annunziato[2]

1 - University of Costa Rica
2 - Joint Research Centre, European Commission

EUR 24783 EN - 2011

JRC EUROPEAN COMMISSION

ipsc Institute for the Protection and Security of the Citizen

The mission of the JRC-IPSC is to provide research results and to support EU policy-makers in their effort towards global security and towards protection of European citizens from accidents, deliberate attacks, fraud and illegal actions against EU policies.

European Commission
Joint Research Centre
Institute for the Protection and Security of the Citizen

Contact information: Giovanni Franchello
Address: JRC Ispra Site, Via Enrico Fermi 2749, I-1027 Ispra (VA), Italy
E-mail: giovanni.franchello@jrc.ec.europa.eu
Tel.: +39 0332 785066
Fax: +39 0332 785154

http://ipsc.jrc.ec.europa.eu/
http://www.jrc.ec.europa.eu/

JRC 62983

EUR 24783 EN
ISBN 978-92-79-19851-9 (print)
ISBN 978-92-79-19852-6 (pdf)
ISSN 1018-5593 (print)
ISSN 1831-9424 (online)

doi:10.2788/859

Luxembourg: Publications Office of the European Union

Printed in Italy

Executive Summary

On April 1st 2007 a large earthquake of magnitude 8.1 occurred offshore Solomon Islands at 20:40:38 UTC. Numerical simulations of the tsunami event caused by the earthquake have been performed to compare the results obtained by the SWAN-JRC code (Annunziato, 2007), the TUNAMI (Imamura, 1996) and the HYFLUX2 (Franchello, 2008). The analysis conducted using these numerical simulations were also compared with NOAA-MOST code unit source results.

The tsunami event has been simulated considering several options for the seismological parameters as input data: Finite Fault Model (USGS, 2007), the Centroid Moment Tensor fault model and other mechanisms derived from the field survey analysis (Tanioka model).

The main aim of this study is to assess how the different fault models affect the overall results and to perform a comparison among the various codes in the wave propagation phase. Another objective of this study is to use HYFLUX2 code to calculate inundation and compare the simulation results with site field measurements.

The study has been separated into two main parts. The first one represents the collection of information about focal mechanisms: the fault analysis in chapter 4 covers one of the main aims of this research where different fault scenarios have been tested using published field data. The second part describes the different calculations that have been performed in order to analyze the response of the wave propagation models to various fault deformation models. For the inundation assessment, more detailed calculations at 300m grid size resolutions have been performed, using the fault model that best represent the deformation.

The calculations in the propagation assessment subsection were performed using: SWAN-JRC, HYFLUX2, TUNAMI-N2 and NOAA-MOST code. In the inundation assessment the HYFLUX2 numerical code, initialized with the Tanioka fault model was used.

The deformation comparison with field measured data shows that none of the “quick” fault mechanism was able to estimate correctly the measured value. The best model is the empirical model by Tanioka which was obtained by trying to reproduce the measured value.

From the published fault mechanism the one that shows a better correlation with measurements is the simple cosinuosoidal model. Results of simulations done with 300 m grid, show a maximum wave height of 7.5 m. Though the maximum run up reported was 10 m in Tapurai site, Simbi Island, the simulation results are encouraging.

INDEX

1. INTRODUCTION

On April 1st 2007 an earthquake of magnitude 8.1 occurred offshore the Solomon Islands at 20:40:38 UTC causing a tsunami which affected the surrounding islands. The tsunami caused approximately 100 fatalities on the islands close to the epicentre. The European Commission Global Disaster Alert and Coordination System (GDACS), an early warning system created to alert the humanitarian community of potential disasters, issued a red alert as a result of the so called UNESCO Matrix (according to this logic an earthquake of Richter scale greater than 7.5 struck a location in the open sea[1]. Simulations were automatically launched by the GDACS system and the calculated maximum wave height was 2.2 m in Vanikuva, Solomon Islands: this simulation was available 30-40 min after the event. The online calculation code is SWAN-JRC.

The JRC Tsunami Assessment Tool has been developed to retrieve and perform new calculations when requested by the GDACS system. When a new event is detected by GDACS using data from the seismological sources (USGS, EMSC), an evaluation of the event is performed to estimate his importance from humanitarian point of view.

As the crustal deformation is one of the main inputs for a reliable tsunami numerical simulation, this research intends to evaluate different fault models together with numerical code behaviours.

In this report more detailed analyses have been conducted using SWAN-JRC code (Annunziato, 2007), the TUNAMI-N2 (Imamura, 1996) and the HYFLUX2 (Franchello, 2008). The analysis conducted using these numerical codes were also compared with MOST code unit source results used by US National Oceanic and Atmospheric Administration (NOAA) The Solomon Island event is a good example to understand and to evaluate the approach of these numerical codes in earthquakes occurring very close to the coast and in which tsunami alert is a challenge due to the small time available. Near field tsunami events are also good to assess the accuracy of ground deformation which constitutes the input of the hydrodynamic models.

First the various deformation models are analysed and compared with field data. Once the best model is identified, it is used to estimate the wave propagation with the codes used for early warning; the inundation is calculated using HYFLUX2 code.

Different bathymetry and topography resolutions have been used in the analysis. In order to reduce the calculation time, the early warning system requires a rather coarse resolution; for this case a 2.6 min cell size was used. Resolutions of 1.6 min and 0.5 min are also used to compare the results.

[1] In 2007 the pre-calculated tsunami scenario matrix was not yet available; in that case an estimate of 2.8 m would have been calculated and thus, the event would have been classified as orange alert. This scenario matrix means that the GDACS system does not perform actual tsunami wave propagation calculations after an earthquake, but instead uses a database of pre-calculated scenarios. These scenarios have the maximum wave height and arrival time for all nearby coastal populated places, which is used to establish an alert level. When no scenario is available, the system falls back on the UNESCO method, which is based on earthquake magnitude only.

2. ADOPTED NUMERICAL CODES

2.1 Tsunami wave propagation models

The numerical codes SWAN-JRC, TUNAMI-N2 and HYFLUX2 solve the shallow water equations using different numerical methods: SWAN and TUNAMI use the finite different method (FD) while HYFLUX2 uses the finite volume method (FV).

The shallow water equation is commonly used to describe tsunami wave propagation and general features of the inundation processes. The shallow water equations can be derived in a number of ways and different numerical approaches, all of which relies on the assumption that the flow is vertically hydrostatic, the fluid is incompressible, the pressure at the free surface is constant and the vertical velocity and the acceleration are negligible.

The finite difference method is largely used to model Tsunami wave propagation and run-up. Models based on finite difference schemes are usually less time consuming than those based on finite volumes. However, most of the FD schemes fail when dealing with flow discontinuities such as wetting and drying interfaces and bore formation.

The finite volume method has been developed in the past to simulate dam-break and recently is used also in Tsunami modelling. The finite volume method is conservative in terms of mass and momentum and, if the dry/wet front is well modelled, the method is particularly suitable for run-up and inundation modelling.

Commonly, most of the numerical tsunami models use nested computational grids from coarse to high-resolution, to get more detail into the area of interest. Nested grids are used to have a minimum number of nodes in a wavelength in order to resolve the wave with minimum error.

SWAN-JRC code

SWAN-JRC is the numerical code implemented for *Global Disaster Alerts and Coordination System (*GDACS). GDACS has been jointly developed by the European Commission and the United Nations and combines existing web-based disaster information management systems, with the aim to alert the international community in case of major sudden-onset disasters and to facilitate the coordination of international response during the relief phase of the disaster. When a new event is detected by the seismological sources (USGS, EMSC), an evaluation of the event is performed to estimate the importance of the event from humanitarian point of view. In case of an earthquake event occurring under water and of magnitude greater than 6.5, the JRC Tsunami Assessment Tool is invoked and a new calculation is requested.

The SWAN-JRC model (Annunziato, 2007) solves the shallow water equations by the finite difference numerical scheme based on Mader code SWAN (1988).

SWAN-JRC code estimates also the fault length, height and direction to determine the initial water displacement. The code initializes the calculation space, performs the travel time propagation calculation, verified at each step if there are locations reached by the wave and thus updates the visualization and animation files. For early warning purposes the model can run in automatic mode in order to publish automatically the results in the GDACS web site. For post event calculations the Okada model and Finite Fault Model as well as other earthquake parameters can be used to compare or enhance simulation results.

TUNAMI-N2 code

TUNAMI-N2 code was developed by the Disaster Control Research Center through the Tsunami Inundation Exchange Modeling (TIME) Program (Goto et al. 1997) and improved by Dao and Tkalich (2007).

The TUNAMI-N2 code is based on the shallow water equation. The TUNAMI code consists of several codes:

(a) TUNAMI-N1, linear theory with constant grids.

(b) TUNAMI-N2, linear theory in deep sea, shallow-water theory in shallow sea and run up on land with constant grids.

(c) TUNAMI-N3, linear theory with varying grids.

(d) TUNAMI-F1, linear theory for propagation in the ocean in the spherical co-ordinates.

(e) TUNAMI-F2. linear theory for propagation in the ocean and coastal waters. \

In this analysis TUNAMI-N2 has been used. TUNAMI code is included in the SWAN-JRC suite and therefore the results can be easily produced with the same environment as the SWAN code.

HYFLUX2 code

The *HyFlux2* model has been developed to simulate severe inundation scenario due to dam break, flash flood and tsunami-wave run-up. The model solves the conservative form of the two-dimensional shallow water equations using a finite volume method. The interface flux is computed by a Flux Vector Splitting method for shallow water equations based on a Godunov-type approach. A second-order scheme is applied to the water surface level and velocity. Physical models are included to deal with bottom steps and shorelines. The second-order scheme together with the shoreline-tracking method makes the model well balanced in respect to mass and momentum conservation laws, providing reliable and robust results. In HYFLUX2, the numerical stability is ensured under the Courant-Friedrich-Levy criteria (Franchello, 2009).

In addition, HYFLUX2 is included in the suite of codes that can be invoked by the SWAN-JRC suite, thus enabling an easy comparison of the code results.

NOAA-MOST code

The MOST (Method of Splitting Tsunami) is a suite of numerical simulation codes capable of simulating three processes of tsunami evolution: earthquake, transoceanic propagation and inundation.

MOST Tsunami modelling proceeds in three distinct stages:

- A Deformation Phase generates the initial conditions for a tsunami by simulating ocean floor changes due to a seismic event.
- A Propagation Phase propagates the generated tsunami across deep ocean using Nonlinear Shallow Water (NSW) wave equations.
- An Inundation Phase simulates the shallow ocean behaviour of a tsunami by extending the NSW calculations using a multi-grid “run-up” algorithm to predict coastal flooding and inundation.

The tsunami generation process is based on a fault plane model of the earthquake source (Gusiakov, 1978; Okada, 1985) which assumes an incompressible liquid layer on an underlying elastic

half space to characterize the ocean and the Earth's crust. The implementation of this elastic fault plane model (Titov, 1997) utilizes a formula for static sea-floor deformation to calculate the initial conditions required for subsequent computations of tsunami propagation and inundation.

The *near–real time calculations* performed by NOAA considered the best fitting scenario used at the moment of an event. NOAA's Pacific Marine Environmental Laboratory (PMEL) forecast system combines real-time seismic and tsunami data with a forecast database of pre-computed scenarios. The database model scenarios for unit sources consist on fault blocks of 100 km along strike and 50 km down dip. The model requirement in this case is similar to hindcast studies: the solution must provide the best fit to the observations (Titov et al., 2005) and use seismic or dart scaling factors to fit the data. The use of these scaling laws may be inadequate for complex events resulting in forecast errors (Weinstein and Lundgren, 2008).

NOAA-MOST initial conditions are adjusted by direct comparison with the Deep-ocean Assessment and Reporting of Tsunamis (DART) buoys stations available records, in order to estimate correctly the source parameters that better represent the results (tsunami forecast) [2]. For this event under analysis, the factor calculated by the inversion of DART recorded data is: 12*nvszb10 (Mw 8.2) and the seismic factor is: 3.96* nvszb12 + 3.96* nvszb11.

2.2 Tsunami inundation model

The coastal flooding and inundation is commonly simulated by extending propagation calculations with a nested grid approach. The code requires as input detailed information on seismic source mechanisms, gridded bathymetric data for the open sea propagation, and a set of gridded Digital Elevation Models (DEM) containing detailed bathymetry and topography in order to model the inundation phase.

The most common procedure to track movements of the shoreline (Imamura, 1996; Liu et al., 1998 Imamura et al., 2006) is the moving boundary treatment. Run up is calculated with nonlinear computations.

HYFLUX2 uses a shoreline tracking method to model the interface between dry and wet. (Franchello, 2009, (Fig. 1). HYFLUX2 inundation 2D scheme has been designed to identify the shoreline as intersection between two planar surfaces which describe the bottom and the water free surface (Figure). With this method a cell can be partially wetted, i.e. the fraction of cell that is wetted is a result of the proposed shoreline tracking methodology.

In HYFLUX2 it has been realized a preservation of mass conservation at almost zero velocity, without the reconstruction of the bottom topography as was proposed by other authors (Audusse et al., 2004; Fabien Marche, 2004; Brufau and Garcia-Navarro, 2000). The HYFLUX2 method does not include a shoreline coordinate transformation or a moving boundary. The numerical codes COMCOT, TUNAMI-N2 and MOST, among others, use the moving boundary approach in inundation quantification (Fig. 2)..

[2] NOAA-MOST results are accessed online through an agreement between NOAA and JRC.

In the TUNAMI-N2 code a numerical algorithm is needed to determine if the total water depth is high enough to flood the neighbouring dry cells (land) and hence to move the shoreline. Momentum equations are used to update the volume in the wet cells only. When water surface is raising (Figure , case 2) the volume flux is no longer zero and the shoreline moves one grid point in the onshore direction.

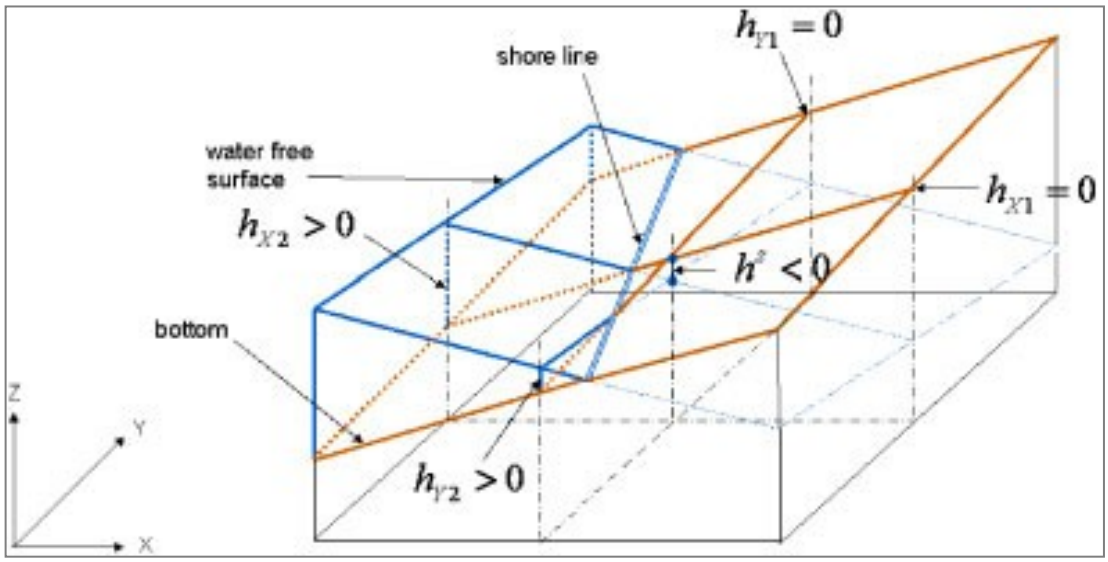

Figure 1. Inundation scheme (shoreline tracking) in HyFlux2

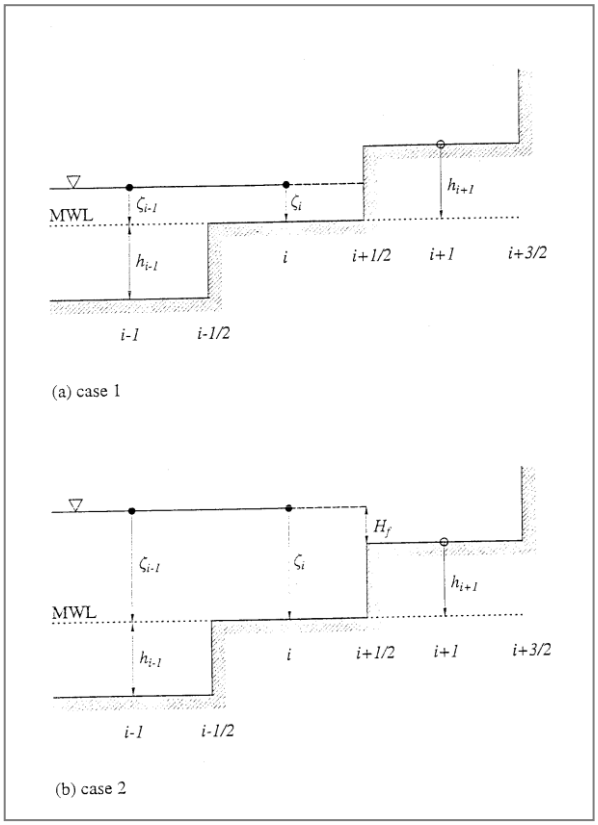

Figure 2. Inundation scheme in TUNAMI-N2

3. TECTONIC SUMMARY AND TSUNAMI EVENT

The Solomon Islands arc (Fig. 3) experiences a very high frequency of earthquake activity and many shocks of Mw 7 and larger have been recorded since the early decades of the twentieth century. The April 1, 2007 (UTC) earthquake, nucleated in a 250 km-long segment of the arc that had produced no shocks of Mw 7 or larger since the early 20th century (USGS)[3].

The event occurred close to Solomon Islands located on the southwestern Pacific plate. In this region the Pacific plate is being subducted by the Solomon Sea, Woodlark and Australian plate. The latter three plates converge to the northeast (Woodlark) or east-northeast (Australia) with the Pacific plate with velocities of 9.0-10.5 cm/yr.

The Solomon Islands arc lies along the south-western boundary of the Pacific plate, where the geometry of the subduction zone is complicated by the presence of several sub-plates, however the overall slip direction of the Indian plate with respect to the Pacific plate is relatively uniform over the entire region (Kagan and Jackson, 1980).

Large, shallow, thrust earthquakes in the Solomon Islands region tend to occur in closely related pairs or doublets. This is where two large magnitude earthquakes occur in a range of hours or days (Kagan and Jackson, 1980) as described in several events in this region (Lay and Kanamori, 1980; Schwartz et al., 1989).

Historic events: Most of the historic doublets in the Solomon Islands have occurred north of the 2007 earthquake in the vicinity of Bougainville Island and along the New Britain subduction zone. The largest of these doublets are a pair of M=8.0 and 8.1 earthquakes that occurred 12 days apart in 1971 (Schwartz et al., 1989). The portion of the fault that ruptured in the first earthquake of the 1971 doublet reruptured in a different manner during a M=7.7 earthquake in 1995 (Schwartz, 1999). Since 1907 (1919-1920, 1923, 1945-1946, 1971, 1974, 1975), and a triplet in 1977 (Lay and Kanamori, 1980; USGS, 2008) six doublet sets ranging on Mw 7-8 have occurred in this region. However none produced a noticeable tsunami, except an unconfirmed event around the turn of the 20th century noted by the locals (Fritz and Kalligeris, 2008).

[3] http://earthquake.usgs.gov/earthquakes/eqinthenews/2007/us2007aqbk/#summary

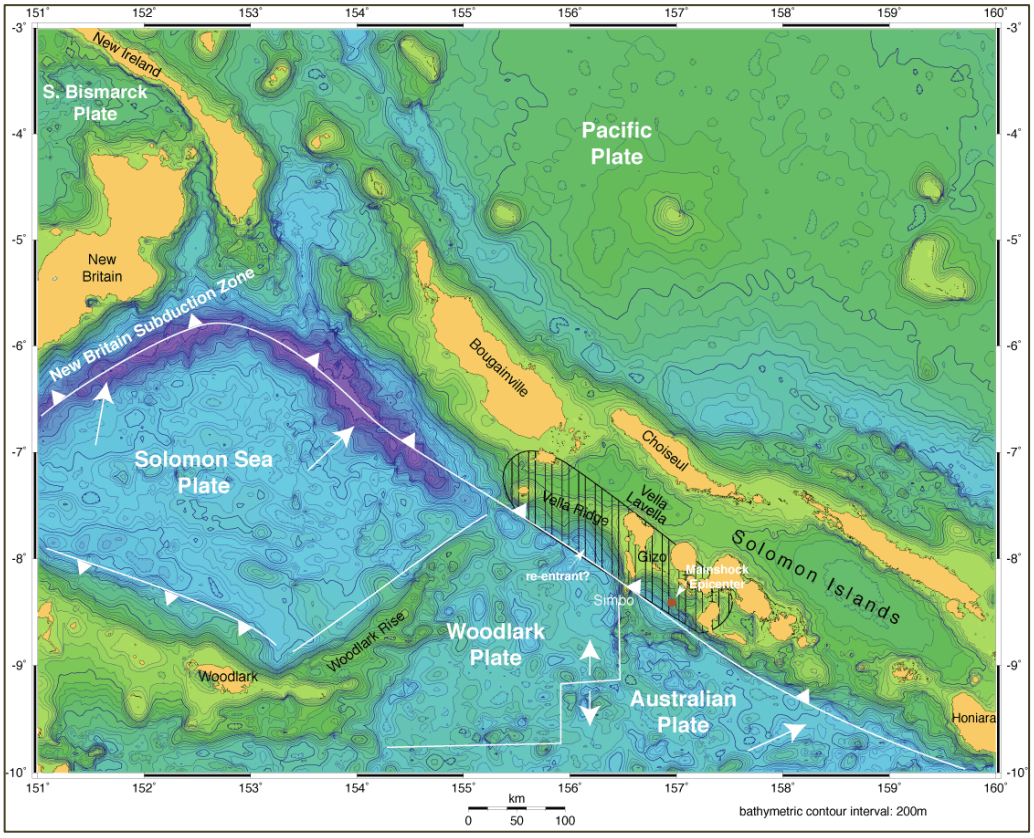

Figure 3. Tectonic setting.
http://walrus.wr.usgs.gov/tsunami/solomon07/

3.1 Description of the deformation zone

The earthquake focal mechanism indicated thrust faulting earthquake. The largest slip area is located near a triple junction among Woodlark, Australia and Pacific plates (Miyagi et al., 2009; Tomita et al., 2008). The main April 2007 Solomon earthquake was not a typical interplate earthquake which ruptured the plate interface, but rather an earthquake that occurred on a dislocation extent of the main fault, maybe because of subduction of the Woodlard ridge system (Fig. 4a). Bathymetric ridges entering the subduction zones like the Woodlark Rise and Woodlark Ridge appear to influence the distribution of slip during the earthquake. It is interesting to note that the fault ruptured directly across where an active spreading center is being subducted (USGS).

Over geologic time, ridge subduction contributes to the uplift of the overriding plate and the generation of islands such as Simbo, Ghizo, and Ranunga very near the Solomon trench. These processes can affect tsunami generation and need to be investigated in the future. A coseismic crustal deformation surveys were conducted in Ghizo, Simo, Ranongga, Vella Lavella, Kolombangara, New Georgia, Parara and Rendova Islands (Fig. 4b). The field data have been used in the evaluation of JRC codes mapping of the deformation as well as the hydrodynamic behaviour (e.g. amplitudes, run up). Different fault parameters were used in the Okada model. The Finite Fault Model and the sinusoidal model were also used in the wave height simulations to be reproduced by the JRC numerical code. Also data from InSAR (Miyagi et al., in press; Lubis and Isezaki, 2009) has been useful to compare proposed major slip patches and the generation of co-seismic uplift or subsidence on the coast with the deformation generated by the numerical codes.

The large displacements gradients on Rannongga Island were measured in the field and also using INSAR techniques. With the latter, a slip of 10 m has been estimated west of Ranongga Island (Miyagi et al., 2009). The slip location is consistent with the centroid determined by the Global CMT Project and according to assessments using InSAR (Miyagi et al., 2009), the slip is higher than the one reproduced by the models. This will be analyzed further in chapter 4.

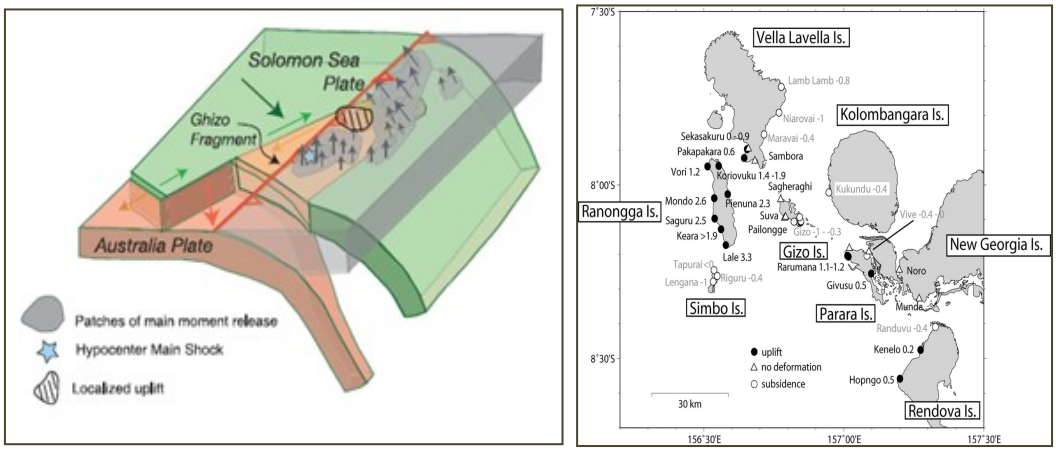

Figure 4. a. Solomon April 2007 event deformation scheme.
b. Deformation measurements (Tomita et al., 2008).

3.2 Description of the tsunami event

The maximum wave height (run up) reported at the US National Geophysical Data Center (NGDC) website was 10 m. There were not available buoys or tidal gauges close to the region analyzed in this study. However, data from field survey done by McAdoo et al. (2007) and data from field surveys have been used to compare the simulation results.

3.3 Impacts

Information about the impacts of the tsunami has been retrieved from several news and field surveys (Tomita et al., 2007; Fritz and Kalligeris, *2008)* that was delivered after the post event survey. Description of the wave height, sediments deposited and damage on the islands of Ghizo, Ranongga, Simbo and the uninhabited reef-islands around Ghizo are available. The tsunami hit the villages of Tapurai where a run up of 10 m had been measured; at Pailongge the runup was 6 m; at Titiana, 6 m (Fritz and Kalligeris, 2008). As it was described, the islands infrastructure suffered severe damage.

In Pailongge and Titiana, on Ghizo, homes made of thatched grasses and palm fronds were lifted off their foundations, floated some tens of meters inland, and deposited with surprisingly minimal structural damage. Vehicles in these villages were not rolled, suggesting that the wave did not come as a turbulent and fast moving bore, but rather as a rapidly-rising tide (Fritz and Kalligeris, 2008).

	Population (% of affected pop.)	Number of Dead (% of village pop.)	Children (under 10) dead (% of dead)
Ghizo			
Gizo	3302 (77.6%)	2 (0.1%)	0
New Manra	*206 (4.8%)*	*8 (3.9%)*	*5 (62.5%)*
Titiana	*366 (8.6%)*	*13 (3.6%)*	*8 (61.5%)*
Pailongge	76 (1.8%)	0	0
Kolombangara	89 (2.1%)	0	0
Nusa Mbaruku	*216 (5.1%)*	*10 (4.6%)*	*8 (80.0%)*
TOTAL	**4255**	**33**	**21**
Simbo			
Tapurai	234 (85.4%)	7 (3.0%)	1 (14.3%)
Riguru	40 (14.6%)	2 (5.0%)	0
TOTAL	**274**	**9**	**1**
Ranongga			
Mondo	341 (100%)	2 (0.6%)	0
TOTAL	**341**	**2**	**0**
Vella Lavella			
Sambora	319 (76.7%)		0
Lambulambu	97 (23.3%)	2 (2.1%)	2 (100%)
TOTAL	**416**	**2**	**2**
Choisuel			
Luti	101 (24.6%)	1 (1.0%)	0
Lologae	9 (2.2%)	1 (11.1%)	0
Sagiae	21 (5.1%)	1 (4.8%)	0
Sepa	165 (40.2%)	1 (0.6%)	0
Sasamunga	114 (27.8%)	2 (1.7%)	0
TOTAL	**410**	**6**	**0**
GRAND TOTAL	**5696**	**52 (0.9%)**	**24 (46.2%)**
Gilbertese	*788 (13.8%)*	*31 (59.6%)*	*21 (87.5%)*

Table1. Mortality statistics. Island name in bold, followed by community name, where it can be noted that the Gilbertese population suffered higher per capita mortality rates. [From McAdoo et al., 2007].

The event generated a tsunami that caused hundreds of affected persons (Table 1). As mentioned above, the tsunami hit both Pailongge and Titiana with similar magnitudes, yet 13 people died in Titiana (6 of which were children under 8 years old), and none died in Pailongge. The people of Titiana are of Gilbertese (Polynesian) descent who migrated to the Solomons in the 1950s, and have no indigenous knowledge of tsunamigenic earthquakes. Many were exploring the lagoon as it emptied with the leading depression wave, and were overwhelmed by the subsequent peak. The Melanesian population of Pailongge, however, gathered together the oldest and youngest members of the community and headed for higher ground after the shaking stopped, demonstrating an effective use of indigenous knowledge that saved their lives.

4. FAULT MODELS ASSESSMENT

4.1 Fault models

The generation stage of tsunami evolution includes the formation of the initial disturbance of the ocean surface due to the earthquake-triggered deformation of the seafloor. This initial water surface disturbance evolves into a long gravity wave radiating from the earthquake source. Modelling of the initial stage of tsunami generation is therefore closely linked to studies of earthquake source mechanisms (Titov, 2005).

In the following sections discussion on the five fault model results are presented (Fig. 6).

a) Cosinusoidal model used in GDACS early warning calculations
b) USGS Global Tensor model, available few hours after the event
c) Harvard Global CMT, available few hours after the event
d) USGS Finite Fault Model, available few days after the event
e) Tanioka model, obtained to fit field data observations

Cosinusoidal model used in GDACS early warning calculations

This model is used in the GDACS online calculations. These calculations are performed using the reported epicentre and the magnitude of the earthquake and calculating the rupture length and width by using empirical relationship proposed by Ward (2002). The deformation is directly applied to the water surface, without using an Okada model. For this reason the model is conservative because the deformation is similar to a very shallow earthquake if the deformation is filtered through an Okada model.

However as could be seen in overlaid field data this model doesn't take into account subsidence. In cases where the fault is close to the shoreline this is very important as had happened at Simbo Island in this event.

USGS Moment Tensor solution, available few hours after the event

This model solution has been determined using the body-wave moment tensor inversion method developed by Sipkin (1982). Globally distributed seismograph stations are used with distances between approximately 30 and 95 degrees to have suitable P waveforms. Only long-period vertical components are used. The source depth used is the depth that gives the smallest normalized mean-squared-error. Depth is the only hypocentral parameter determined since the inversion procedure is insensitive to small errors in both epicenter and origin time. Data in the National Earthquake Information Center (NEIC) catalog are available starting January 1980. The resulted fault mechanism of location of epicenter (lat/lon), depth, strike, dip, slip and Mw is used in the Okada Model to represent deformation area.

Harvard CMT, available few hours after the event

These solutions have been determined using the long period body and mantle wave moment tensor inversion method described by Dziewonski, et.al. (1981). considering corrections due to an aspherical earth structure of model SH8/U4L8 (Dziewonski and Woodward, 1991).

Currently GSN and IDA/IRIS data are used. Long-period body waves and mantle waves are also used. Mantle waves are routinely used in inversion for sources with moments greater than $5*10^{18}$ Newton-meters (Nm). Data are available starting from January 1977. Moreover, the resulted fault mechanism of location of epicenter (lat/lon), depth, strike, dip, slip and Mw is used in the Okada Model to represent deformation area.

USGS Finite Fault Model, available few days after the event

The Finite Fault Model (Fig. 8) is proposed as one of the best approaches for tsunami source estimation (Weinstein and Lundgren, 2008). For the case of Solomon Islands earthquake, the Finite Fault Model is represented by 180 subfaults (15 km x 10 km) delivered a smaller slip than what had been measured in reality. Similar situation occurred when using the Global CMT and USGS CMT parameters in the Okada Model (Fig.6).

Tanioka model, obtained to fit field data observations

The Tanioka Fault parameters (Fig. 11) were obtained based on measured field data, taking into account regions of major ground dislocation and extent of deformation. This fault model was judged as the best one, therefore it was chosen for inundation calculations and for the subsequent evaluation of HYFLUX2 numerical code.

4.2 Fault model and related simulation results

The fault scenarios generated with different parameters and fault models provide the basis to obtain the tsunami model initialization. Different fault models have been compared with ground deformation field measurements (Fig 7-11).

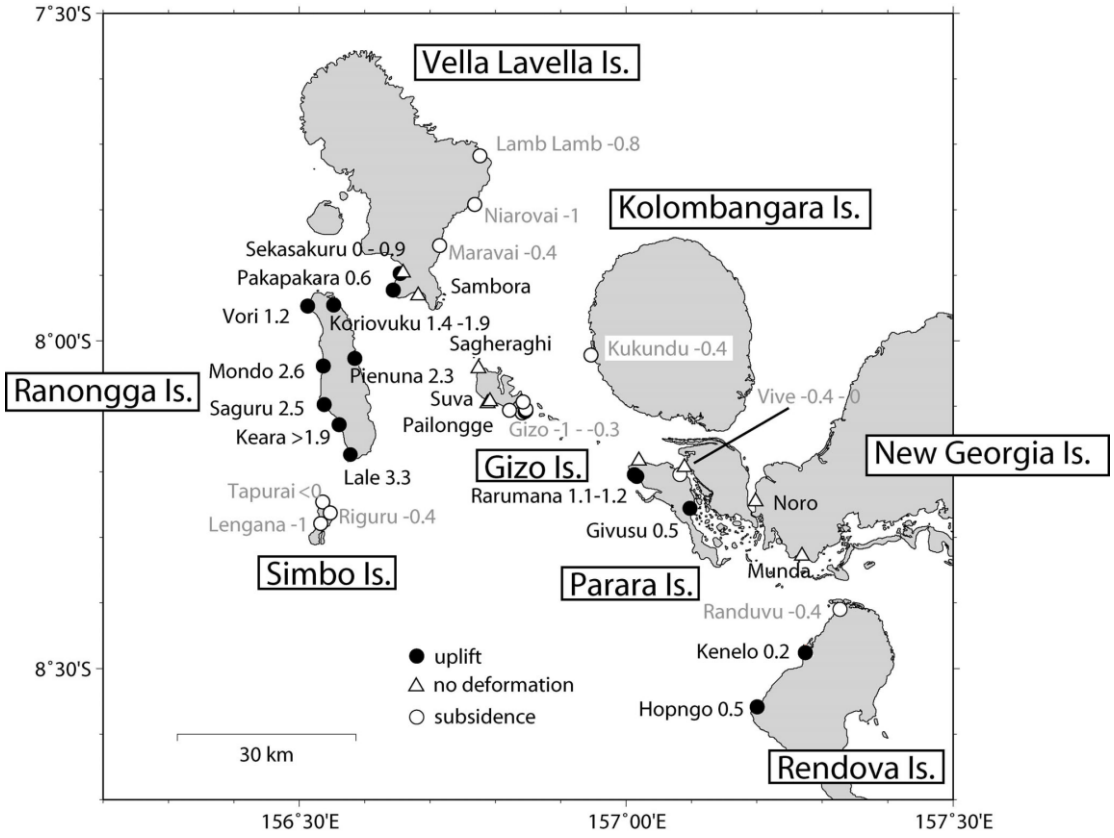

Figure 5. Measured deformation data [Tomita et al., 2007].

Post seismic deformation might have occurred, although our analysis was done on the results provided by Tomita et al. (2008) and other publications where co-seismic data has been discussed. The above mentioned models provide the profiles indicated in the following figures. The various models are also compared individually with the measured uplift or subsidence

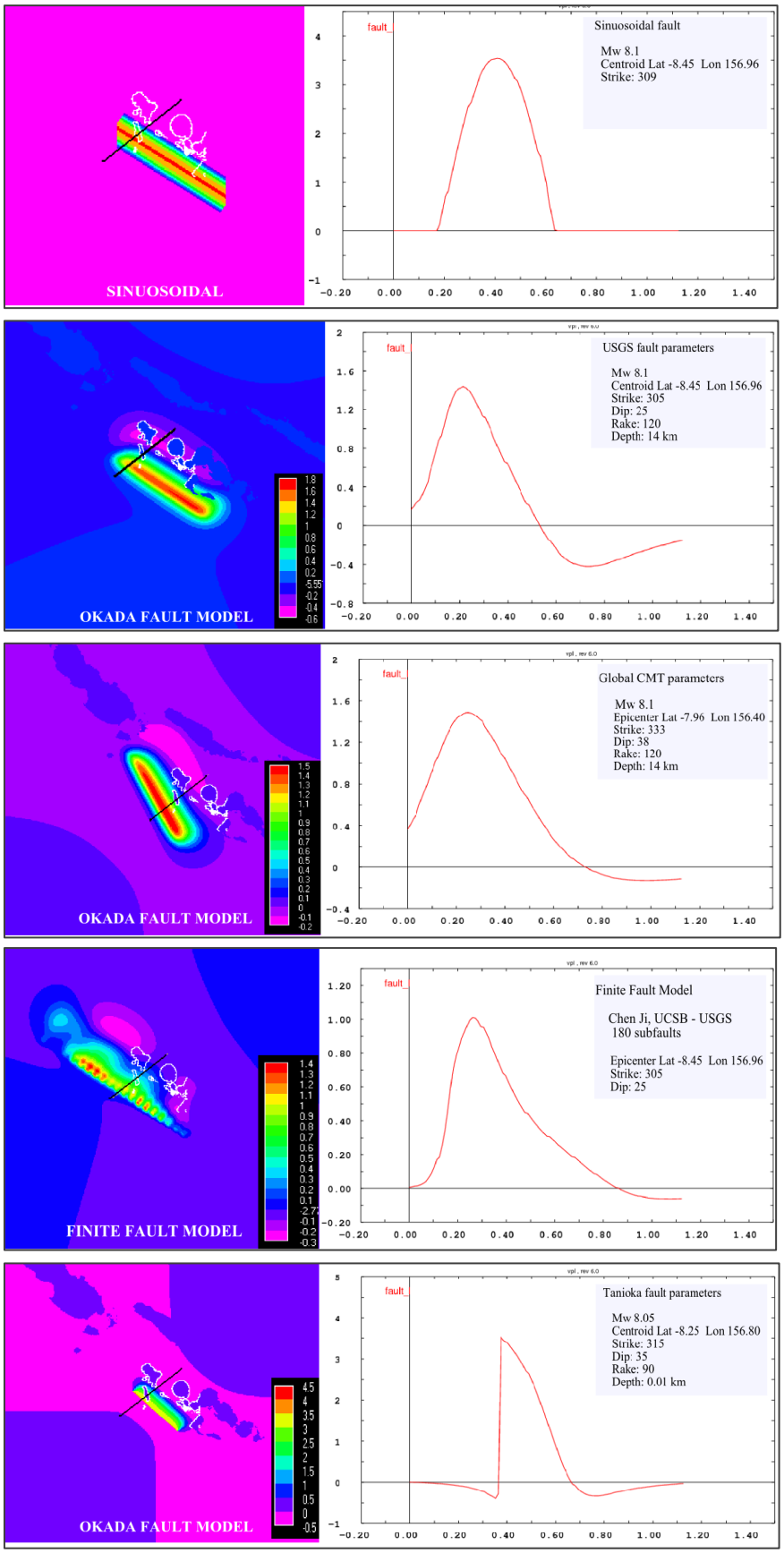

Figure 6. Deformation models and profiles.

The best agreement between field measurements and deformation values calculated by the fault models is achieved by the Tanioka fault model (Figure 7), and followed by the Cosinuosoidal model.

Profile comparison of field data with fault models deformation values are presented (Fig. 7). The ratio between Cosinussoidal crust deformation model and averaged field measurements is 2.5.

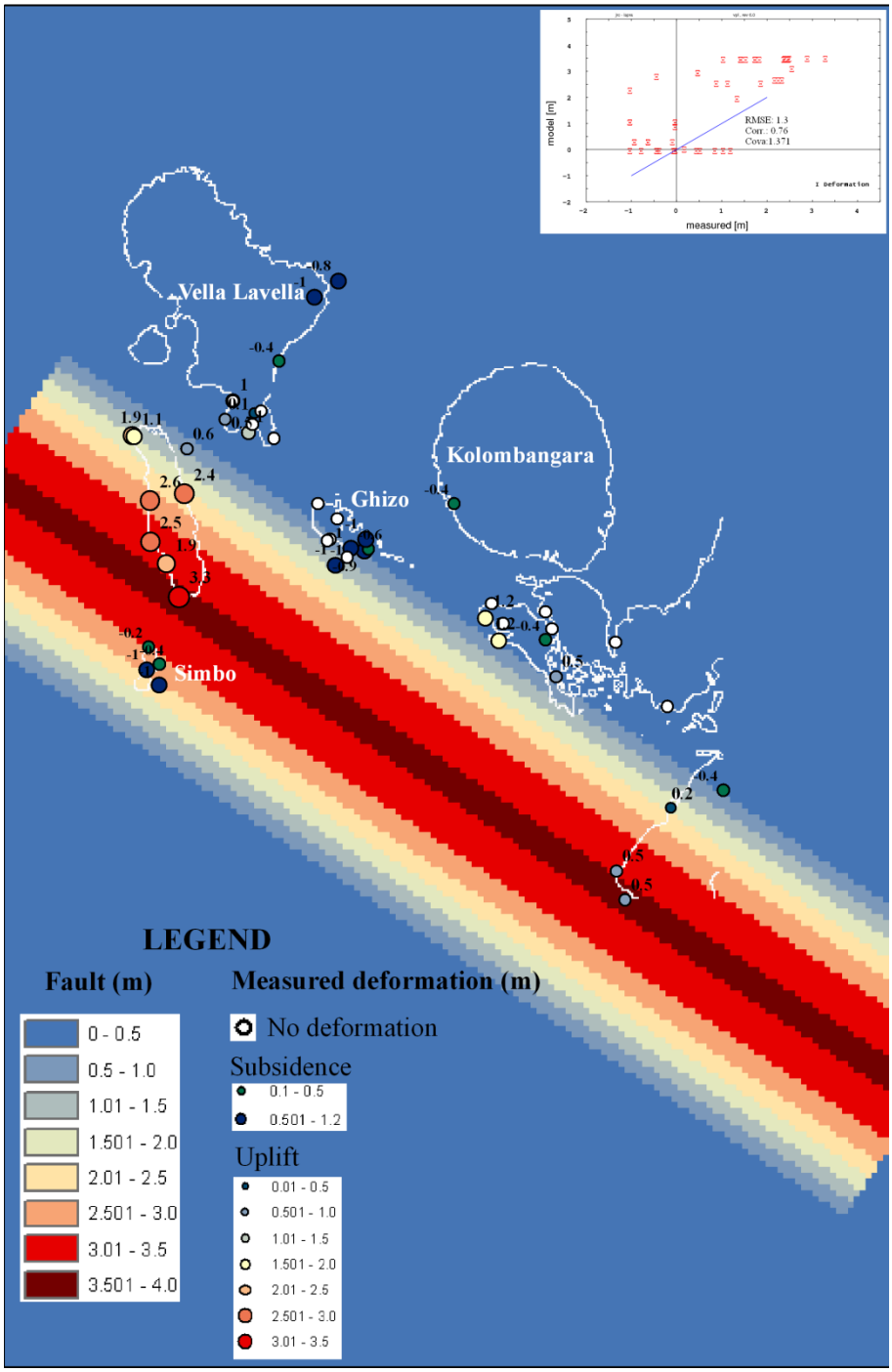

Figure 7. Fault distribution – Sinusoidal form and the measurements of ground deformation.

Profile comparison of field data with fault models deformation values are presented (Fig. 8). The ratio between the wave heights calculated with Okada model - using the fault parameters published by USGS - and the field measurements is 0.45.

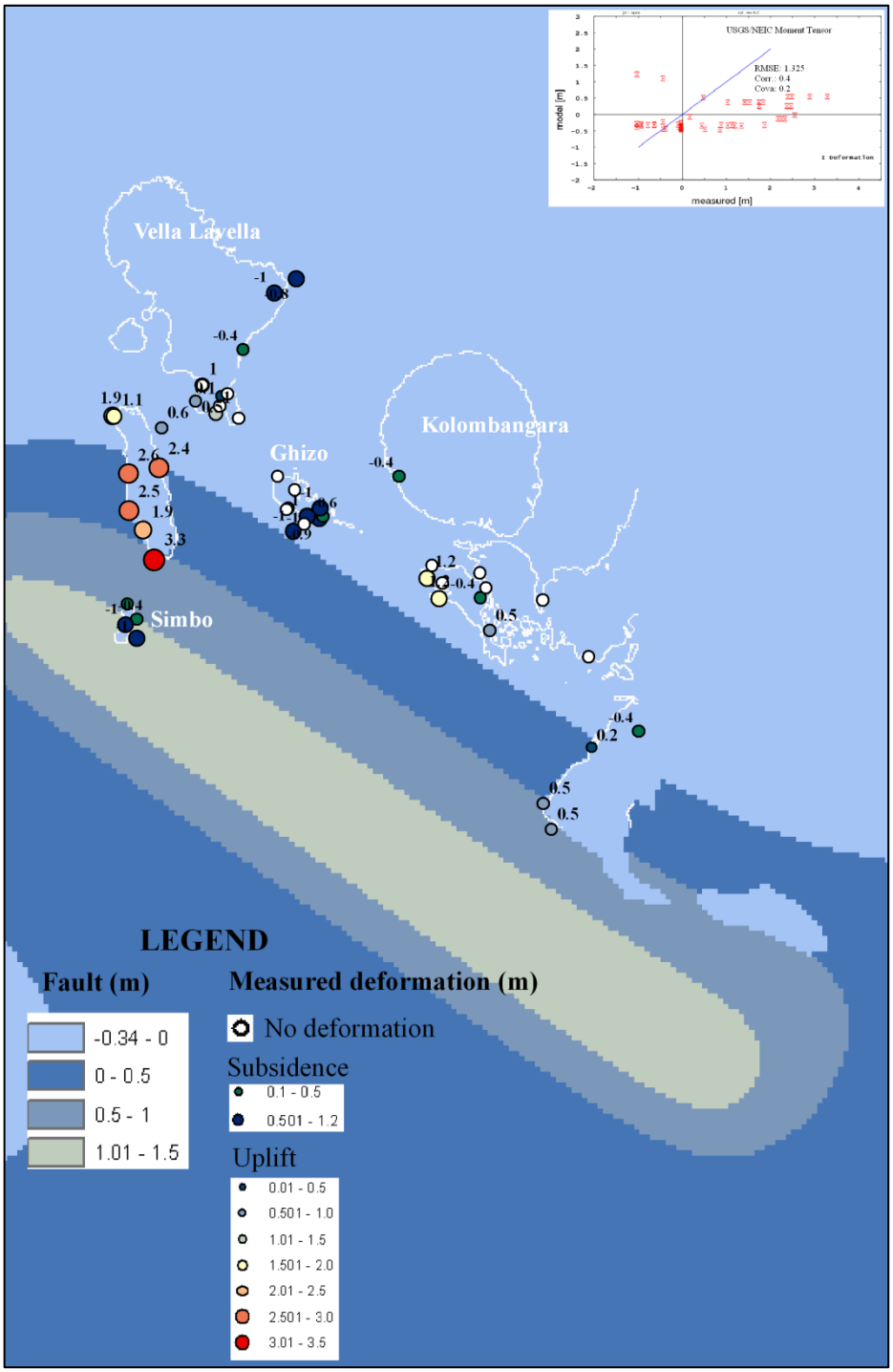

Figure 8. Fault distribution –Okada Model USGS/NEIC Centroid Moment and the measurements of ground deformation.

Profile comparison of field data with fault models deformation values are presented (Fig. 9). The ratio between the wave heights calculated with Okada model - using the fault parameters published by Harvard CMT - and the field measurements is 0.27.

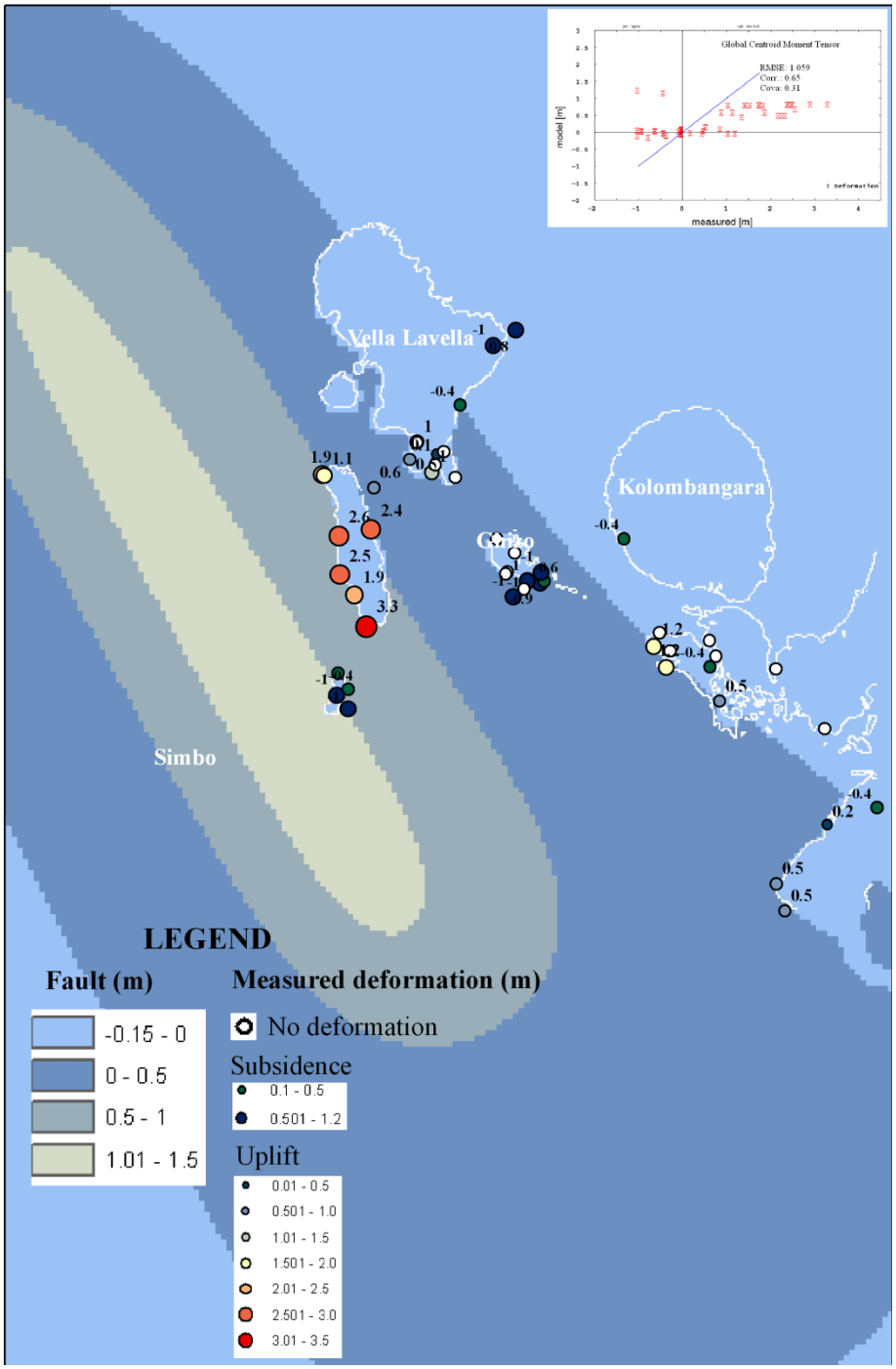

Figure 9. Fault distribution –Okada Model Global Centroid Moment and the measurements of ground deformation.

Profile comparison of field data with fault models deformation values are presented (Fig. 10). The ratio between the wave heights defined with the Finite Fault Model and the field measurements is 0.32.

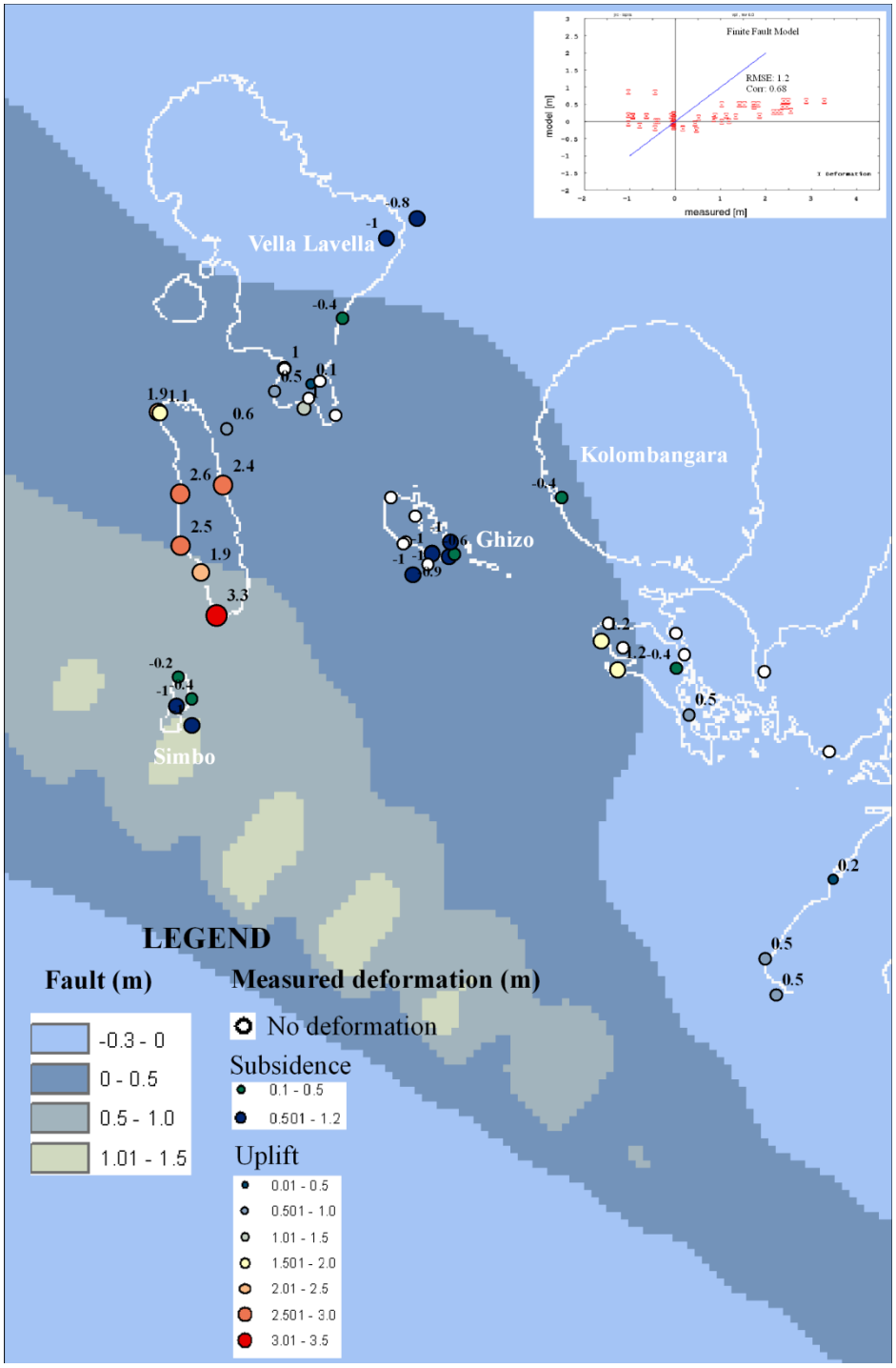

Figure 10. Fault distribution – Finite Fault Model and the measurements of ground deformation.

Profile comparison of field data with fault models deformation values are presented (Fig. 11). The ratio between the wave heights propsed by Tanioka (Tomita et al., 2008) and the field measurements is 1.14.

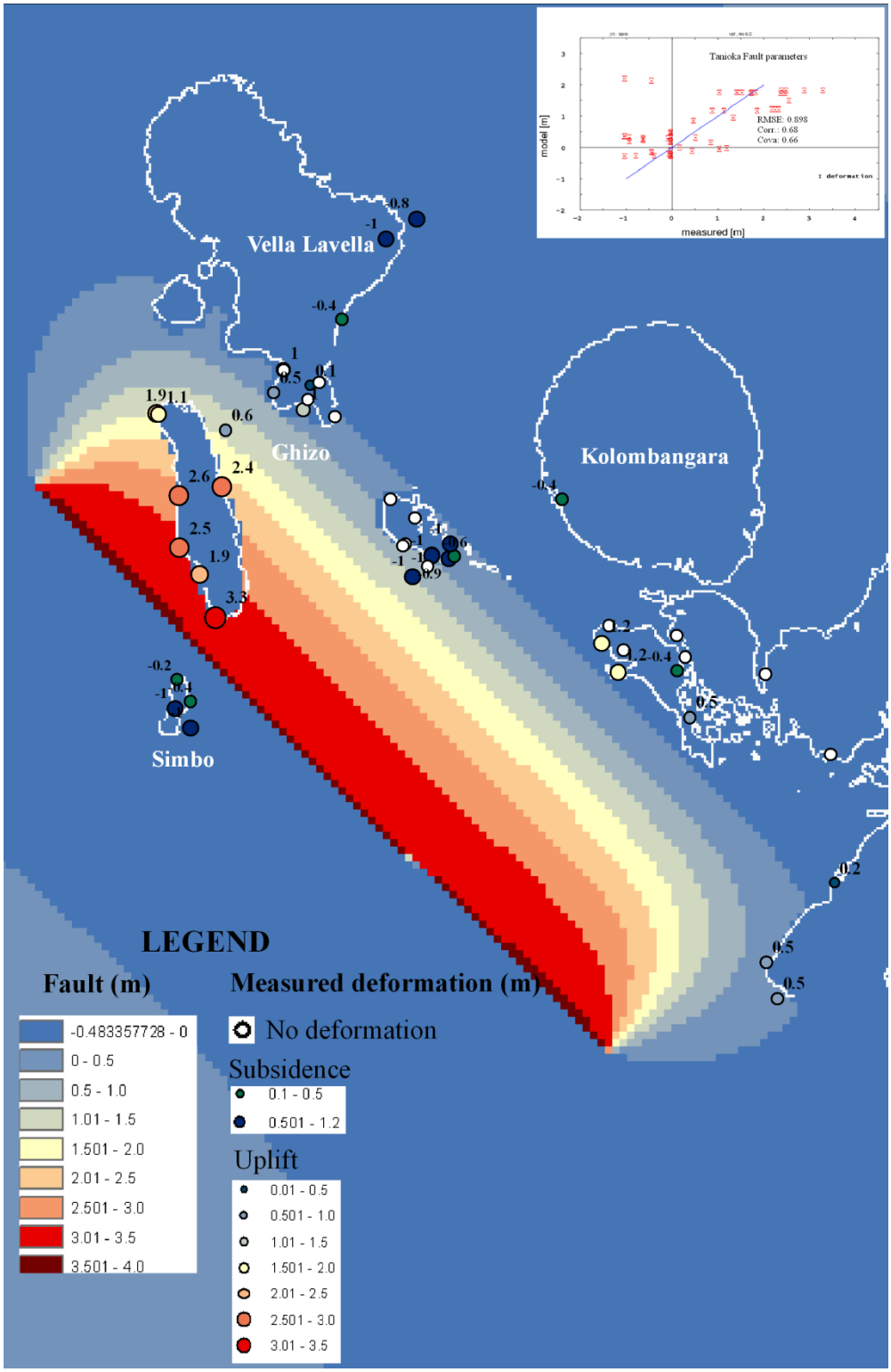

Figure 11. Fault distribution – Okada Model (Tanioka fault parameters) and the measurements of ground deformation.

5. PROPAGATION CALCULATIONS

The use of one of the models described in the previous section could drive different wave height results at different locations. Although it has been deeply discussed how fault scenarios influence the directivity, amplitude and inundation pattern, among others, this chapter is intended to show the difference of the use of several models reflected on the wave heights obtained from the calculations.

5.1 Calculations with CMT, Finite Fault, USGS and with Tanioka models

The fault mechanism is one of the most significant aspects for a reliable tsunami propagation and inundation assessment. In this subsection we compare 4 fault parameters using the HYFLUX2 code. Those 4 faults are Global CMT, NEIC/USGS, Finite Fault Model and Tanioka fault parameters as shown in Chapter 4.

The following map shows the location of the watch points analyzed. These points are consistent with the field measurements. The maps have been separated by islands to facilitate the view of different results. Although error calculation and correlation of the data has been done for each simulation (Fig. 12) and the field measurements.

The results showing a comparison of 5 fault scenarios was done using the above section fault mechanism. Most of the calculations done with different fault scenarios delivered very different data when compared to the field measurements. However it could be recognized that the best approach is given by the Tanioka (Tomita et al., 2008) fault parameters.

The subsequently figures show the differences in the wave heights that are generated according to the fault parameters used.As it is expected the major differences are related to the strike and consequently the directivity of the wave and the closeness to major slip.

As could be seen in. Iringila the measurements are very high compared with the results. The measurement plot presents the highest wave height value; the wave height and run up values measured around this site ranges from 1.86 m - 4.5 m. Similar situation is shown for Lengana where measurements range from 3.5 – 5.0 m.

The range of field wave height measurements in Ghizo site is 1.4 m - 2.08 m and in Givusu 0.9 m - 1.4 m. At Suve the wave height measurements vary from 4.0 m - 5.5 m. The major variety in the wave height measurements were found in Titiana and Tapurai where major run up had been measured (9.0-10 m respectively). The range of run up varies from 4 m – 10 m (Fig. 12).

Chapter 4 demonstrated that a better comparison is obtained when using the Tanioka model. It is interesting now to understand the impact of the various crustal deformation models or focal mechanisms, on the sea level behaviour. Therefore the HYFLUX2 or SWAN code has been selected and the various models have been applied.

The conclusion is that the Tanioka parameters using Okada Model, was one of the fault deformation model to predict the correct behaviour on the coast.

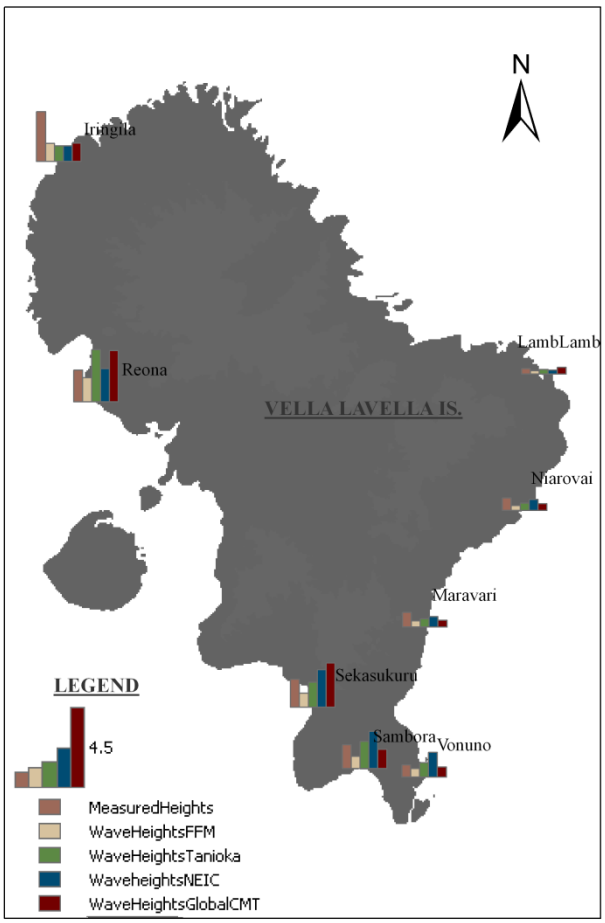
N
Iringila
Reona
LambLamb
VELLA LAVELLA IS.
Niarovai
Maravari
Sekasukuru
Sambora
Vonuno
LEGEND
4.5
MeasuredHeights
WaveHeightsFFM
WaveHeightsTanioka
WaveheightsNEIC
WaveHeightsGlobalCMT

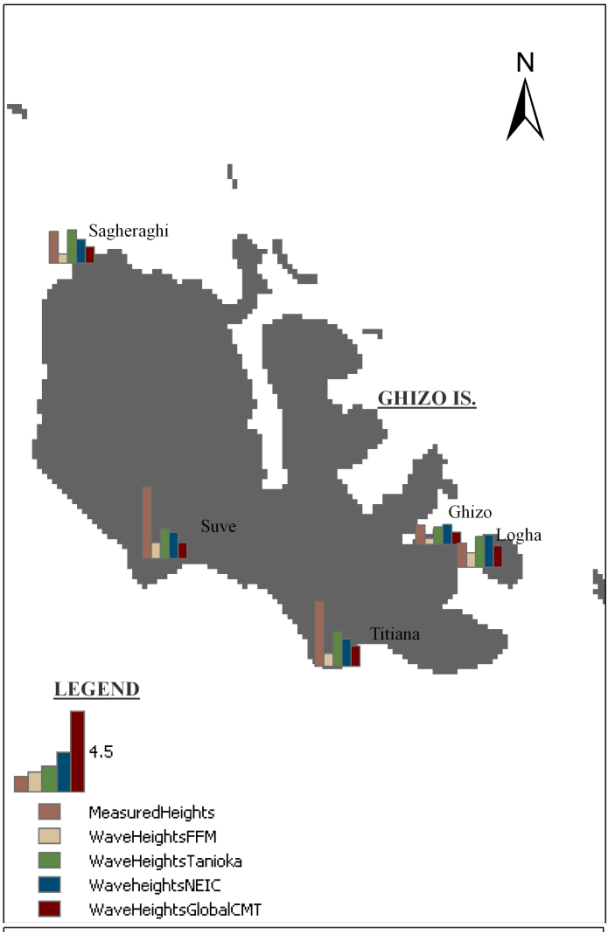
N
Sagheraghi
GHIZO IS.
Suve
Ghizo
Logha
Titiana
LEGEND
4.5
MeasuredHeights
WaveHeightsFFM
WaveHeightsTanioka
WaveheightsNEIC
WaveHeightsGlobalCMT

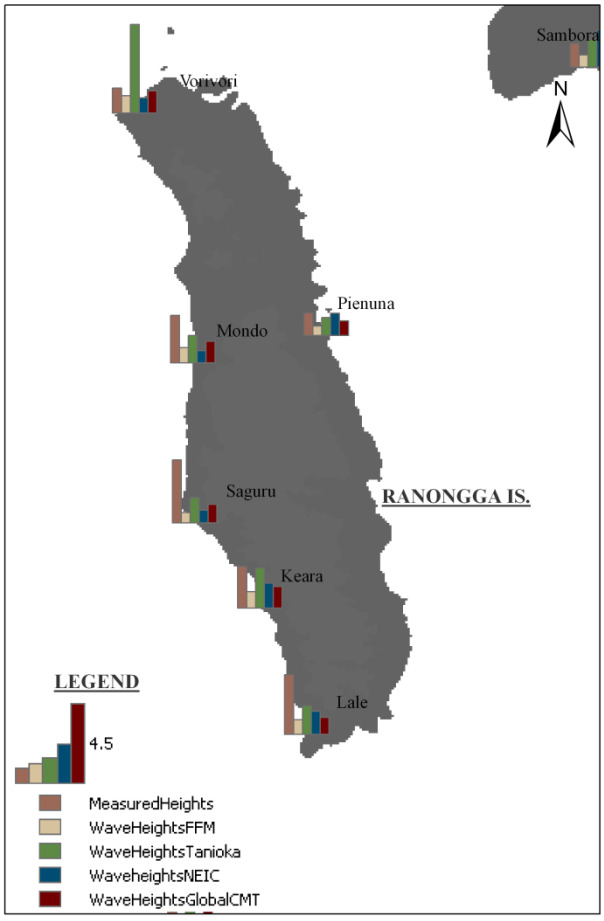
Sambora
N
Vonivoni
Pienuna
Mondo
Saguru
RANONGGA IS.
Keara
Lale
LEGEND
4.5
MeasuredHeights
WaveHeightsFFM
WaveHeightsTanioka
WaveheightsNEIC
WaveHeightsGlobalCMT

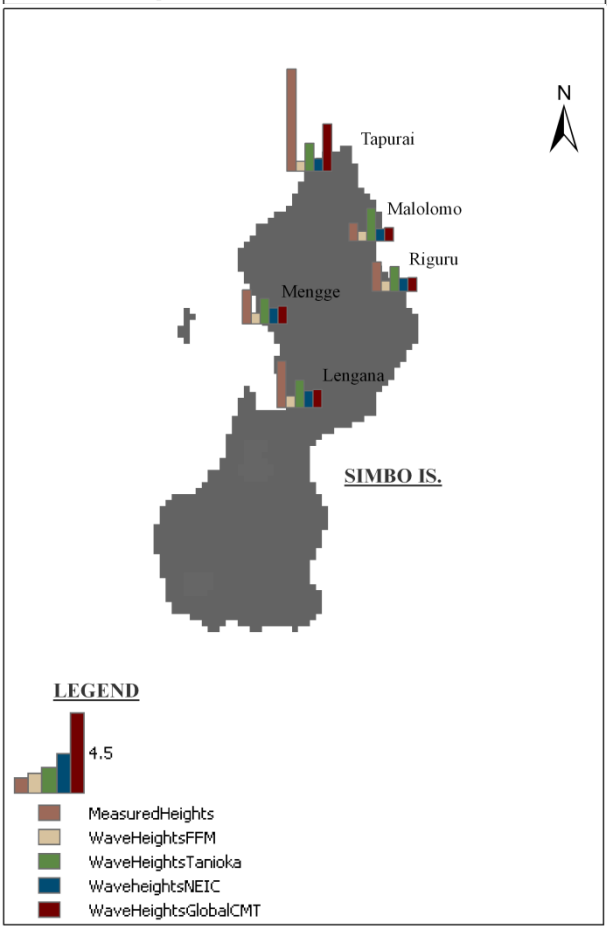
N
Tapurai
Malolomo
Riguru
Mengge
Lengana
SIMBO IS.
LEGEND
4.5
MeasuredHeights
WaveHeightsFFM
WaveHeightsTanioka
WaveheightsNEIC
WaveHeightsGlobalCMT

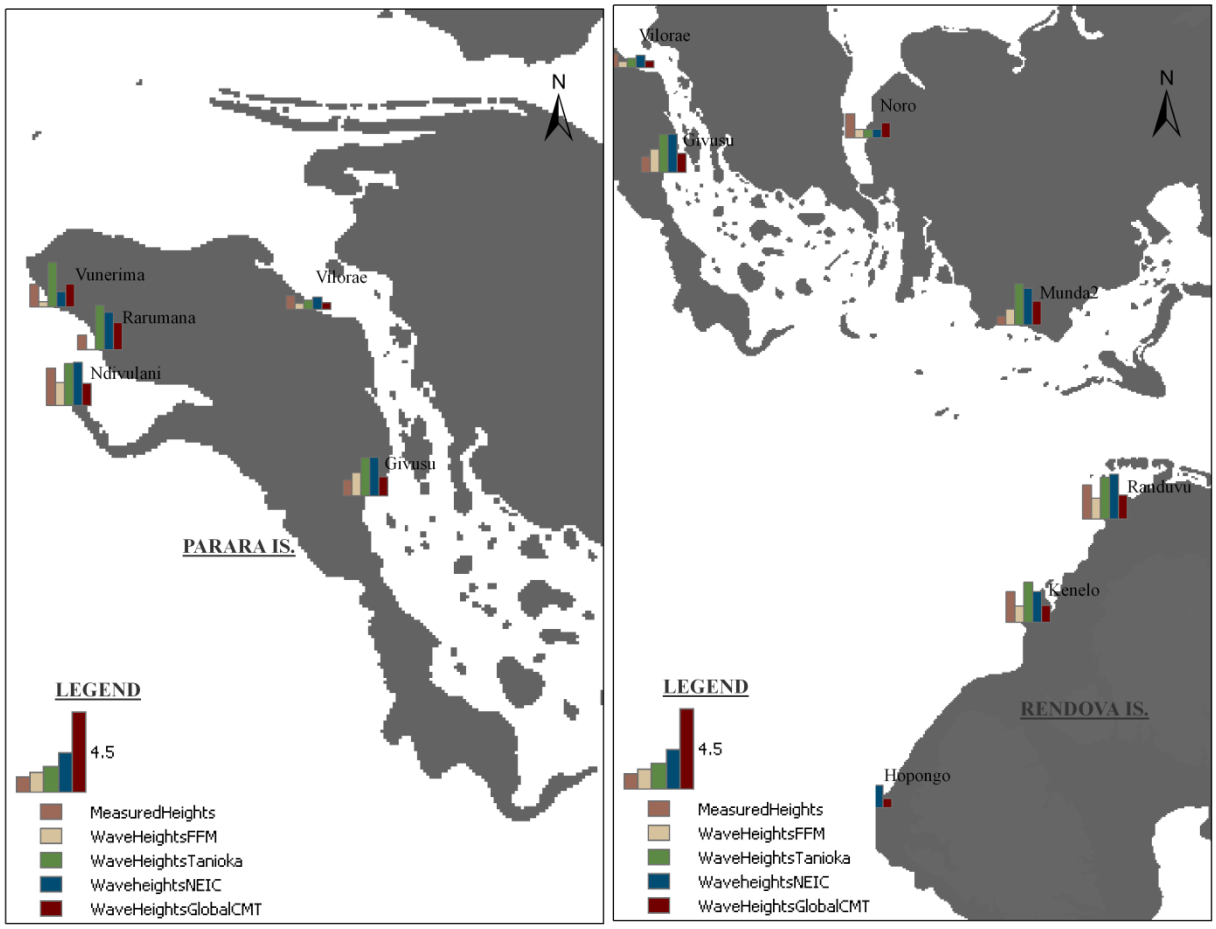

Figure 12. Wave heights calculations and field measurements.

The comparison of each wave height value resulted from the different fault models is shown in table 2. The best fitting model is Tanioka when comparing the average ratio between the simulated wave heights and field measurements. The calculations have been done with HYFLUX2 code.

Statistics of deformation	
Fault parameters	**Ratio AV[sim/meas]**
Cosinuosoidal Mw 8.2	2.5
USGS Centroid Moment Tensor solution	0.45
Global Centroid Moment Tensor	0.27
Finite Fault Model	0.32
Tanioka fault parameters	1.14

Table 2. Statistics of deformation: measured data and simulated data.

In the following graph comparisons of wave height measurements and simulations, obtained by using the different fault models are presented. The purpose of the simulations was to assess how the selection of a fault source will impact the results. Understanding these parameters is important especially in case of near coast fault scenarios like this Solomon rupture.

The higher run up was measured in Tapurai at Simbo Island. The calculated wave heights summarize values more greater than 0.5 m. Graphs in figure 13 show in better scale the wave heights presented in figure 12.

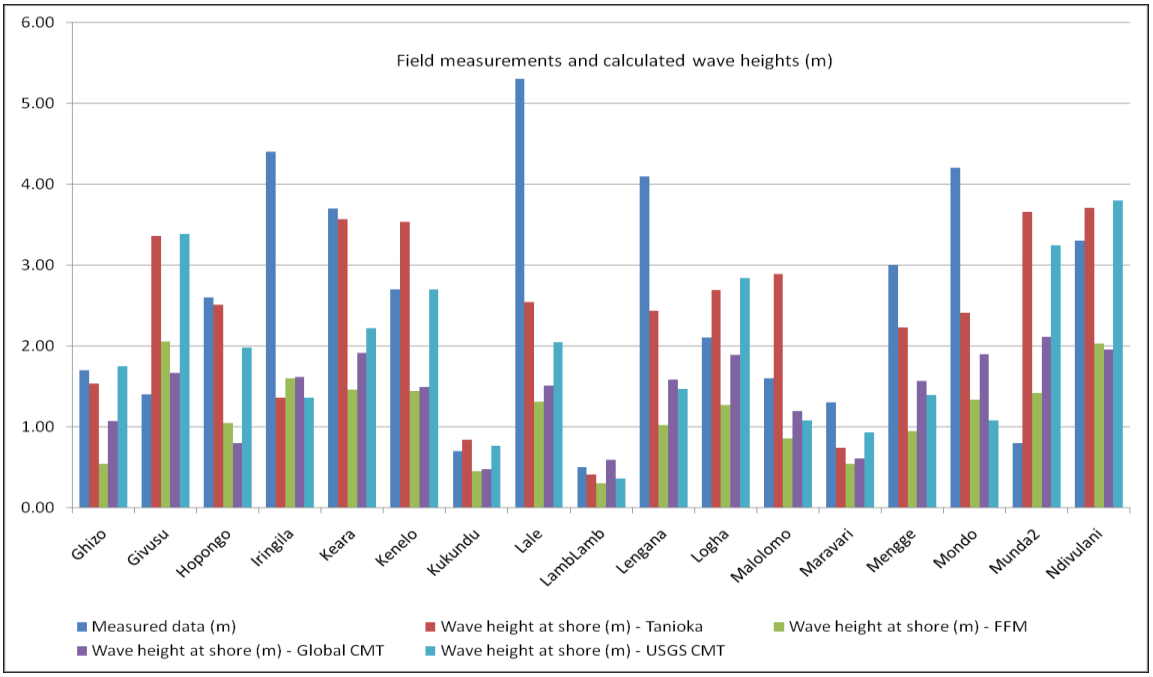

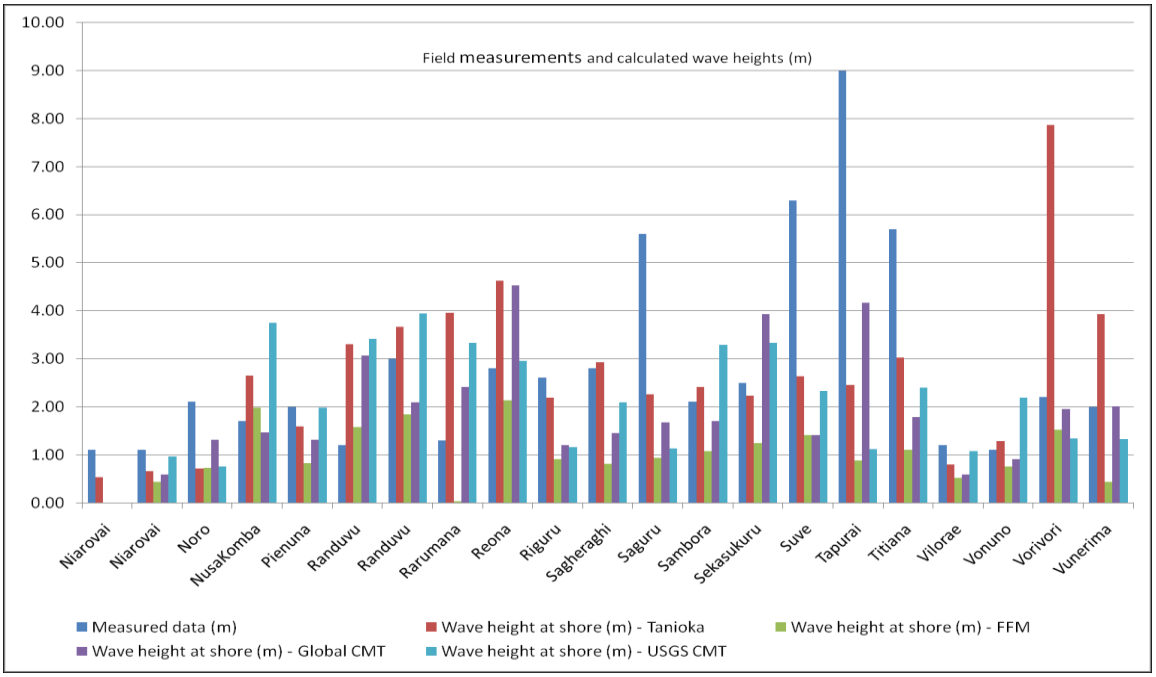

Figure 13. Calculated wave heights using different scenarios.

The profiles in Figure 15 indicate differences of sea level trends when using the available seismic information. Results of two site off shore and two sites close to the shoreline have been presented (see Figure 14 for the sensor position).

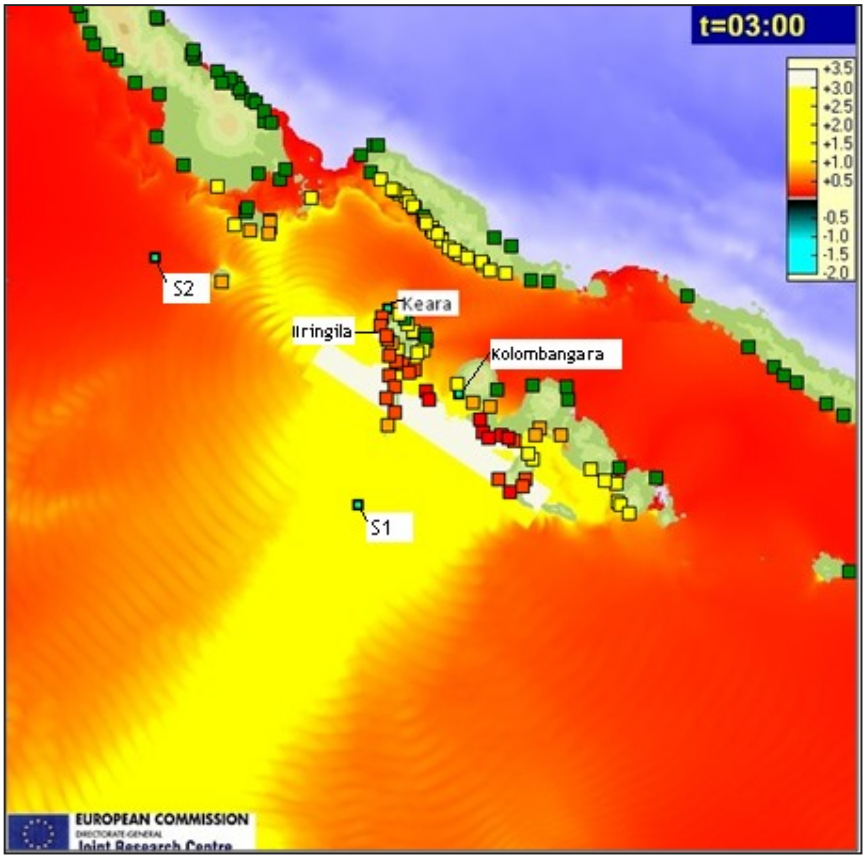

Figure 14. The sensor position (light green, sensor S1, S2, Keara, Kolobangara). [Run Grid size: 900 m].

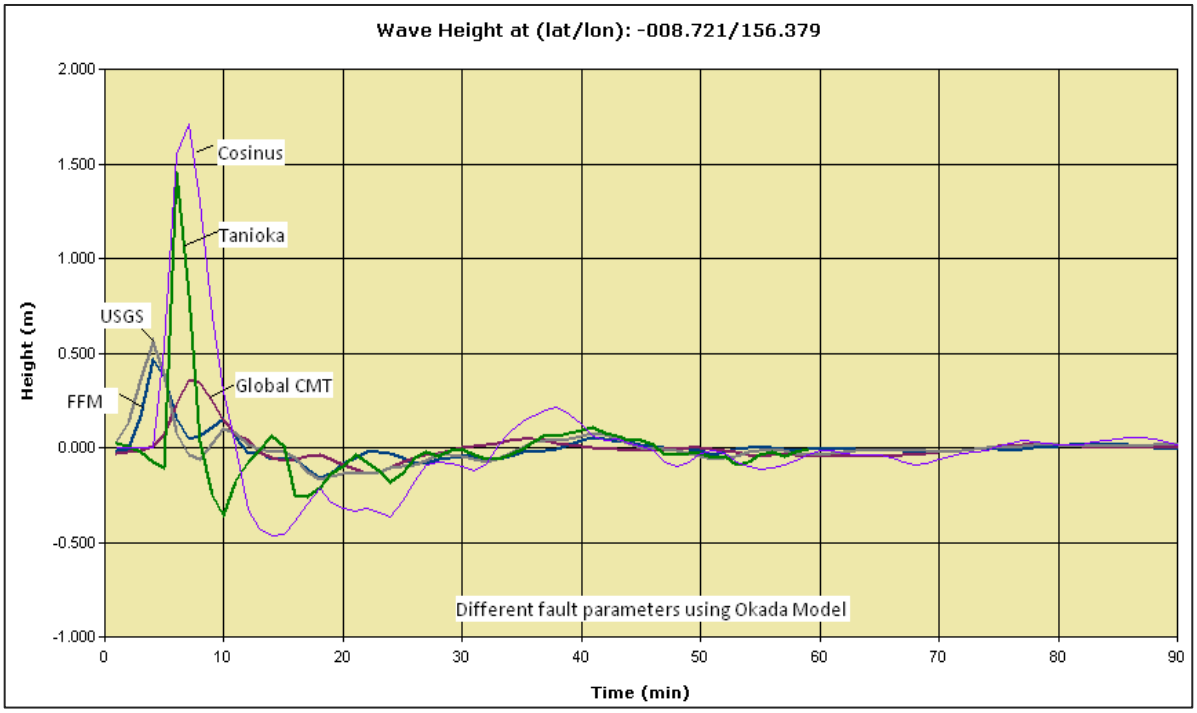

a. Offshore S1

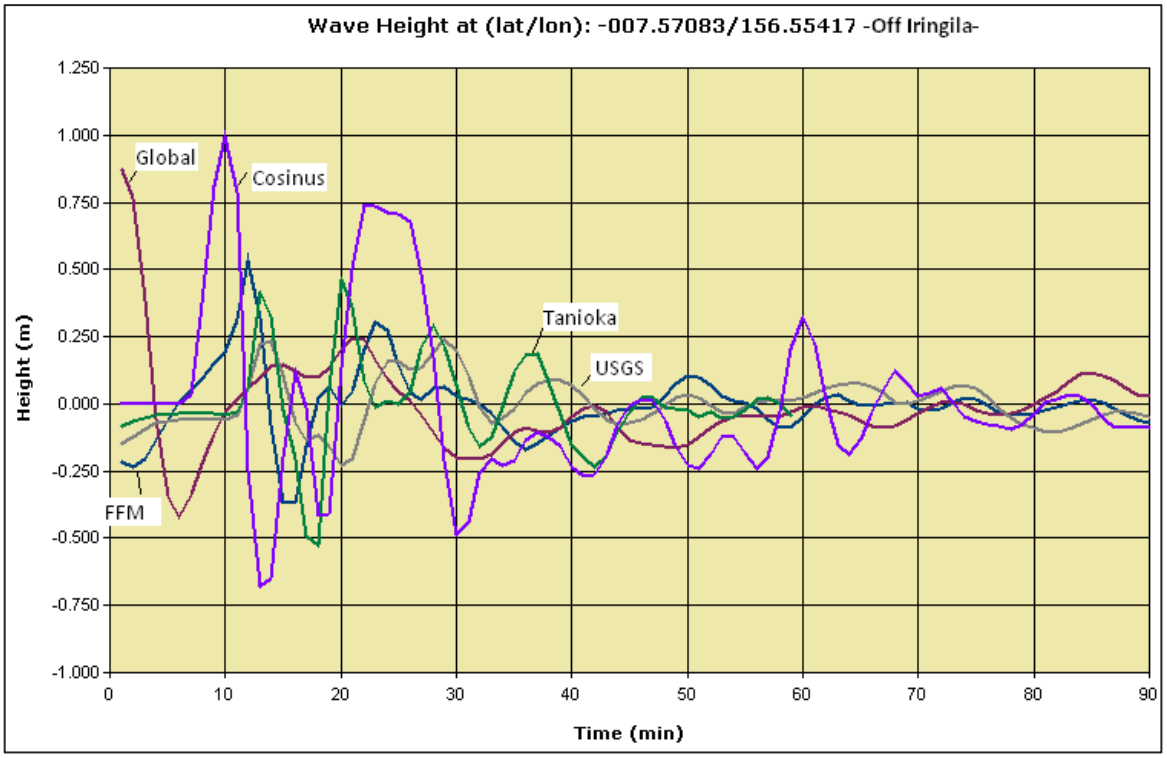

b. Off Iringila

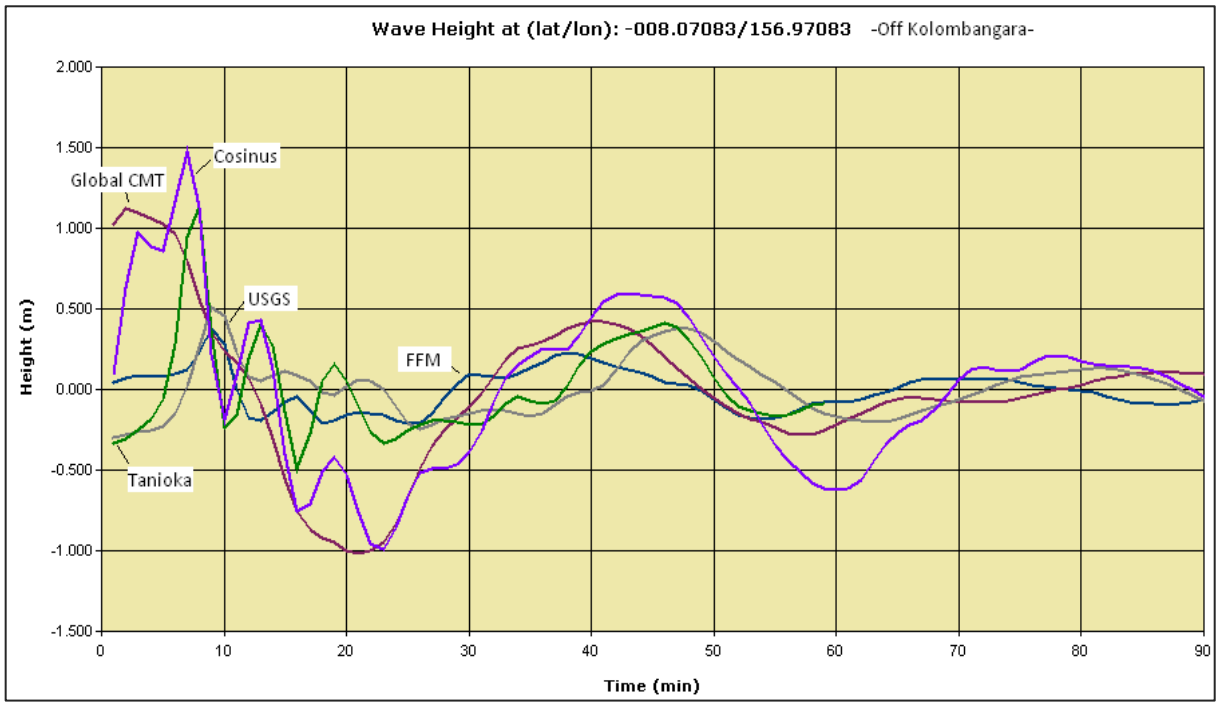

c. Off Kolombangara

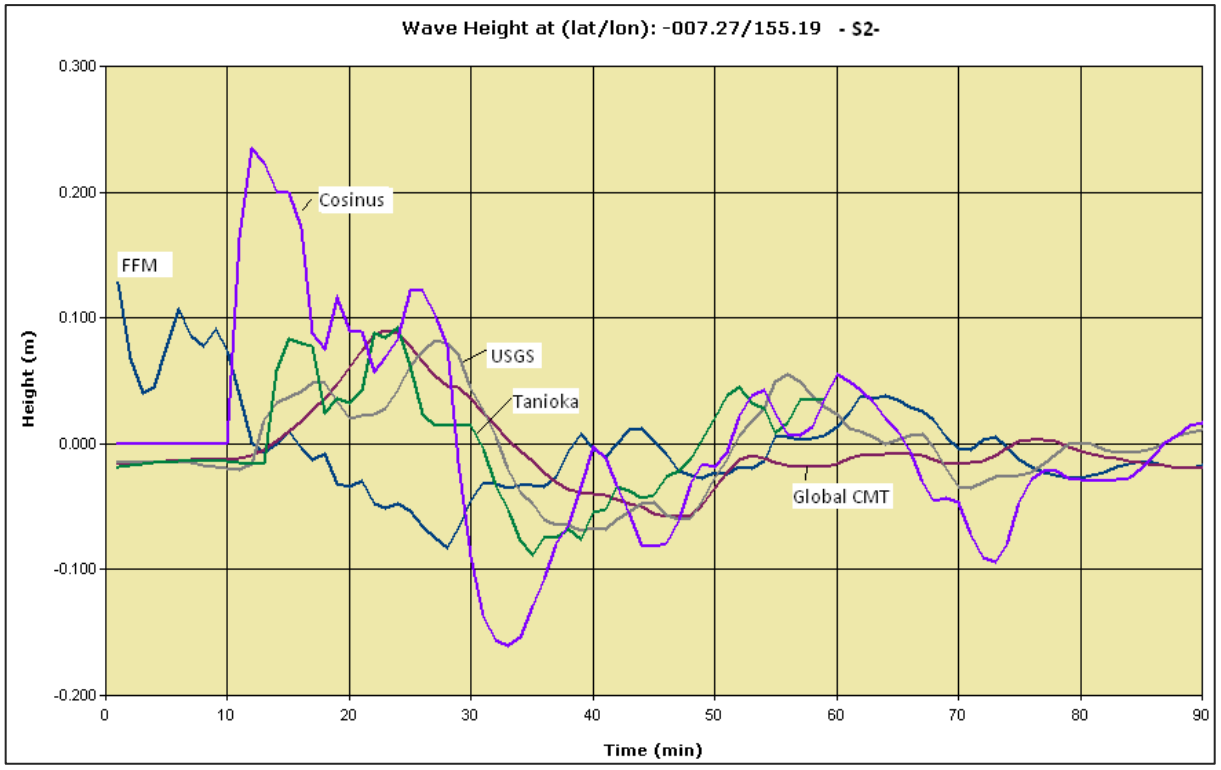

d. Sensor S2 offshore.

Figure 15. Sea level trends at several sensors. All faults are shown together to highlight differences related to fault mechanism and fault model.

5.2 Early Warning Calculations (JRC model in GDACS)

JRC systems detected the earthquake 16 minutes (Table 2; 3) after the event as soon as it was published by the United States Geological Survey[4]. Subsequently, the online JRC SWAN model was activated, spending about 20 minutes to complete the wave height propagation calculation. The online JRC SWAN model calculated maximum tsunami wave heights of 3.2 m in Kunji and 2.7 m in Vanikuva and Harai in the Solomon Islands.

The assumed initial fault conditions for these calculations are shown in Table 3. The major difference in respect to other models is the strike angle which is due to the fact that the system looks for the closer fault line direction.

Calculation details		
Initial conditions, fault geometry and calculation time.		
Grid calculations **Mw 8.0**	Lat/Lon Fault Length Fault Width Slip Fault Angle Bathymetry cell size Calculation time	-8.5, 157 158 km 44 km 3.16 m 124 2.64 min 2.2 hr
Earthquake data **Mw 8.1**	Lat/Lon Fault Lenght Fault Width Slip Fault Angle Bathymetry cell size CPU Time/Calculation	-8.4807, 156.9781 177 km 49 km 3.54 m 141.11 2.937 min 20 min for 2.5 hr

Table 3: Simulation parameters of the JRC pre-calculated grid scenario (Mw 8.0) and the online JRC SWAN model (Mw 8.1)

The analysis is performed by showing the results of the calculations in some points (S1 to S5) in some interesting locations. In order to have other reference the results of the JRC-SWAN are compared with the ones of NOAA-MOST and with the grid pre-calculations available for this equivalent event, i.e. the calculation that would be currently selected by the large JRC pre-calculated scenario.

[4] After the event detection a grid pre-calculation would immediately be retrieved from the JRC pre-calculated scenario. Unfortunately at the time of the earthquake such a database was not yet completed.

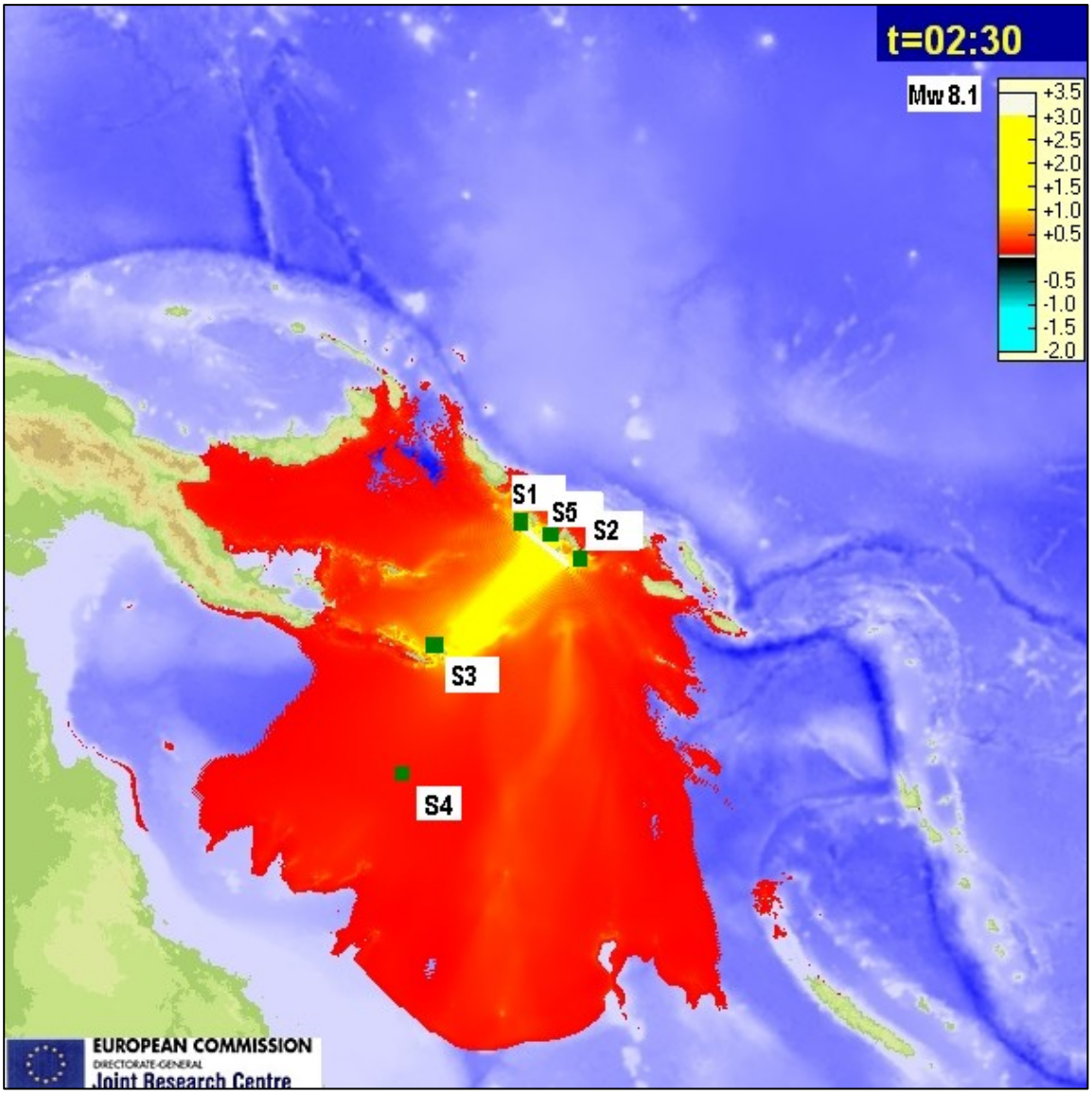

Figure 16. Location of sensors [5 km -2.937' grid size].

The main difference between the pre-calculated grid scenario and the online calculation are in the amplitudes. This is expected because basically the seismic input parameters used at the beginning were slightly different in the magnitude respect to the final values of the event. However, when compared with MOST code calculations an important difference could be assessed, mostly due to the different strike in the fault parameters used by the two calculations.

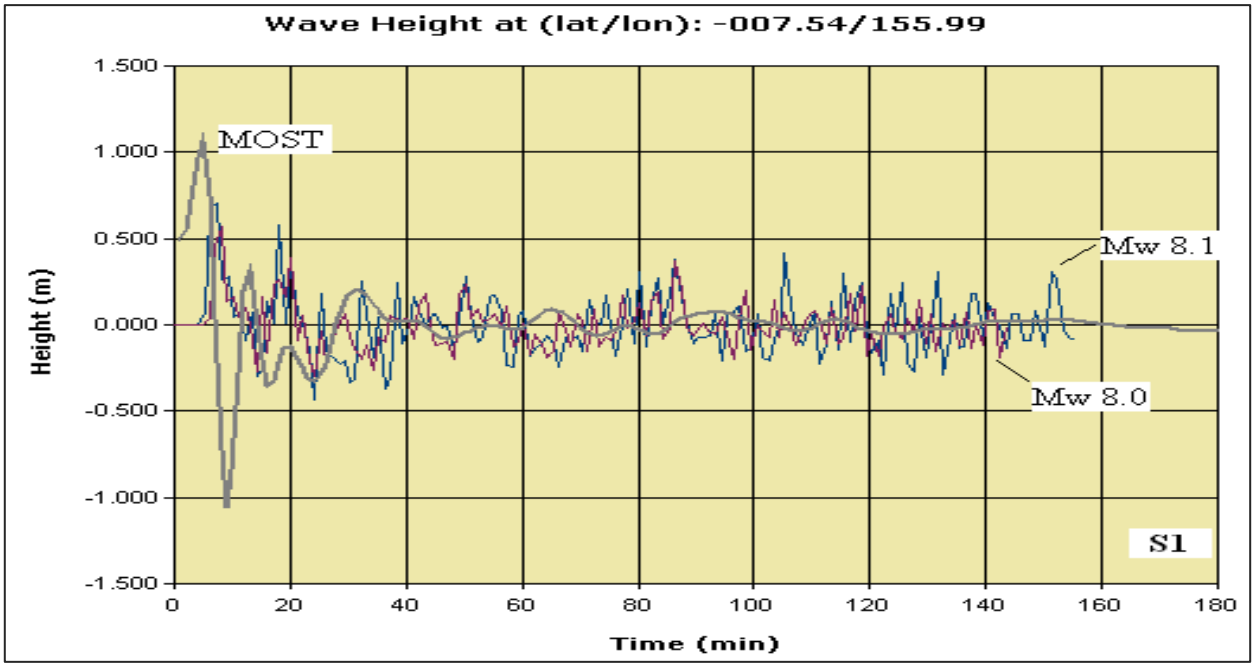

Figure 17. Sea level at sensor S1. Pre-calculated grid scenario (Mw8.0), online calculations (Mw 8.1) and MOST code results

.

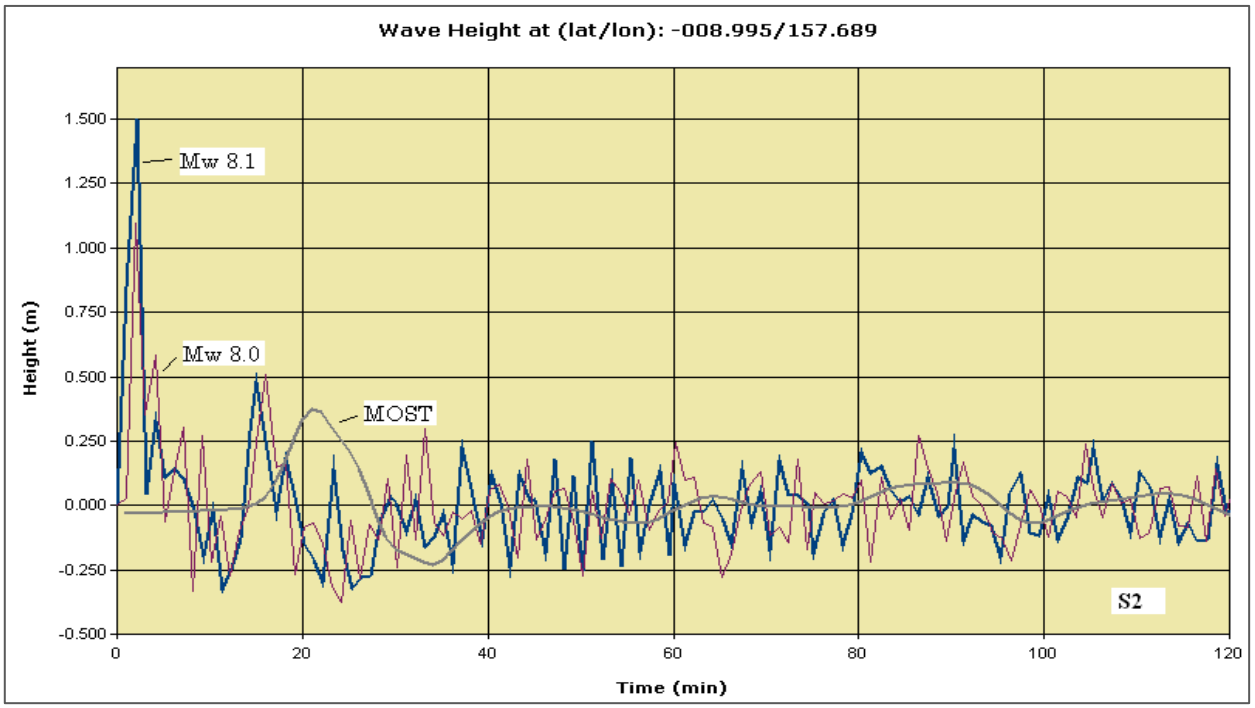

Figure 18. Sea level at sensor S2. Pre-calculated grid scenario (Mw8.0), online calculations (Mw 8.1) and MOST code results

.

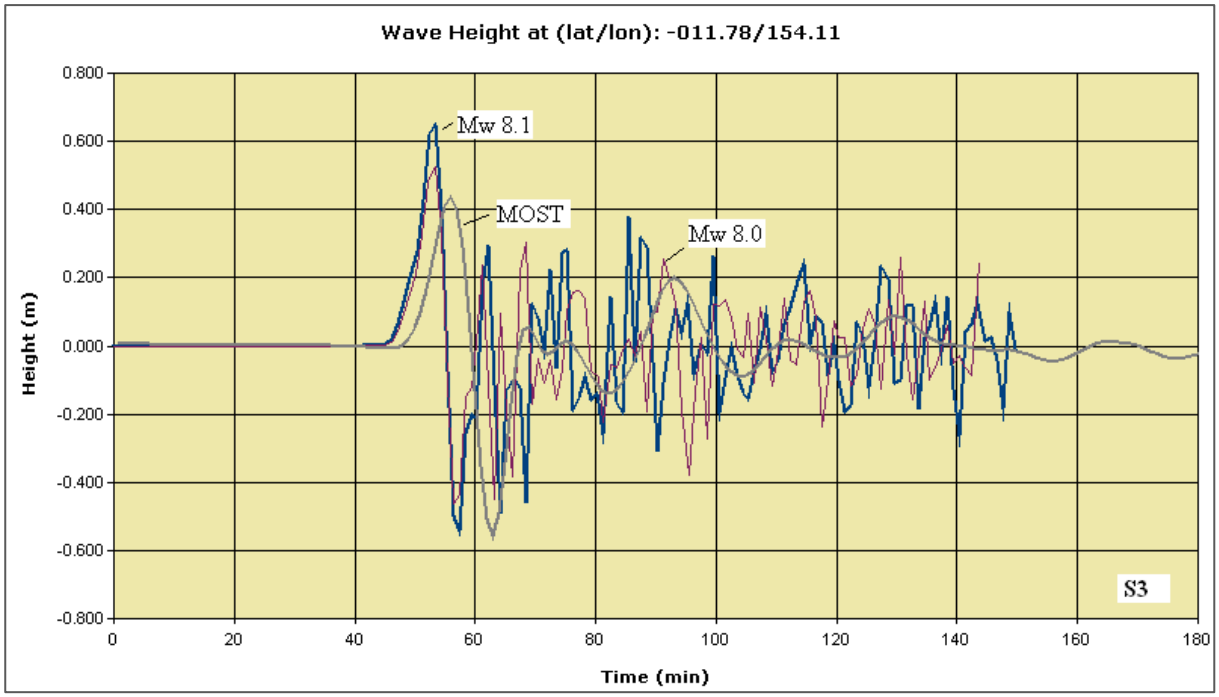

Figure 19. Sea level at sensor S3. Pre-calculated grid scenario (Mw8.0), online calculations (Mw 8.1) and MOST code results.

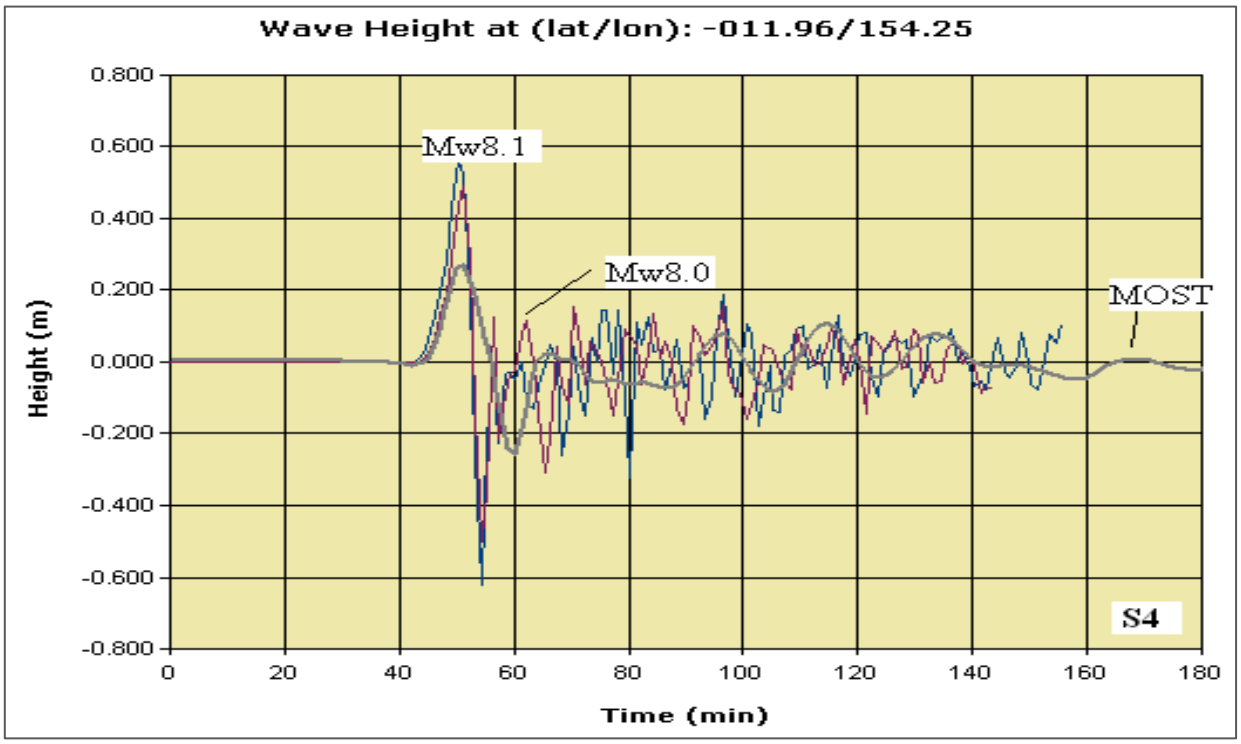

Figure 20. Sea level at sensor S4. Pre-calculated grid scenario (Mw8.0), online calculations (Mw 8.1) and MOST code results.

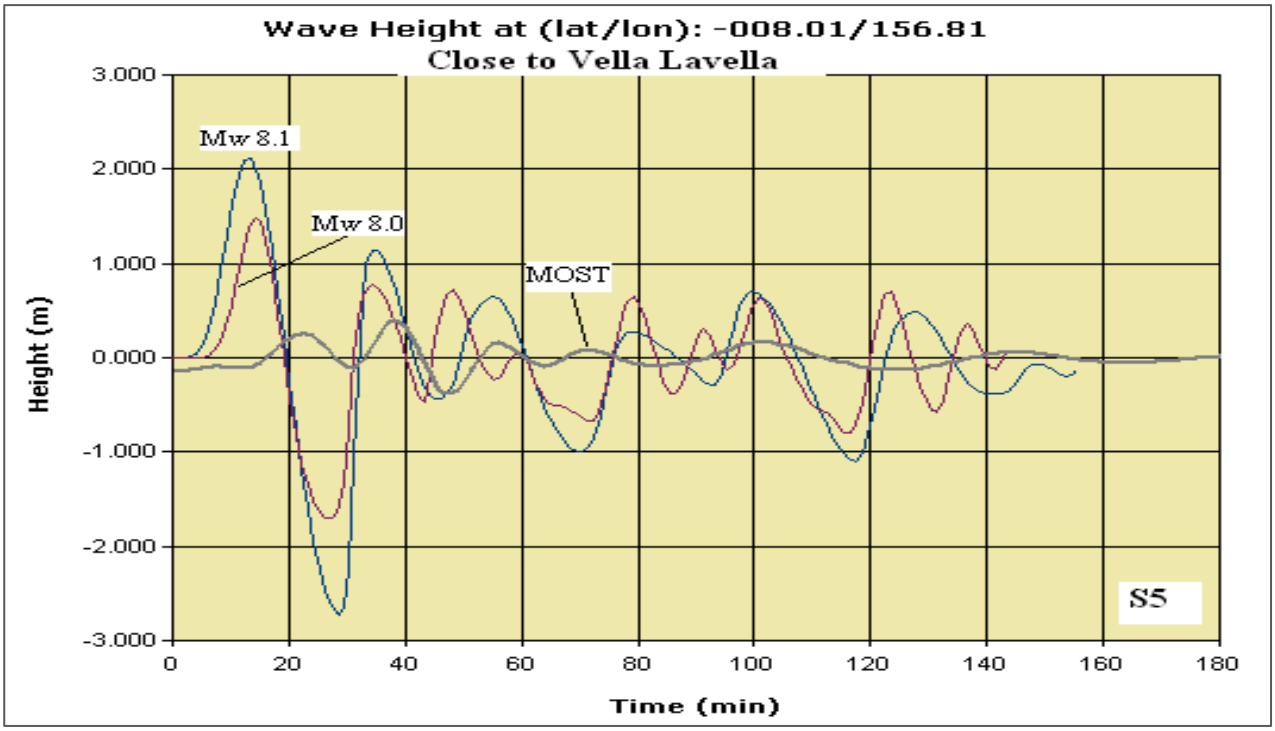

Figure 21. Sea level at sensor S5. Pre-calculated grid scenario (Mw8.0), online calculations (Mw 8.1) and MOST code results.

Depending on the location of the sensor (e.g. offshore, close to shoreline) wave differences could be found. The comparison of calculated wave heights is done with run up measurement. The following graph shows wave height trends.

Although an overestimation of the calculation resulted in the majority of sites (Fig. 22), at Iringila the wave height is underestimated. According to the JRC-SWAN, the expected value was 1 m. However the value of the inundation wave height and run up ranged between 1.9 – 4.4 m.

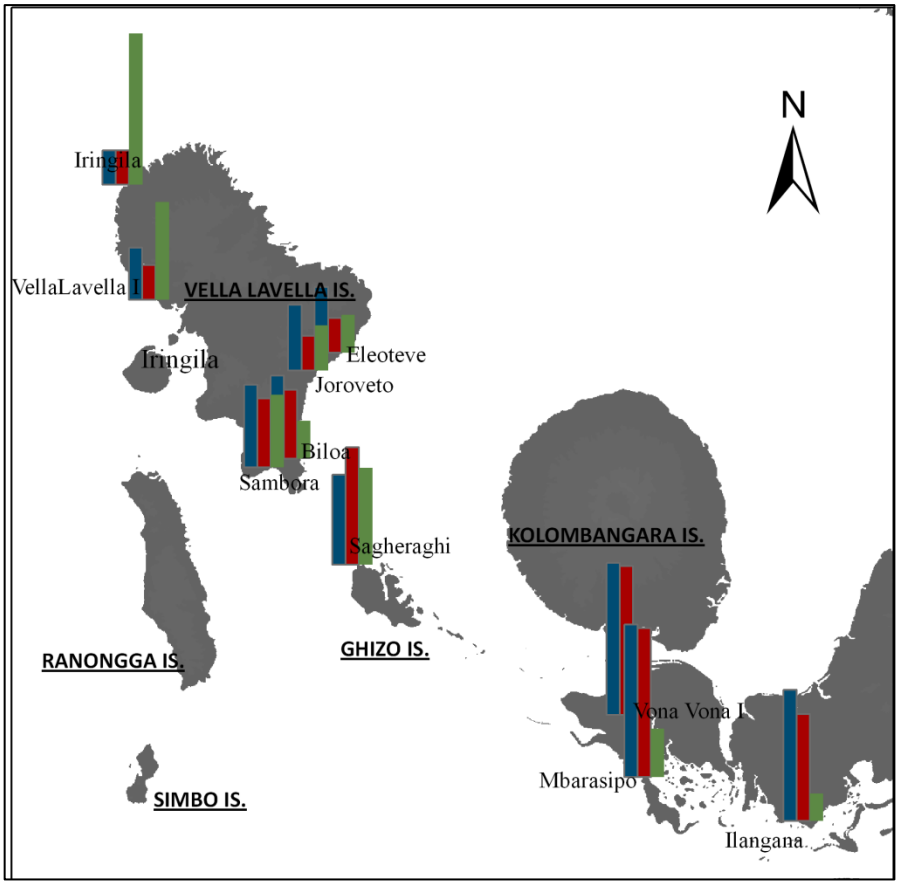

Figure 22. Wave height comparison in selected sites.
(Legend Colours: 8.1Mw Blue, 8.0Mw Red, mesurements Green)

5.3 Code to code comparison with Tanioka model [900 m resolution grid]

A comparisons of the propagation waves simulated by various codes, Swan-JRC, HYFLUX2 and TUNAMI-N2, have been performed. A resolution of 0.5 min (900 m) was used for the simulations (Fig. 23). The Tanioka model was used to initialize the crust deformation.

Six locations (sensors S) were selected for this analysis and are shown in the following figures. Amplitude and arrival times are very similar in HYFLUX2 and SWAN-JRC calculations, while time is different for TUNAMI-N2 calculations which is delayed in respect to the previous codes. The sea level trends are similar although for HYFLUX2 the sea level curve is always smoother. (Fig. 24-30).

At location S1 the first wave is negative for all the codes and the maximum wave height is about 40 cm at about 30 min. Sea level trend off shore (sensor S3) resulted with TUNAMI-N2 is very oscillatory. Sensor 5 located off shore is very consistent among the codes except that the trend of the TUNAMI-N2 is more oscillatory.

In all the cases a main first wave is present followed by a second smaller wave. The highest calculated sea level trend is close to the epicenter, on Rendova island.

In terms of CPU time HYFLUX2 processing time was 4 hours 59 minutes, the numerical code SWAN-JRC duration for this simulation was 0.5 hour and the TUNAMI-N2 numerical code duration was 0.8 hour (48 minutes).

EPICENTER:

Epicenter- Lat -8.655° Lon: 157.0°

Center- Lat: -8.25° Lon: 156.8°
Magnitude: 8.1
Date tsunami: 4/1/2007 8:40:38 PM

FAULT PARAMETERS:
Flenght: 100 km
fwidth: 35 km
strike: 315° (geog North=0)
slip: 7 m
dip: 35°
rake: 90 °

CALCULATIONS PARAMETERS:

FinTime: 1 hr

Tsave: 1 min
dtMax: 0.5 s
fanning: 0.015

GRID PARAMETERS:
Width: 2.5° Batgrid: 0.5 min
Lonmin154.3° Lonmax: 159.3°
Latmin: -10.75° Latmax: -5.75°
Bathymetry: SWAN

Table 4. Simulation main parameters [Tanioka proposed fault]

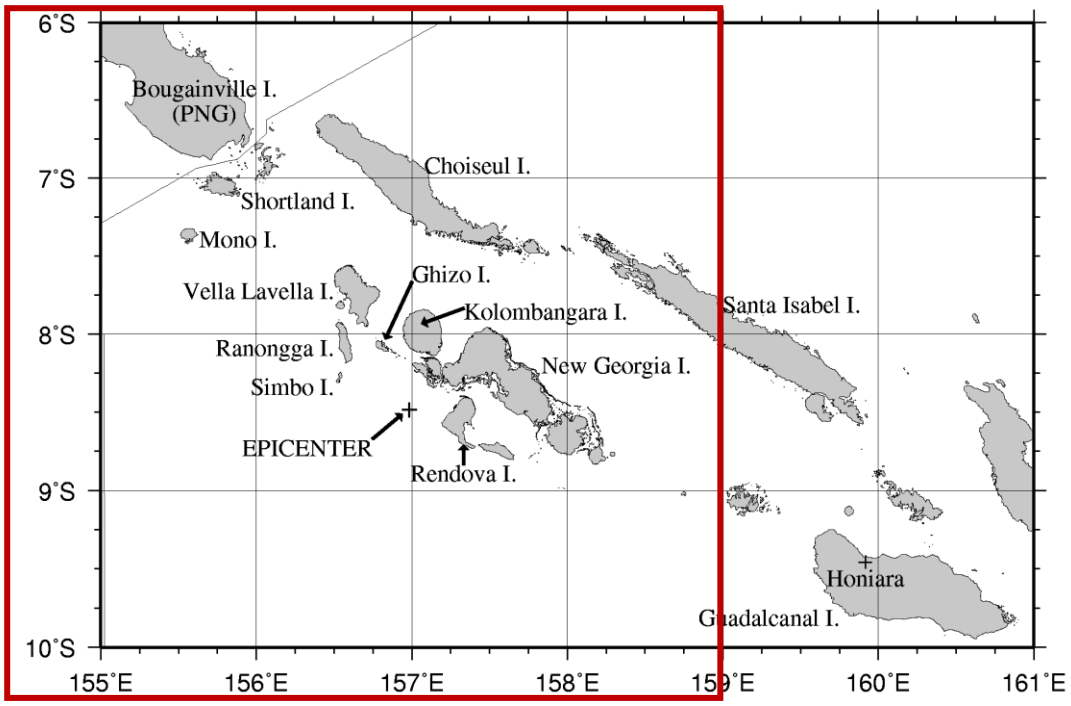

Figure 23. Grid delimitation [red -900 m bathymetry resolution-].

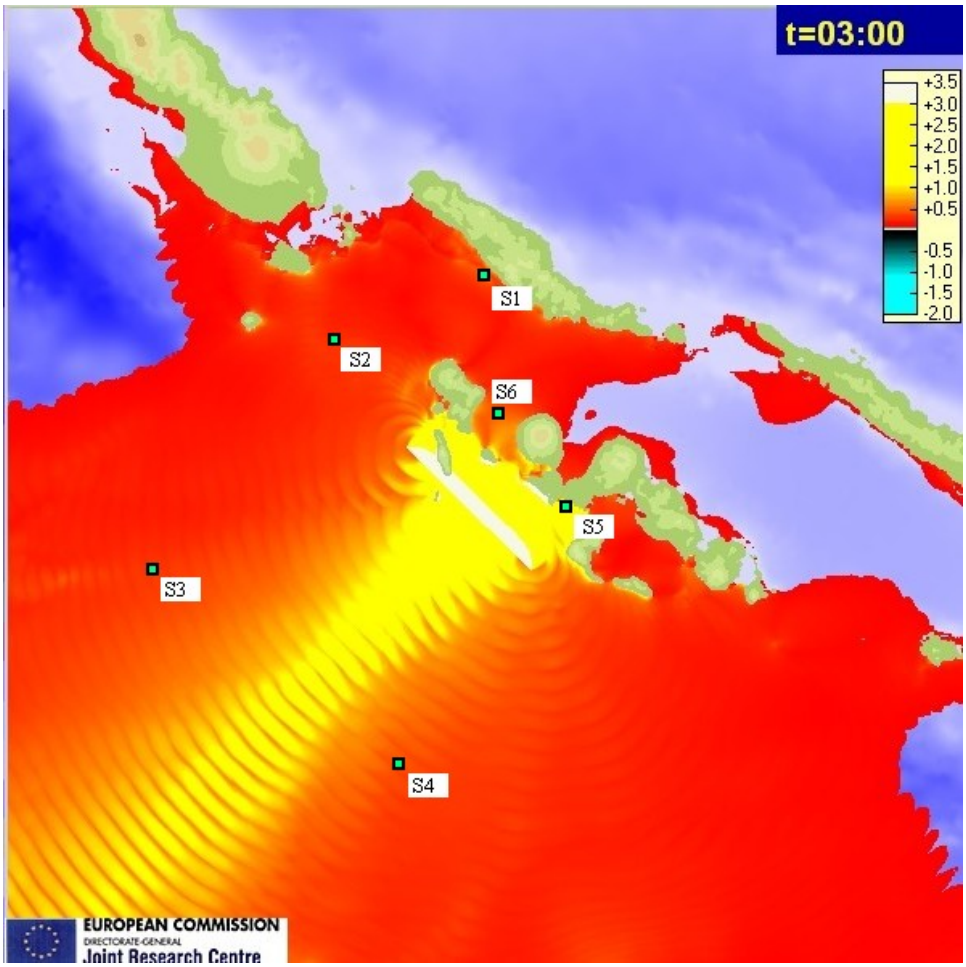

Figure 24. Sensor location [900 m resolution grid].

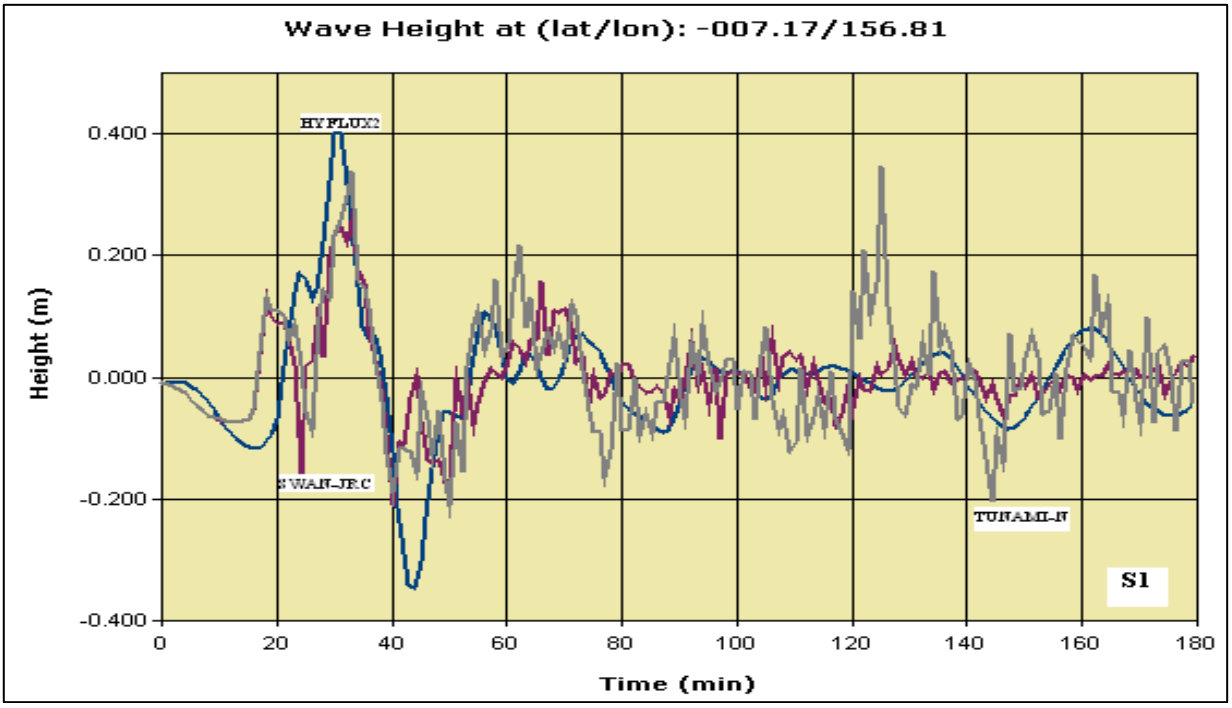

Figure 25. Calculations at S1 done with 900 m resolution. HYFLUX2 (blue), SWAN-JRC (pink) and TUNAMI-N2 (grey).

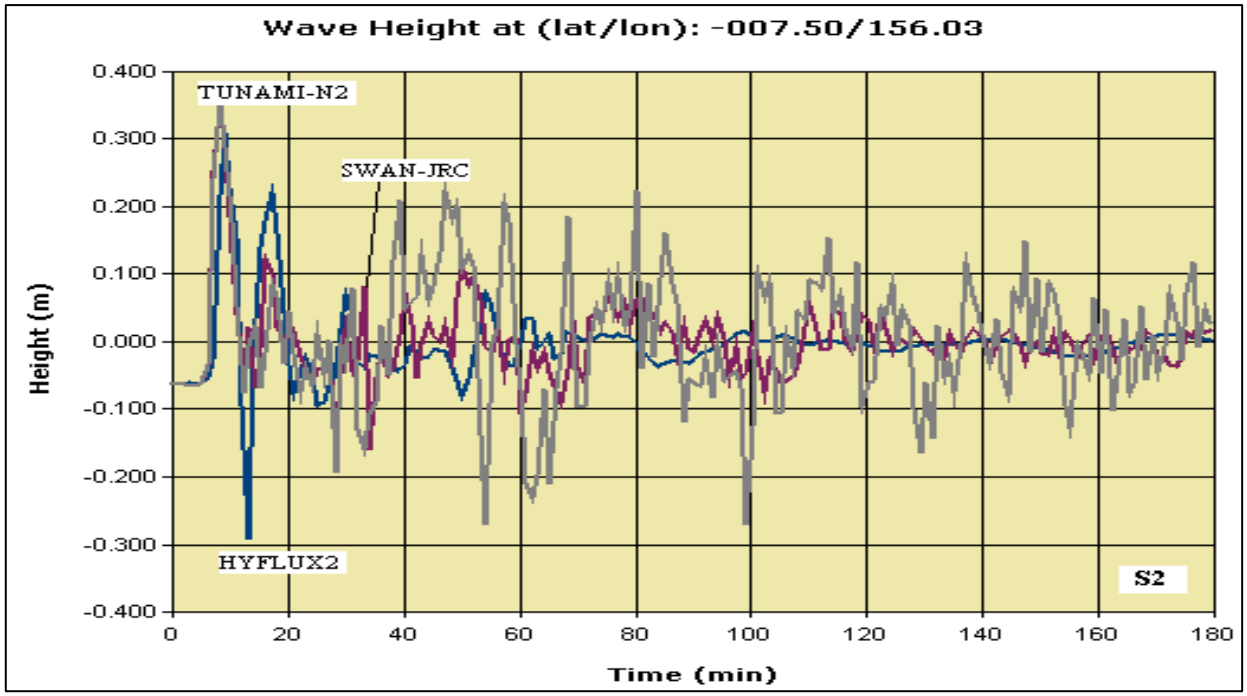

Figure 26. Calculations at S2 done with 900 m resolution. HYFLUX2 (blue), SWAN-JRC (pink) and TUNAMI-N2 (grey).

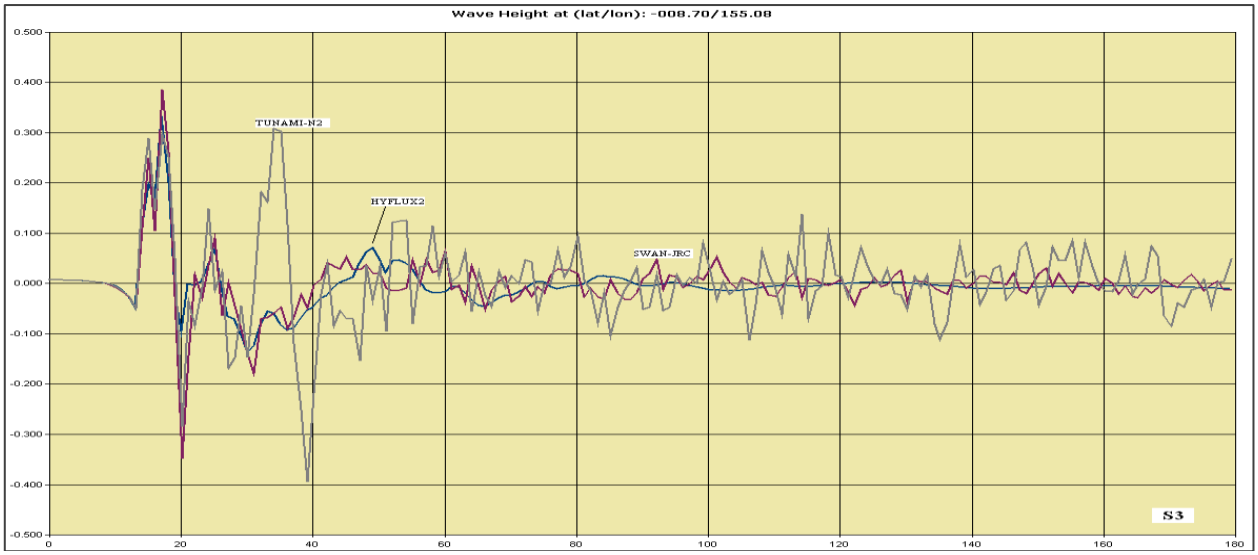

Figure 27. Calculations at S3 done with 900 m resolution. HYFLUX2 (blue), SWAN-JRC (pink) and TUNAMI-N2 (grey).

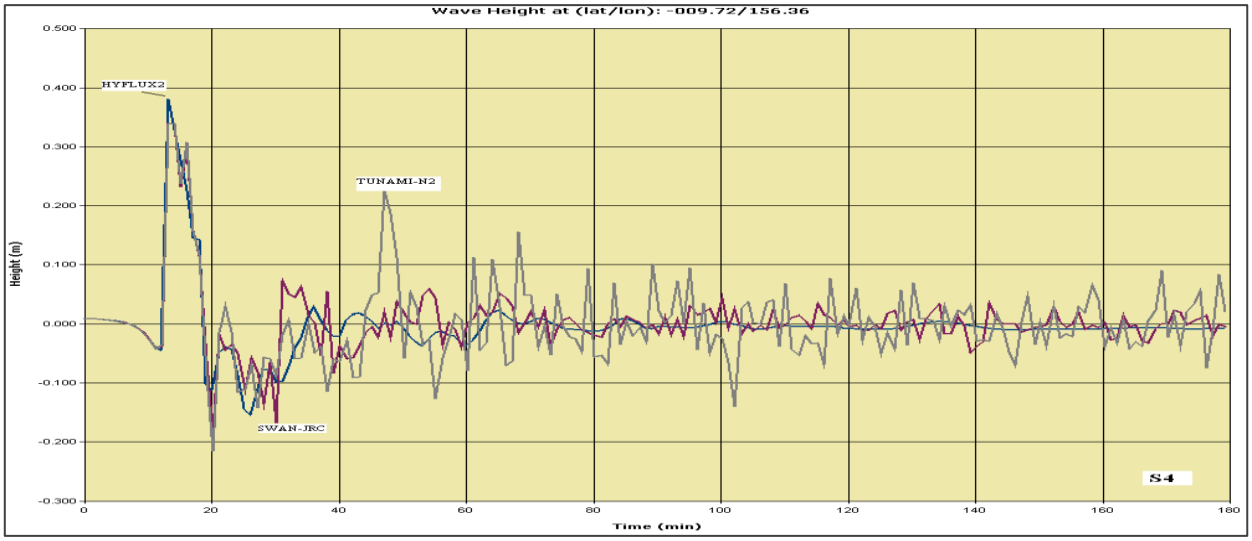

Figure 28. Calculations at S4 done with 900 m resolution. HYFLUX2 (blue), SWAN-JRC (pink) and TUNAMI-N2 (grey).

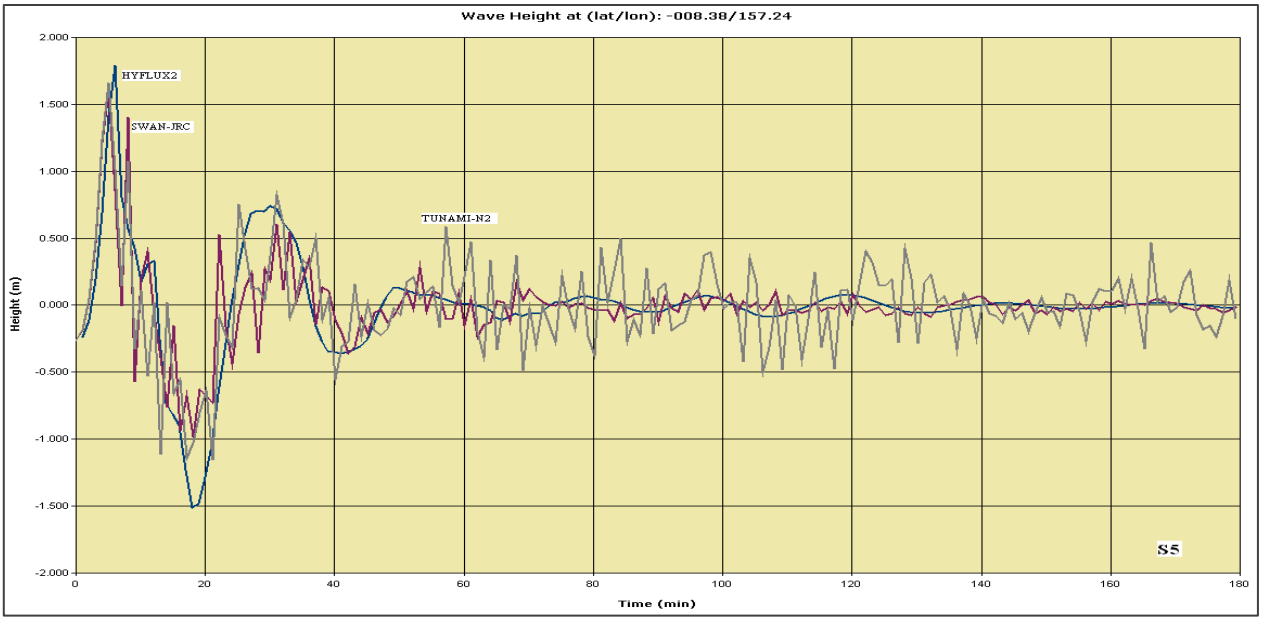

Figure 29. Calculations at S5 done with 900 m resolution. HYFLUX2 (blue), SWAN-JRC (pink) and TUNAMI-N2 (grey).

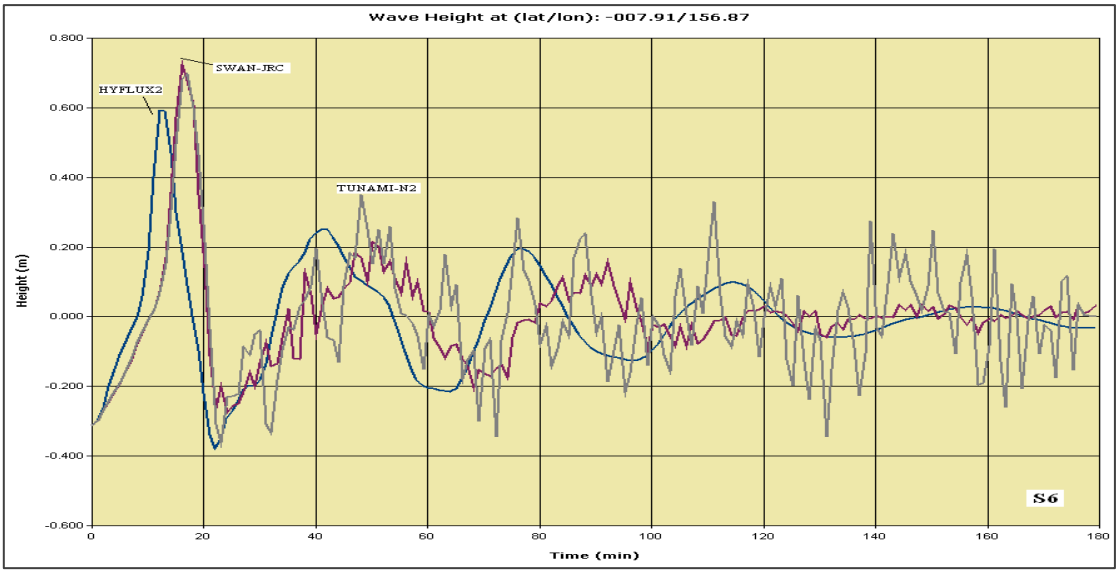

Figure 30. Calculations at S6 done with 900 m resolution. HYFLUX2 (blue), SWAN-JRC (pink) and TUNAMI-N2 (grey).

The ratio (HYFLUX2 code/ SWAN-JRC code) between the simulated maximum wave heights at the analyzed locations is 0.732 (Fig. 31). The ratio between the simulated maximum wave heights - calculated with HYFLUX2 and TUNAMI-N2 codes - is 0.5. The greater sea level height estimated by SWAN_JRC code and TUNAMI-N2 code in respect to HYFLUX2 can be explained by the fact that such finite difference codes show oscillations which increase near-shore. As can be seen in Figures 25 to Figure 30 the higher predicted wave height is given by TUNAMI-N2

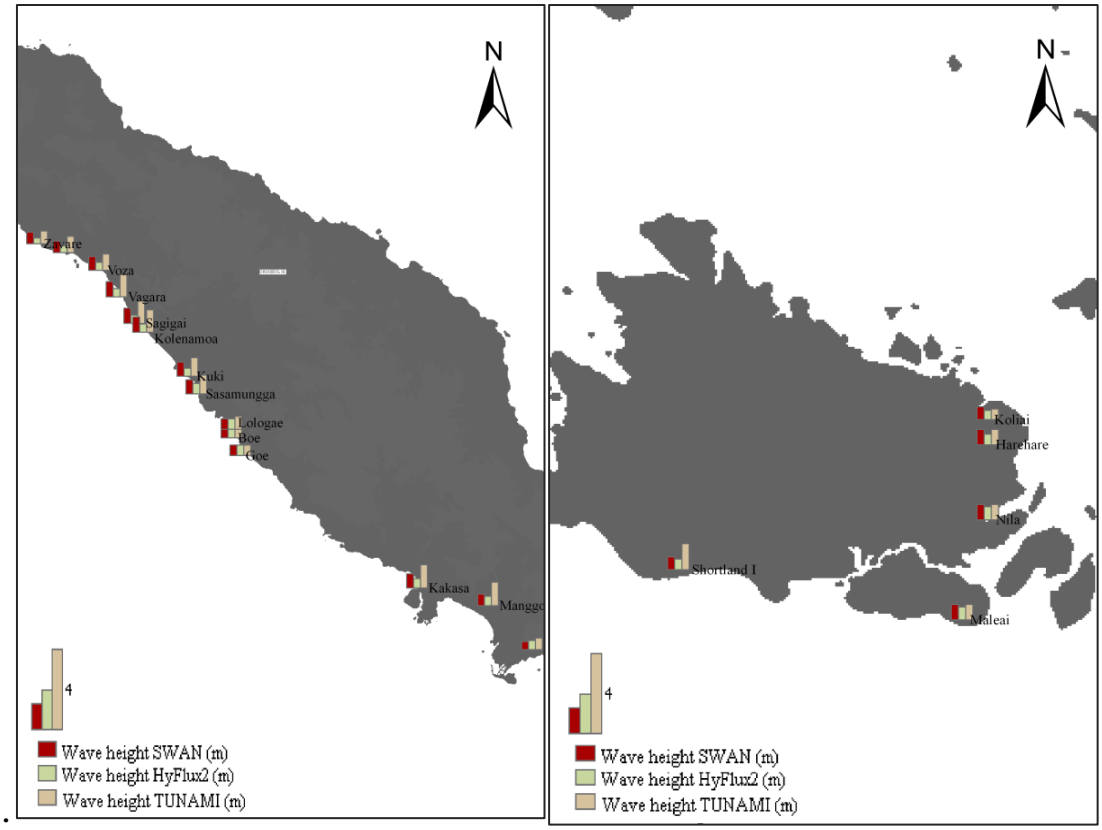

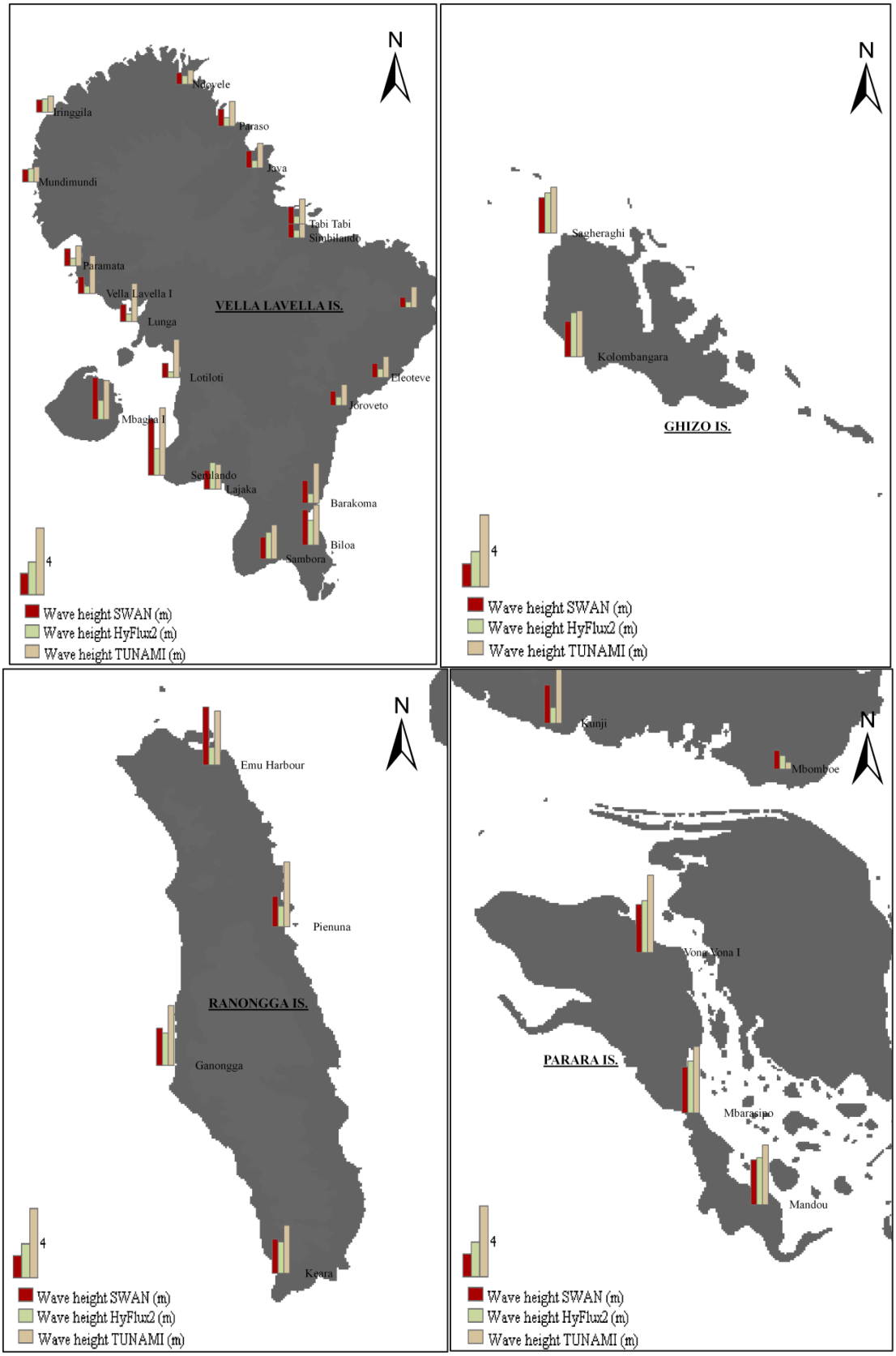
N
Ndovele
Iringgila
Paraso
Jaya
Mundimundi
Tabi Tabi
Shubilando
Paramata
Vella Lavella I
VELLA LAVELLA IS.
Lunga
Lotiloti
Eleoteve
Joroveto
Mbaghia I
Seghilando
Lajaka
Barakoma
Biloa
Sambora
4
Wave height SWAN (m)
Wave height HyFlux2 (m)
Wave height TUNAMI (m)
N
Sagheraghi
Kolombangara
GHIZO IS.
4
Wave height SWAN (m)
Wave height HyFlux2 (m)
Wave height TUNAMI (m)
N
Emu Harbour
Pienuna
RANONGGA IS.
Ganongga
Keora
4
Wave height SWAN (m)
Wave height HyFlux2 (m)
Wave height TUNAMI (m)
N
Kunji
Mbomboe
Vona Vona I
PARARA IS.
Mbarasipo
Mandou
4
Wave height SWAN (m)
Wave height HyFlux2 (m)
Wave height TUNAMI (m)

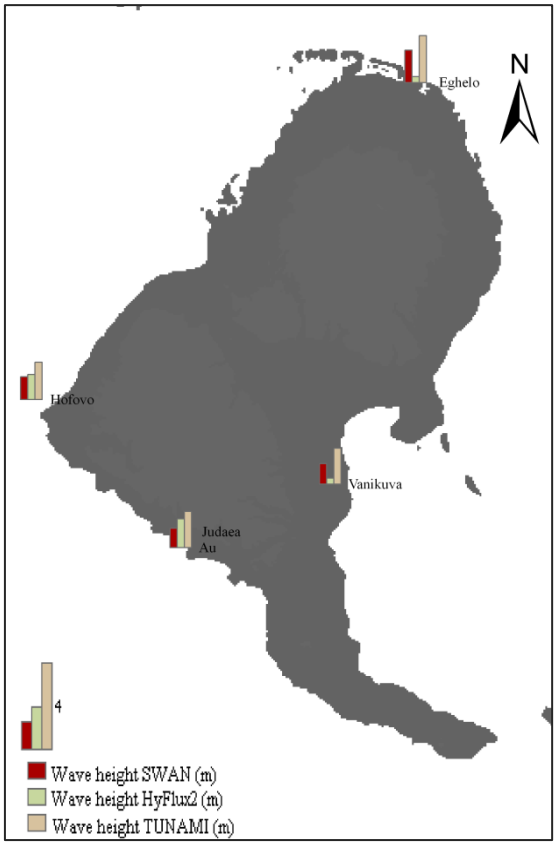

Figure 31. Location of wave heights resulted from 3 codes using the Tanioka fault parameters.

6. INUNDATION CALCULATIONS [300 m resolution]

The aim of this section is to evaluate in more detail the local sea level trends to make comparisons with the measured field data. When the wave reaches shallow water its length becomes shorter and the amplitude increases. Such phenomena are emphasized in the bays, where reflection and resonance took place. Therefore in order to describe with more details the wave, the adopted grid size resolution must be higher. Consequently, a grid size in the order of 10-30 m is requested if an inundation impact assessment is intended. In other report (Franchello et al., 2010) it was shown that a 30 m grid size resolution could have noticeably improved the simulation, providing information on the inundation extent. However, in the above mentioned report it was shown that the simulation performed at 300m grid size resolution allowed to evaluate the maximum wave height at the shoreline with an acceptable accuracy, providing also an indication on which are the localities where inundation were occurred.

Unfortunately the best resolution of available data on bathymetry and topography on a global scale is 30 arc sec (~ 900 m). The interpolation of the available DEM to very low grid size (i.e. lower tan 100 m) does not make sense, considering that the elevation of hills and bays of size lower than 1 km are averaged to 1 point. A compromise for inundation simulations can be 300 m grid size (Fig. 32), which is interpolated from the 900 m available information. With such resolution the wave length at the shore is quite well represented, but the information on run up distance and inundation extent are quite poor when the measured values are lower than the chosen 300 m grid size. Therefore, despite the onsite survey provided detailed information on horizontal inundation and run up distance (which is always lower the 300m), the bathymetry grid is still a limitation for a real inundation assessments. Therefore, in the present section the field measurement data are compared with the calculated wave height at the shoreline.

The fault parameters are based on the previously described Tanioka Model (Tomita et al., 2008) while the HYFLUX2 code has been used for these calculations (Franchello, 2009). Three nested simulations have been performed as indicated in the figure below: the simulation results at 900 m grid size resolution (the bigger window) are used as boundary conditions of the simulations with 300 m grid size (smaller windows).

The comparison with the simulated results and the inundation field measurements have been done by setting a 1 km search radius of the maximum values inland. Since the best resolution used for this calculations is 300 m, and the maximum inundation distance reported is 200 m (at Rendova Is.), analysis for horizontal inundation cannot be carried out in detail.

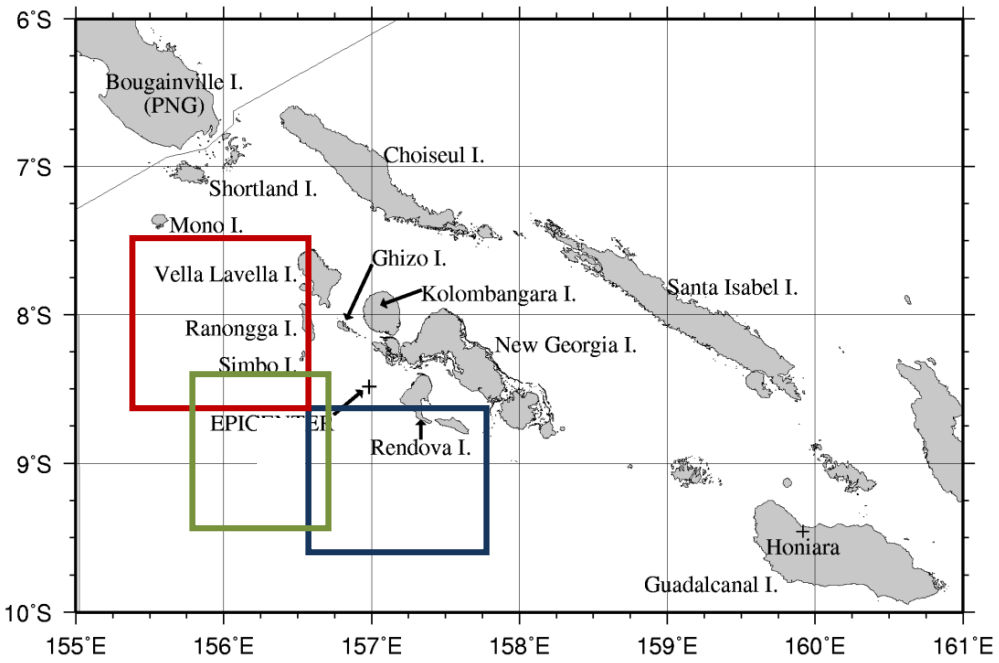

Figure32. Delimitation of simulations at 300 m bathymetry resolution.

8.1 Grid I: Vella Lavella, Ranongga and Gizo

The maximum simulated sea level is represented in figure 33. The maximum water height value at the shoreline is 7.5 m SE of Ranongga Island.

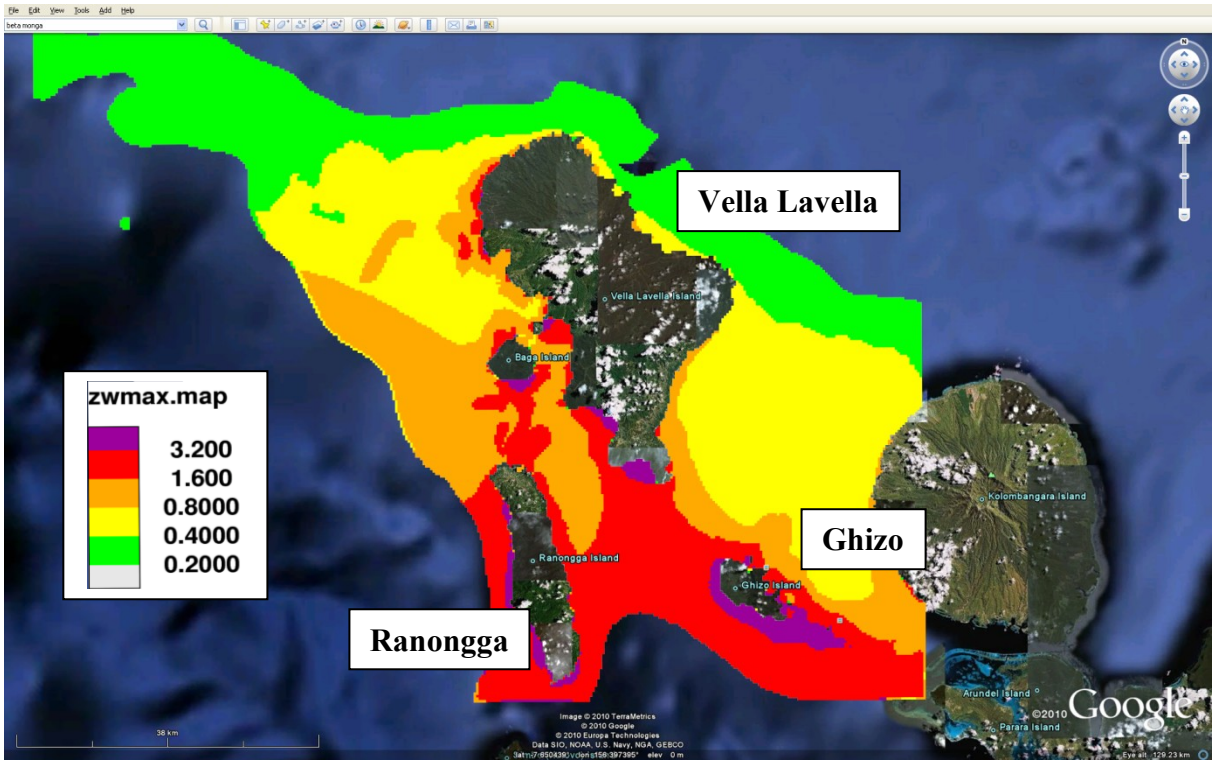

Figure 33. Grid I - Simulated Maximum sea level

❖ **Vella Lavella Island**

The island was severly affected by the tsunami, mainly the town of Iringgila located N-NW of Vella Lavella Island. According to Tomita et al (2008) the inundation height measured on the field was 4.37 m and inundation depth on the ground level was 2.90 m.

In several sites of Vella Lavella Island (Fig 36), the HYFLUX2 code calculations results are in good agreement although detailed bathymetry resolution is still a strong constraint for the tsunami impact analysis. As shown (Tomita et al., 2008), the local change of tsunami height around Iringgila is probably attributed to the complicated bathymetry and topography. As it was described (Tomita et al., 2008) very shallow water area in front of the village may have converged energy of tsunami generating high local tsunami height.

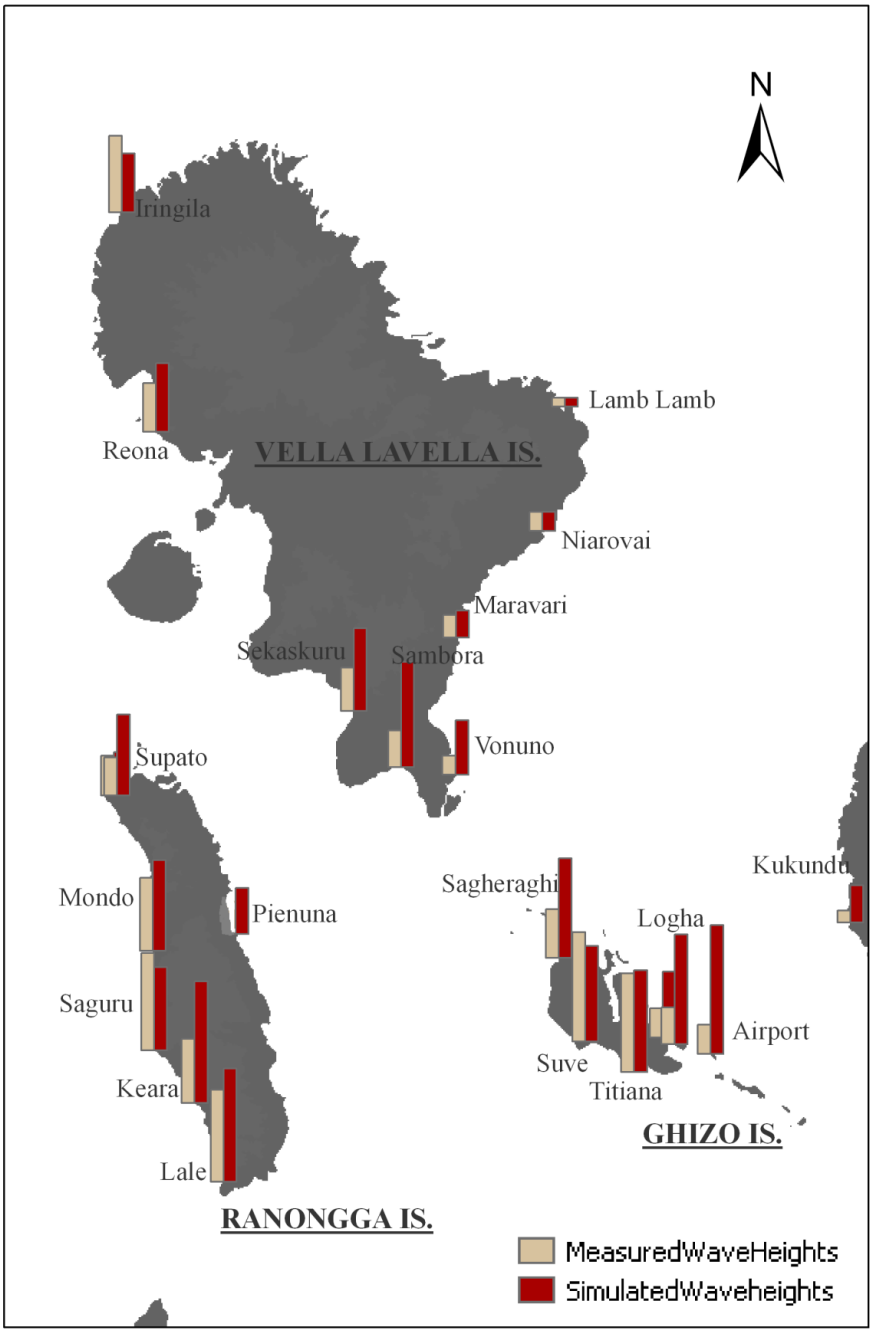

Figure 34. Maximum wave height comparison.

The difference between the maximum wave height measured on the field and the wave height at the shoreline obtained with HYFLUX2 varied for more than 1 meter. The average ratio between simulated and measured data is 1.3, i.e., the code overestimate at several sites (Fig.37). Although the poor DEM resolution used for the simulations, the overall comparisons for these sites has an acceptable behaviour.

Maximum measured inundation distance is 124 m for Vella Lavella Island, which is much lower than the grid size resolution of 300 m.

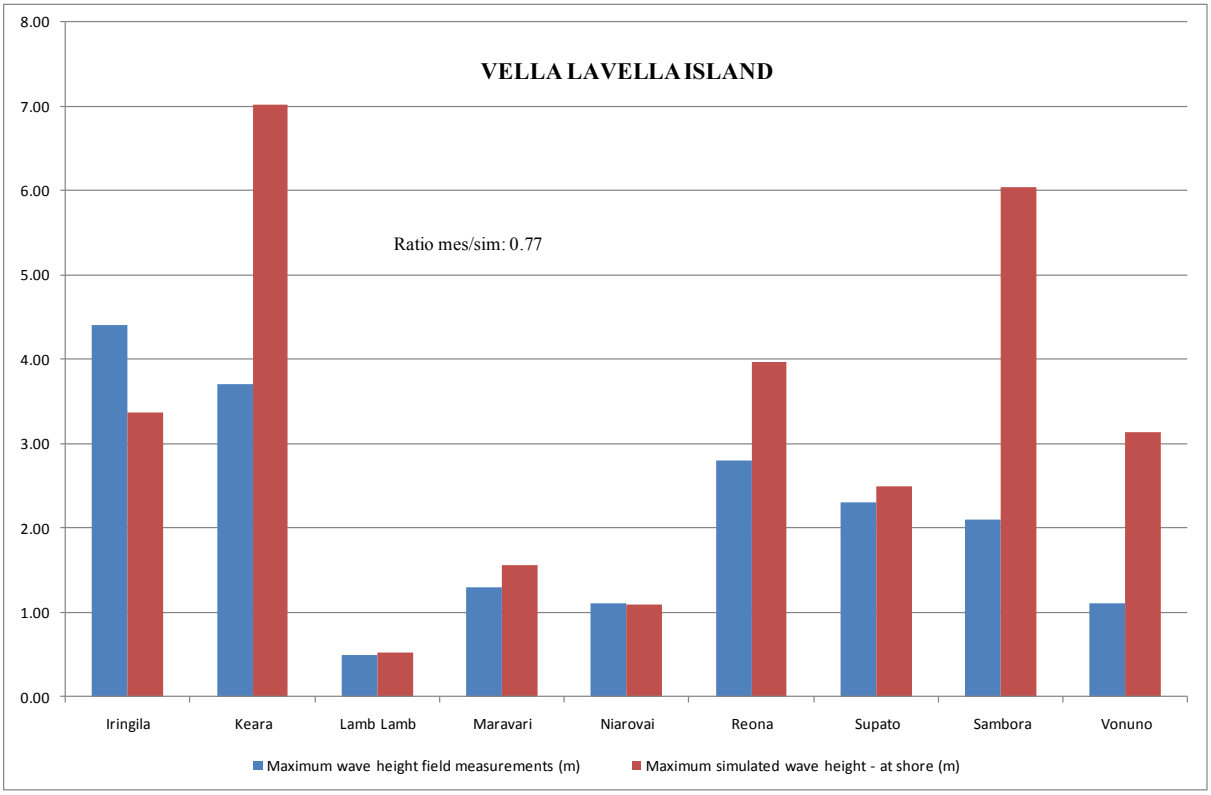

Figure 35. Vella Lavella Isl. Maximum wave height simulated with HYFLUX2 (red) compared with field measurements. (blue)

❖ Ranongga Island

This island was one of the most affected by the earth quake and tsunami. The ground uplifting values range from about 0.9 m (Vori and Vori Point) to about 3 m (Lale).

The tsunami run up and inundation heights ranged from about 1.9 (Vori and Koriovuku) to about 5.5 m (Lale) from north to south, except for a measurement of 5.6 m at Saguru located on the west coast in the middle of the island. At Lale ground uplift and wave heights were the highest of Ranongga Island (Fig. 36). The ratio between simulated and measured data is 1.5.

The main differences on wave amplitudes appear to be at VoriVori, where according to observed images, reefs appear to be very shallow. Herein, the resolution and local site effects might be giving an overestimation of wave height calculations because the higher friction due to the reef has not been taken into account. In addition, the maximum inundation distance of 131 m was measured in Keara.

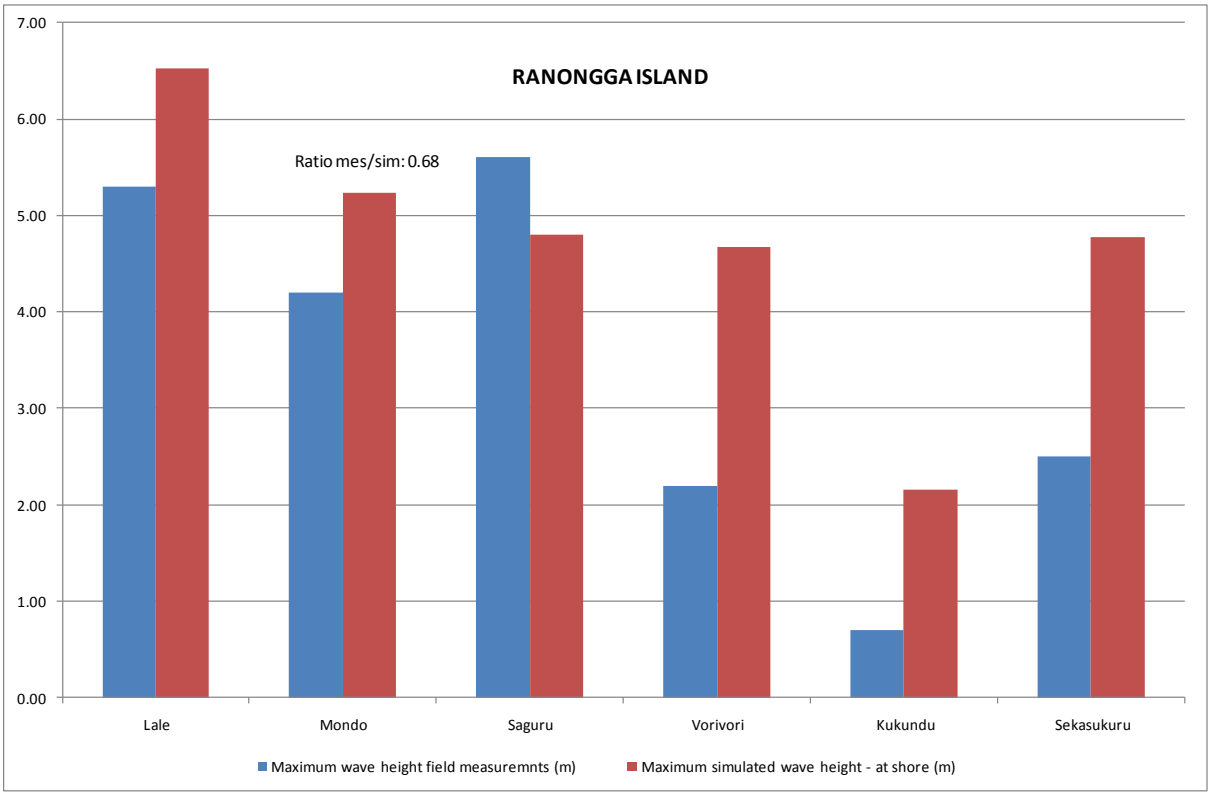

Figure 36. Ranongga Isl. Maximum wave height simulated with HYFLUX2 (red) compared with field measurements. (blue)

❖ **Ghizo Island**

This island is located about 45 km NW of the epicentre (Fig. 32). The southern coast of Ghizo was strongly affected by high tsunami waves that had a maximum inundation distance measured in Ghizo Island of 128 m. The maximum run up measured at Ghizo Island was in the site of Titiana (8.92 m), where almost no houses were destroyed by earthquake, but 10 people were killed by the tsunami (Tomita et al., 2008).

In this island the calculations have given different results when comparing with field data (Figure 37). The ratio between simulated and calculated data is 1.7.

Figure 37. Ghizo Isl. Maximum wave height simulated with HYFLUX2 (red) compared with field measurements. (blue)

8.2 Grid II: Simbo Island.

This calculation includes Simbo Island (Fig. 38) and some details of south Ranongga and Ghizo Islands. The highest wave heights are simulated between 7m to 8 m in Simbo Island and SW Ranongga Island.

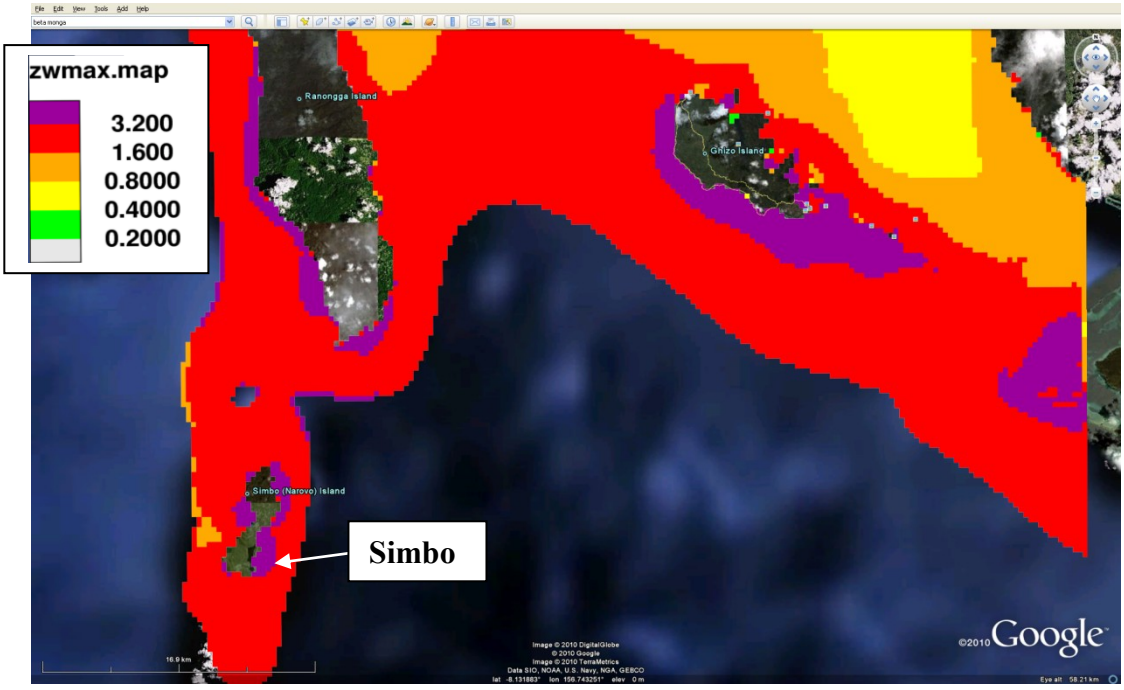

Figure 38. Grid II - Simulated Maximum sea level

- **Simbo Island**

The highest ground subsidence was measured at Simbo Island (3.2 m). In addition, the highest run up value (10 m) was measured in Tapurai, the northernmost tip of Simbo Island. This island was strongly affected by the tsunami that killed people and swept away all houses. Field measurements on Tapurai described widespread damage; in this site all structures were destroyed by a possible higher turbulence due to local bathymetry influence (Fritz and Kalligaris, 2008). The maximum inundation distance of 175 m at Simbo Island was measured in Lengana.

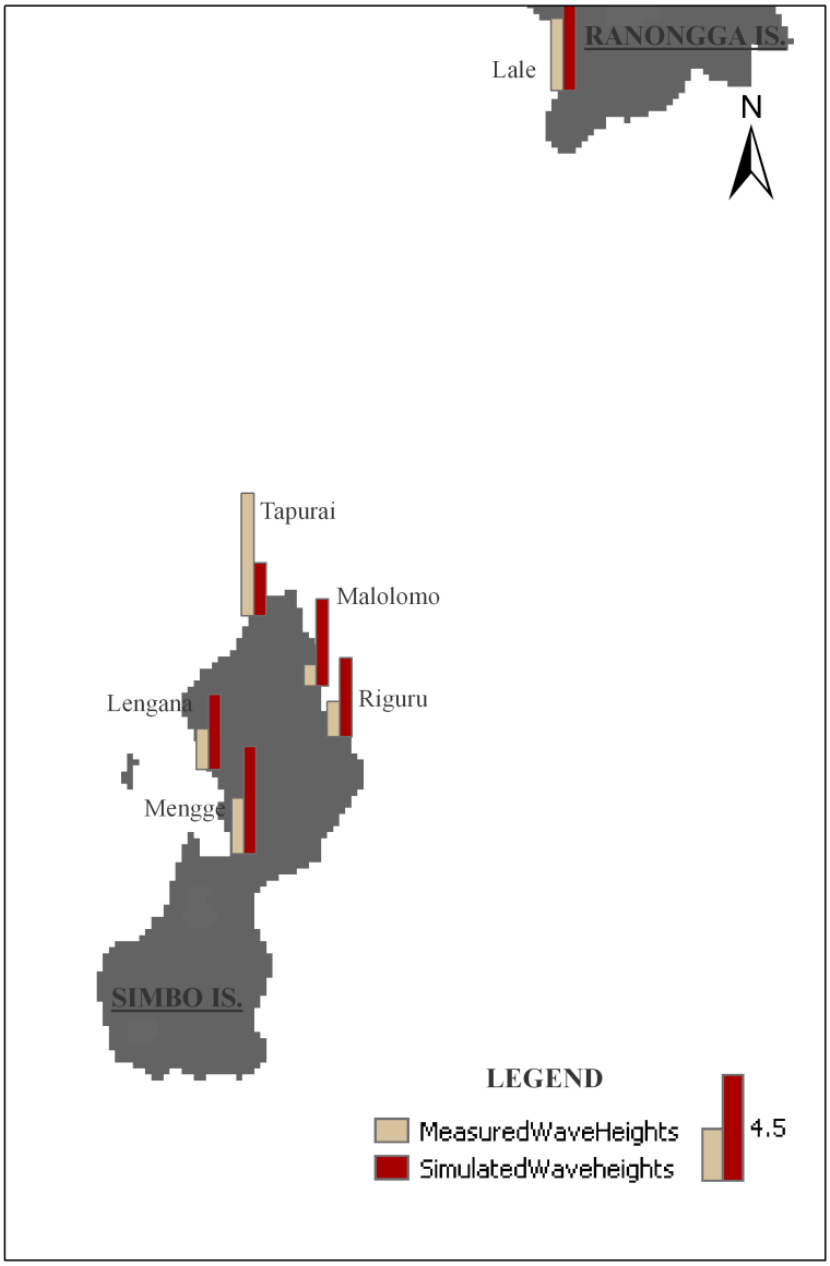

a. Maximum wave height comparison.

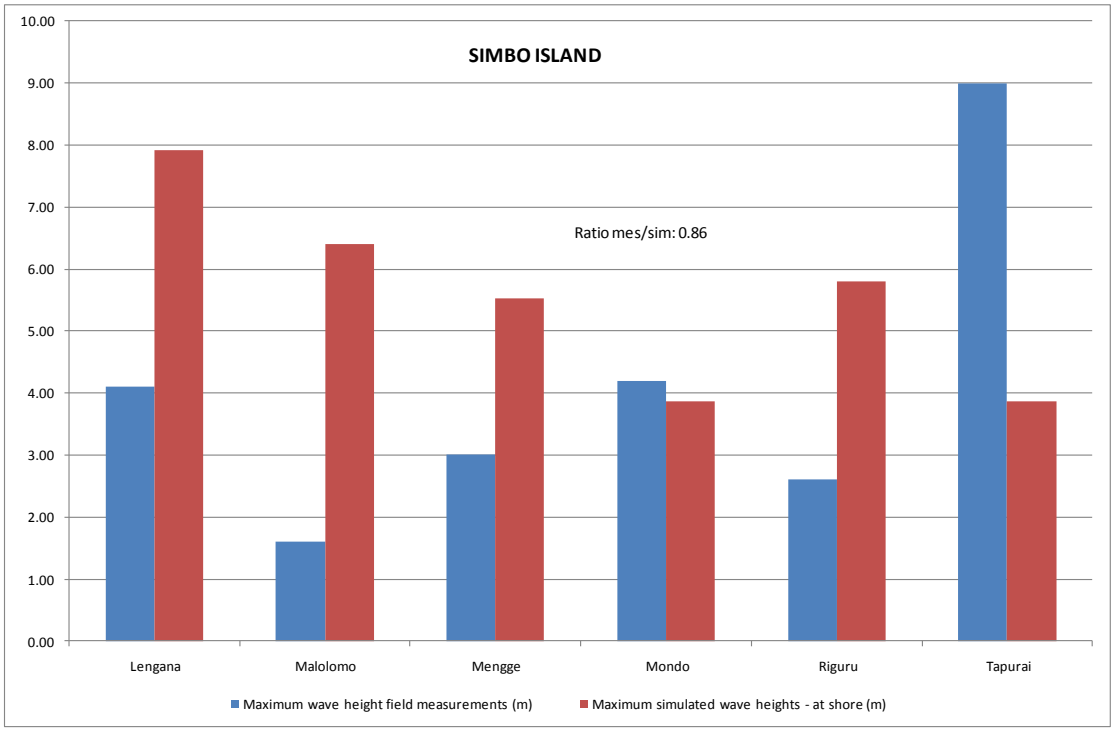

b. Comparison of waves of Simbo Island.

Figure 39. a. Selected sites to be compared b. Comparison of waves of Simbo Island.

8.3 Grid III: Rendova, New Georgia and Parara Islands.

This calculation includes a detail of south Parara, Rendova and New Georgia Island. The highest wave heights are simulated between 7m to 8 m in Parara Island and SW Ranongga Island (Fig. 40).

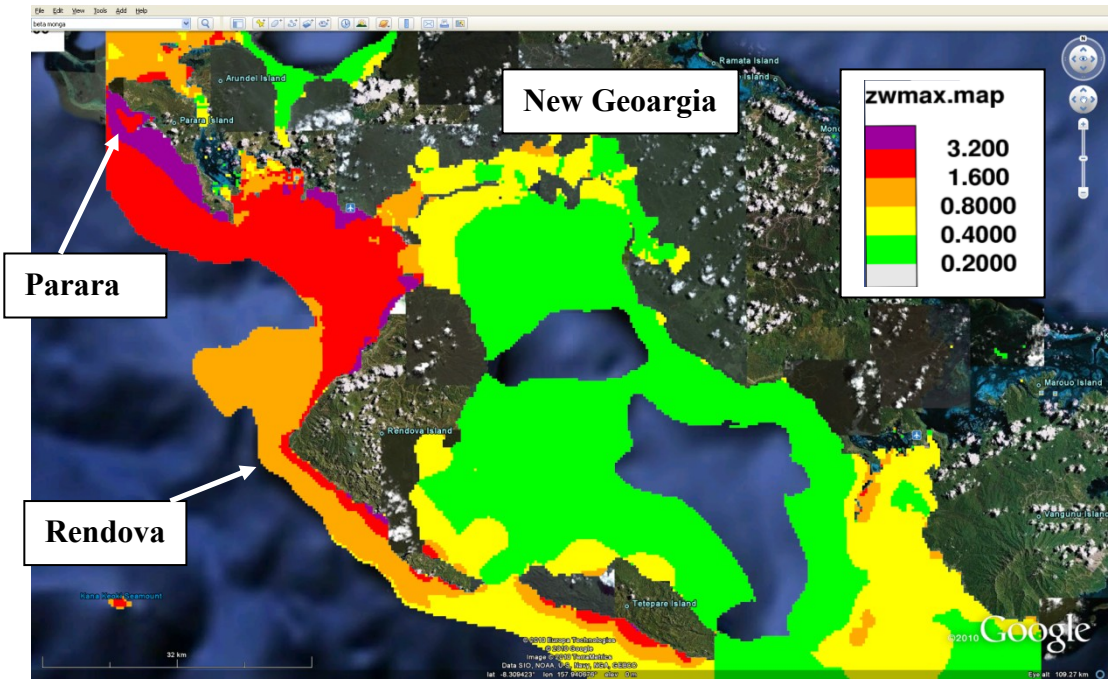

Figure 40. Grid III – Simulated Maxim Sea level.

❖ Rendova Island

This island is on the eastern boundary of the deformation area. This calculation indicated important differences with the field measurements. This site was less studied in the field and the

differences in the amplitudes at Givusu, Vunerima, Munda2, Kenelo and Randuvu could have several explanations in the local bathymetry behaviour. In addition, further analysis of the friction coefficient could be done to understand why this big differences. The maximum inundation distance of 204 m was measured at Randuru in Rendova Island. The ratio between simulated and measured data is 1.56 (Figs. 41, 42).

- **New Georgia Island**

In this side of the island reefs have developed 800 m and 3000 m offshore along the south Munda coast; these reefs act as natural breakwaters. The measured inundation height was 1.05 m, while the simulated wave height at the shoreline was 7.1 m (Figs. 41,43). These values have a big bias from the measured one that could be related to the increased friction due to the reef. This friction has not been taken into account in these simulations. However if finer resolution bathymetry is found a higher friction should be considered.

- **Parara Island**

This island has few inhabitants, no witness description exist: however marks of wave heights were found. A run up height of more than 3.3 m was measured at Ndivulani, which is part of the chain of islands on the extending coral reef. The uplift of the ground was estimated at about 1m. A run up height of 1.3 m was measured at Rarumana, the village on the main island of Parara. The uplift at this site was estimated of 0.8 m. This village suffered no damage, maybe because the coast is sheltered by the extending reef and the ground was uplifted by the earthquake. The simulated maximum height is of the order of 8 m (Figs 41, 44).

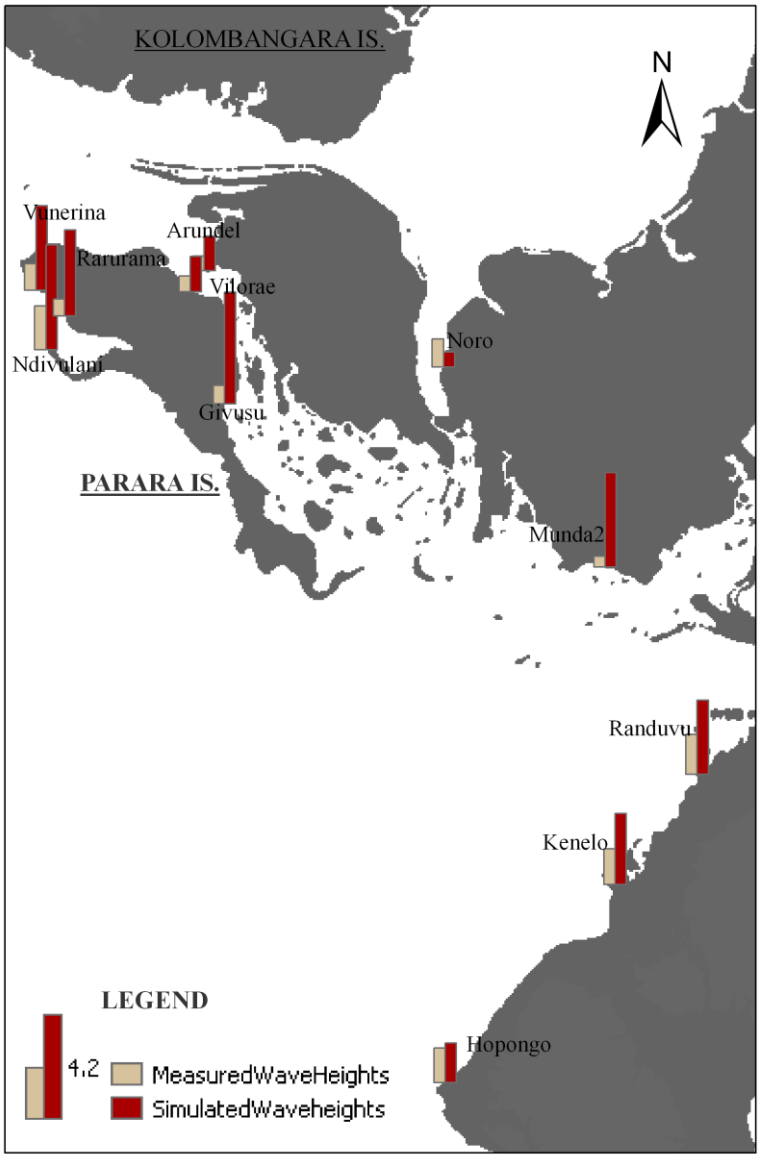

Figure 41. Wave heights calculations at Kolombangara Island, Rendova Island and Parara Island.

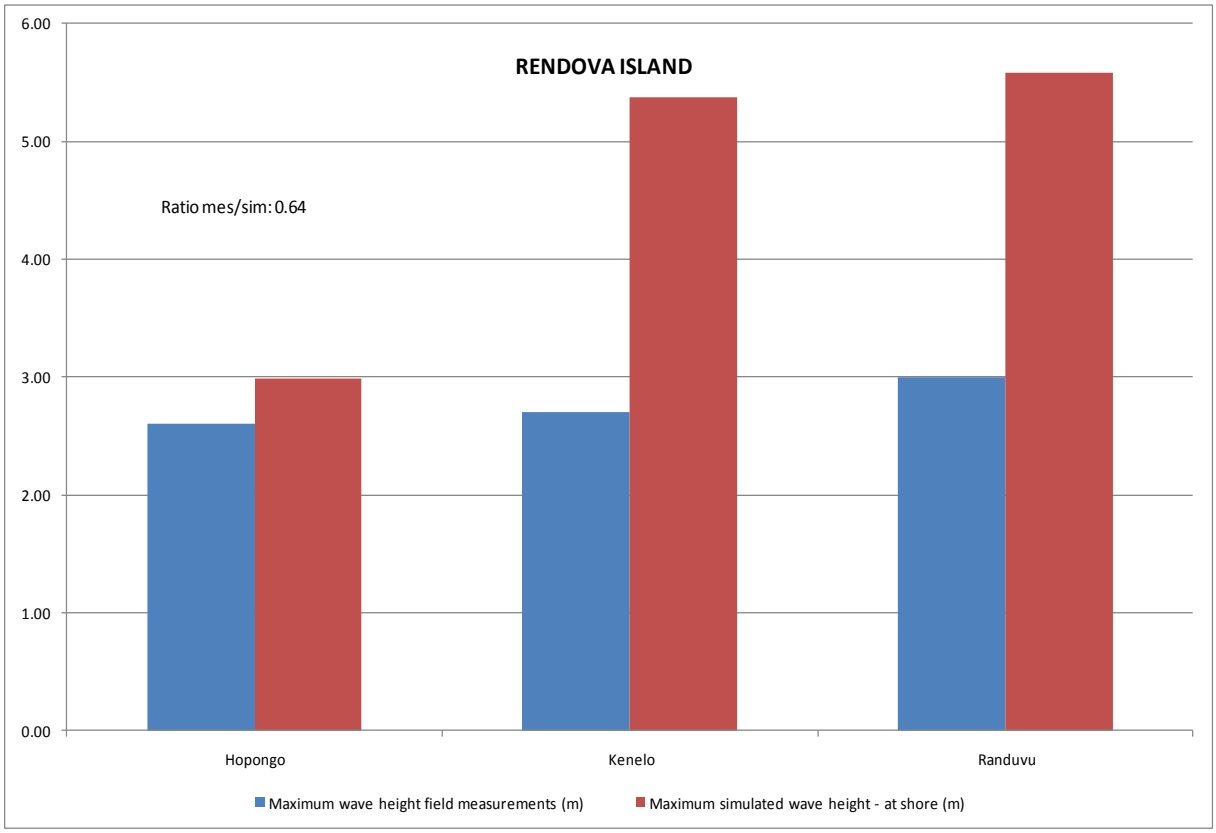

Figure 42. Wave heights calculations Rendova Island.

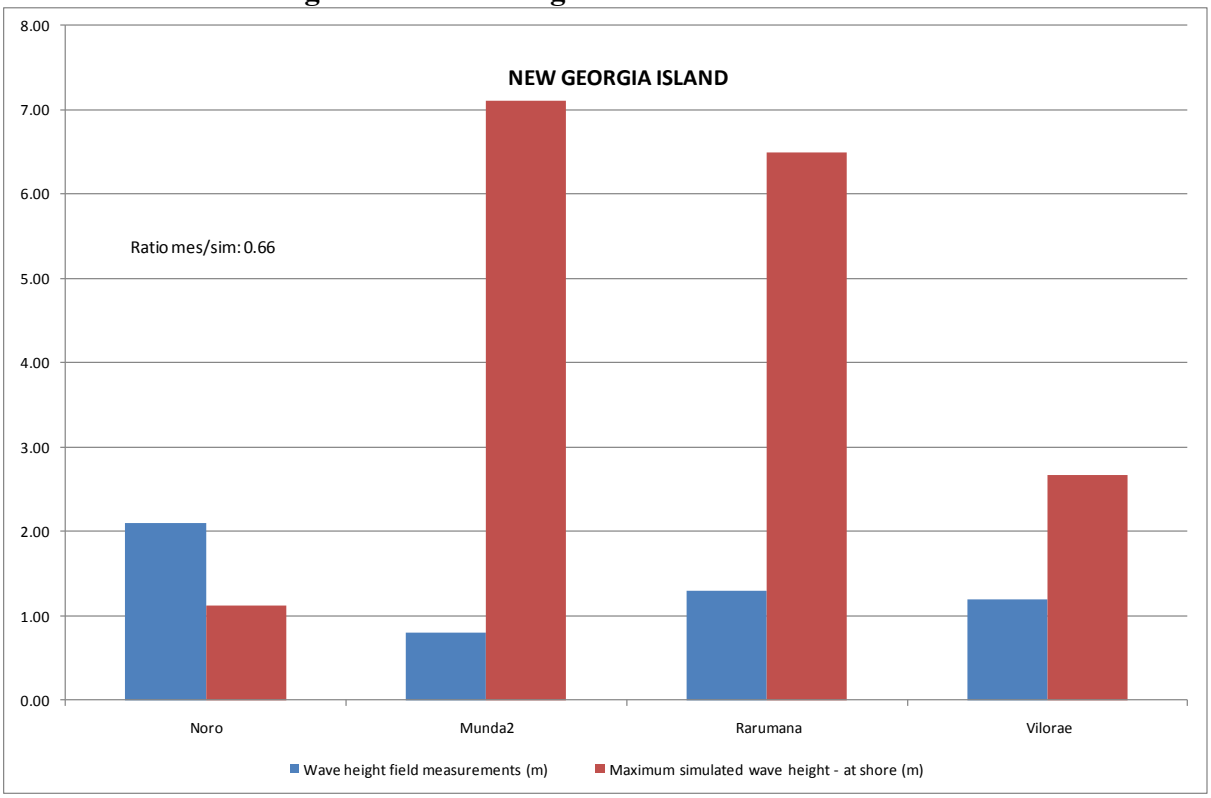

Figure 43. Wave heights calculations at New Georgia Island.

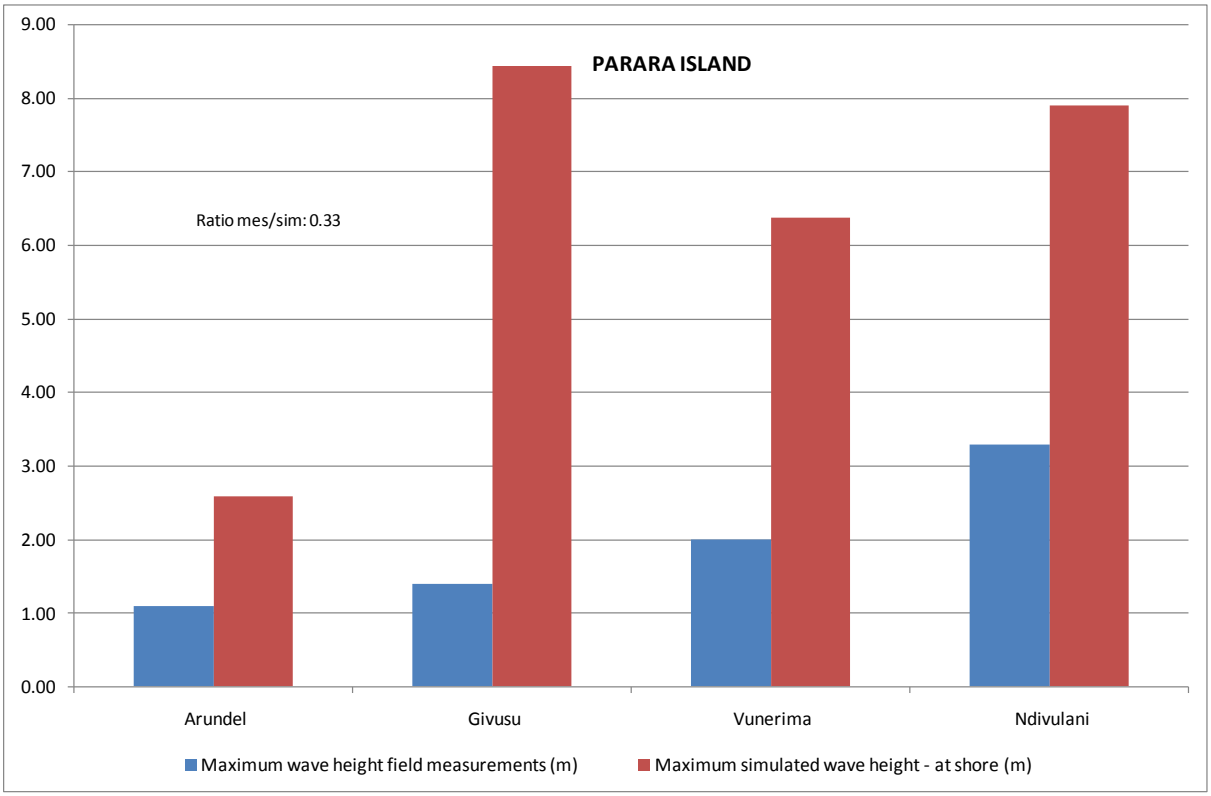

Figure 44. Wave heights calculations at Parara Island.

7. FINAL REMARKS

In this report the influence of the fault model on the coseismic deformation was studied by comparing modelling results with measured values. It was shown that none of the classical models were able to estimate correctly the measured value. The best comparison with experimental data is obtained using the fault mechanism parameters of the so called Tanioka model, obtained by fitting the surveyed measured data points. However, it should be noted that this type of parameters estimation can be available only after the field surveys are carried out.

The second part of the report was dedicated to assess the hydrodynamic models which are currently used at the JRC. Several codes were used with the initial boundary conditions provided by "Tanioka model". The main differences among the codes were related to the high oscillations present in finite difference methods codes when compared with finite volumes code. However, the overall behaviour of the simulations was rather similar and correctly identified most of the affected locations. We find that the resulted offshore wave heights are in good correlation for the three codes that were assessed.

In order to have a reliable sea level prediction on the coast it is necessary to use much finer nodalizations. This was done by using a 300 m resolution grid and the finite volume HYFLUX2 code was used for the simulations. A better bathymetry resolution could have even improved the results but it was not available. However, the simulation performed at 300m grid size resolution allowed to evaluate the maximum wave height at the shoreline, showing a quite good agreement with the measured inundation and run-up.

Finally, differences have been noticed within CPU time among the various codes. The CPU needed when using HYFLUX2 numerical code is higher than when calculations are performed with TUNAMI-N2 or SWAN-JRC. Activities are under way to improve the performance and to produce a parallel version of the code in order to get quicker results.

As a final remark, the fact that the Tanioka model was able to reproduce both the seafloor deformation as well as the sea level wave propagation, it gives more credit to the idea that if the deformation could be estimated accurately and be available immediately (i.e. with GPS online measurements), this would allow to have a more reliable early warning calculation. Of course GPS measurements can be available only in case of near-field crustal deformation, not offshore.

8. REFERENCES

Annunziato, A. 2005. Development and implementation of a tsunami wave propagation model at JRC. Fifth International Symposium on Ocean Wave Measurement and Analysis. WAVES 2005, Madrid 3-7 July 2005.

Annunziato, A. 2007. The Tsunami Assessment Modelling System by the Joint Research Centre. Science of Tsunami Hazards, Vol. 26, (2):

Briggs R.W., Sieh, K. E., Meltzner, A.J., Natawidjaja, D. H., Galetzka, J., Suwargadi, B.W., Hsu, Y., Simons, M., Hananto, N. D., Prayudi D. and Suprihanto, I. 2006. Deformation and slip along the Sunda megathrust in the great 2005 Nias-Simeulue earthquake. Science 311(5769): 1897- 1901.

Falck, C., Ramatschi, M., Bartsch, M., Merx, A., Hoeberechts, J. and Schmidt, G. 2010. Near real-time GPS applications for tsunami early warning systems. Nat. Hazards Earth Syst. Sci., 10, 181–189.

Franchello, G. 2008. Modelling shallow water flows by a High Resolution Riemann Solver. 2008. JRC Scientific and Technical Reports. EUR 23307 EN.

Franchello,G. 2009. Shoreline tracking and implicit source terms for a well balanced inundation model. *Int. J. Numer. Meth. Fluids* 2010; 63:1123–1146.

Franchello,G., Annunziato,A. 2010 "29 September 2009 Samoa Tsunami: Early Warning System and Inundation Assessment", paper submitted to Natural Hazard

Fritz, H., and N. Kalligaris (2008). Ancestral heritage saves tribes during 1 April 2007 Solomon Islands tsunami. *Geophys. Res. Lett. 35*, L01607, doi:10.1029/2007GL031654.

Furlong, K.P. *et al. 2009.* A Great Earthquake Rupture across a Rapidly Evolving Three-Plate Boundary. Science 324, 226.

Geist, E. L., Bilek, S. L., Arcas, D. and Titov, V. V. 2006. Differences in tsunami generation between the 26 December 2004 and 28 March 2005 Sumatra earthquakes. Earth Planets Space, 58**,** 185–193.Global CMT *www.**globalcmt**.org/* -

Imamura, F. 2006. Tsunami Modeling manual - TUNAMI-N2 (Tohoku University's Numerical Analysis Model for Investigation of Near Field Tsunamis ver. 2) http://www.tsunami.civil.tohoku.ac.jp/hokusai3/J/projects/manual-ver-3.1.pdf. (Accessed 15/02/2010).

Ji, C., Wald, D.J. and Helmberger, D.V. Source description of the 1999 Hector Mine, California earthquake; Part I: Wavelet domain inversion theory and resolution analysis, Bull. Seism. Soc. Am., 92, (4): 1192-1207, 2002.

Kagan, Y.Y., and Jackson, D.D., 1999, Worldwide doublets of large shallow earthquakes: *Bulletin of the Seismological Society of America*, v. 89, p. 1147-1155.

Lay, T. and Kanamori, H., 1980, Earthquake doublets in the Solomon Islands: *Physics of the Earth and Planetary Interiors*, v. 21, p. 283-304.

Lubis, A.M., and N. Isezaki (2009). Shoreline changes and vertical displacement of the 2 April 2007 Solomon Islands earthquake Mw 8.1 revealed by ALOS PALSAR images. *Physics and Chemistry of the Earth 34*:409-415, doi: 10.1016/j.pce.2008.09.008.

Mader, C. 1988. Numerical modelling of water waves, University of California Press, Berkeley, California.

Mader C. 2004. Numerical modeling of water waves. CRC Press – ISBN 0-8493-2311-8, 2004.

McAdoo, B. G., Jackson, K., Kruger, J., Bonte-Grapentin, M., Moore, A., Rafiau, W., D. Billy, and Tiano, B. 2007. Geologic Survey of the 2 April 2007 Solomon Islands Earthquake and Tsunami, UNESCO [Field Report].

McAdoo, B.G., Fritz, H., Jackson, K., Kalligeris, N., Kruger, J., Bonte-Grapentin, M., Moore, A., Rafiau, W., Billy, D. and Tiano, B. Solomon Islands Tsunami: One Year Later, *EOS,* Transactions, American Geophysical Union 89, no. 18, p. 169-170, 29 -04-2008.

McAdoo, B.G., Moore, A. and Baumwoll, J. 2009. Indigenous knowledge and the near field population response during the 2007 Solomon Islands tsunami. Nat. Haz. *48* (1):73-82, doi: 10.1007/s11069-008-9249-z.

Miyagi, Y., Ozawa, T. and Shimada, M. 2009. Crustal deformation associated with an M8.1 earthquake in the Solomon Islands, detected by ALOS/PALSAR. Earth and Planetary Sci. Lett., 287: 385–391.

NGDC http://www.ngdc.noaa.gov/hazard/hazards.shtml

NOAA website: http://nctr.pmel.noaa.gov/tda_documentation.html

Okada, Y. 1985. Surface deformation due to shear and tensile faults in a half-space. Bulletin of the Seismological Society of America. 75. 1135–1154.

Schwartz, S.Y., 1999, Noncharacteristic behavior and complex recurrence of large subduction zone earthquakes. Journal of Geophysical Research, 104: 111-125.

Schwartz, S.Y., Lay, T. and Ruff, L.J., 1989. Source process of the great 1971 Solomon Islands doublet. Phys. Earth Planet Int, 56: 294-310.

Sipkin, S.A., 1982. Estimation of earthquake source parameters by the inversion of waveform data: synthetic waveforms. Phys. Earth Planet Int. 30, pp. 242–259.

Song, T. Detecting tsunami genesis and scales directly from coastal GPS stations. Geoph. Res. Let., 34 L19602, DOI 10.1029/2007GL031681.

Shuto, N., Imamura, F., Yalciner, A.C. and Ozyurt, A. TUNAMI-N2 Tsunami modeling manual. http://tunamin2.ce.metu.edu.tr/

Titov, V.V. and Gonzalez, F.I. 1997. Implementation and testing of the Method of Splitting Tsunami (MOST) model NOAA Technical Memorandum ERL PMEL-112, 11 p.

Titov, V.V., Gonzalez, F., Bernard, E.N., Eble, M.C., Mofjeld, H., Newman, J.C and Venturato, A.J. 2005. Real-Time Tsunami Forecasting: Challenges and Solutions. Natural Hazards, 35: 41–58.

Report on Field Survey of Solomon Islands Earthquake Tsunami in April 2007. www.pwri.go.jp/eng/ujnr/joint/39/paper/22tomita.pdf

Tomita, T., Arikawa, T., Tatsumi, D., Honda, K., Higashino, H., Watabnabe, K., and Takahashi, S. 2008. Joint report for tsunami field survey for the Solomon Islands earthquake of April 1, 2007. Tsunami Engineering Report of Research, 25. www.pwri.go.jp/eng/ujnr/joint/39/paper/22tomita.pdf

Tanioka et al. 2007. Joint Report for Tsunami Field Survey for the Solomon Islands Earthquake of April 1, 2007. www.nda.ac.jp/cc/users/fujima/**solomon**-pdf/contents/contents-final.pdf

USGS, 2007.Preliminary Analysis of the April 2007 Solomon Islands Tsunami, Southwest Pacific Ocean. http://walrus.wr.usgs.gov/tsunami/solomon07/

Uslu, B., Y. Wei, H.M. Fritz, V. Titov, C. Chamberlin (2008). Solomon Islands 2007 Tsunami Near-Field Modeling and Source Earthquake Deformation, *Eos Trans. AGU, 89*(53), Fall Meet. Suppl., Abstract OS43D.

Ward, S .N., 2002. Tsunamis, Encyclopedia of Physical Science and Technology, Vol. 17, pp. 175–191, ed. Meyers, R.A., Academic Press.

Wei, Y. Uslu, B., H. M. Fritz, V. Titov, C. Chamberlin (in press). Solomon Islands 2007 Tsunami Near-Field Modeling and Source Earthquake Deformation, for submission to *J. Geophys Res. Oceans*.

APPENDIX

I. Historic events originated in the Solomon Islands Subduction Zone

Date						Assoc	Earthquake Location			Earthquake Parameters	
										Focal Depth	
Year	Mo	Dy	Hr	Mn	Sec	Tsu	Name	Latitude	Longitude		Mag
1900	7	29					SOLOMON ISLANDS: SANTA CRUZ ISLANDS	-11	166.1		8.1
1909	12	9	23	23			SOLOMON ISLANDS	-10	165		7.7
1926	9	16	17	59	12	Tsu	SOLOMON ISLANDS	-11.5	160	50	7.1
1931	10	3	19	13	13	Tsu	SOLOMON ISLANDS: SAN CRISTOBAL ISLAND	-10.5	161.75	33	7.9
1931	10	10	0	19			SOLOMON ISLANDS	-10	161	60	7.7
1934	7	18	19	40	15	Tsu	SOLOMON ISLANDS: SANTA CRUZ ISLANDS	-11.75	166.5	25	7.2
1938	3	6	1	56		Tsu	SOLOMON ISLANDS	-5.1	153.1		
1950	11	8				Tsu	SOLOMON ISLANDS: SOLOMON SEA	-10	159.5	33	
1955	9	8	3	27	16	Tsu	SOLOMON ISLANDS	-6.9	155.7	33	6.5
1957	11					Tsu	SOLOMON ISLANDS				
1957	12	17	13	50			SOLOMON ISLANDS: SANTA CRUZ ISLANDS	-12.3	166.7	120	7.8
1959	8	17	21	4	40	Tsu	SOLOMON ISLANDS	-7.5	156		7.3
1966	12	31	18	23	3.9	Tsu	SOLOMON ISLANDS: SANTA CRUZ ISLANDS	-11.8	166.5	33	7.5
1966	12	31	22	15	14	Tsu	SOLOMON ISLANDS: SANTA CRUZ ISLANDS	-11.3	164.8	33	7.3
1969	1	5	13	26			SOLOMON ISLANDS: SANTA ISABEL ISLAND	-7.9	158.9	47	7.5
1974	1	31	23	30	5.3	Tsu	SOLOMON ISLANDS	-7.5	155.9	34	7
1974	2	1	3	12	33	Tsu	SOLOMON ISLANDS	-7.4	155.6	40	7.1
1977	4	20	23	13	10	Tsu	SOLOMON ISLANDS	-9.828	160.323	33	6.8
1977	4	20	23	42	51	Tsu	SOLOMON ISLANDS	-9.89	160.348	19	7.6
1977	4	20	23	49	13		SOLOMON ISLANDS	-9.844	160.822	33	7.5
1977	4	21	4	24	9.6	Tsu	SOLOMON ISLANDS	-9.965	160.731	33	8.1
1980	7	8	23	19	20		SOLOMON ISLANDS: SANTA CRUZ ISLANDS: BANKS	-12.41	166.381	33	7.5
1980	7	17	19	42	23	Tsu	SOLOMON ISLANDS: SANTA CRUZ ISLANDS; VANUATU	-12.525	165.916	33	7.9
1982	8	5	20	33	53		SOLOMON ISLANDS: SANTA CRUZ ISLANDS	-12.597	165.931	31	7.5
1984	2	7	21	33	21		SOLOMON ISLANDS: GUADALCANAL	-10.012	160.469	18	7.5
1985	9	27	3	39	8.5		SOLOMON ISLANDS: HONIARA, GUADACANAL	-9.829	159.854	32	6.9
1988	8	10	4	38	26	Tsu	SOLOMON ISLANDS: SAN CRISTOBAL, GUADALCANAL	-10.366	160.819	34	7.4
1991	2	9	16	18	58	Tsu	SOLOMON ISLANDS	-9.929	159.139	10	6.9
1991	10	14	15	58	13	Tsu	SOLOMON ISLANDS	-9.094	158.442	23	7.2
1992	5	27	5	13	39	Tsu	SOLOMON ISLANDS: SANTA CRUZ ISLANDS	-11.122	165.239	19	7
1996	4	29	14	40	41		SOLOMON ISLANDS: BOUGAINVILLE ISLAND	-6.518	154.999	44	7.2
1997	4	21	12	2	26	Tsu	SOLOMON ISLANDS: SANTA CRUZ ISLANDS; VANUATU	-12.584	166.676	33	7.7
2003	1	20	8	43	6	Tsu	SOLOMON ISLANDS: HONIARA, SAN CRISTOBAL	-10.491	160.77	33	7.3
2007	4	1	20	39	56	Tsu	SOLOMON ISLANDS	-8.466	157.043	24	8.1
2007	9	2	1	5	18	Tsu	SOLOMON ISLANDS: SANTA CRUZ ISLANDS	-11.61	165.762	35	7.2
2009	10	7	22	18	51		SOLOMON ISLANDS: SANTA CRUZ ISLANDS	-12.517	166.382	35	7.8
2010	1	3	21	48	6	Tsu	SOLOMON ISLANDS	-8.88	157.325	10	6.5
2010	1	3	22	36	30	Tsu	SOLOMON ISLANDS	-8.912	157.307	30	7.2
2010	1	5	12	15	36	Tsu	SOLOMON ISLANDS	-8.886	157.522	35	6.9

II. Tsunami events documented from 1900-2010 (NGDC data base)

Date						Tsunami Cause				Tsunami Source Location				Tsunami Parameters
						Val	Code	Earth-quake	Vol-cano					Max Water
Year	Mo	Dy	Hr	Mn	Sec					Country	Name	Latitude	Longitude	Height
1926	9	16	17	59	12	4	1	7.1		SOLOMON ISLANDS	SOLOMON ISLANDS	-11.5	160	2
1931	10	3	19	13	13	4	1	7.9		SOLOMON ISLANDS	SAN CRISTOBAL ISLAND	-10.5	161.75	9
1939	4	30	2	55	30	3	1	8.1		SOLOMON ISLANDS	SOLOMON ISLANDS	-10.5	158.5	10.5
1957	11					2	1	*		SOLOMON ISLANDS	SOLOMON ISLANDS			2.7
1959	8	17	21	4	40	4	1	7.3		SOLOMON ISLANDS	SOLOMON ISLANDS	-7.5	156	1
1961	3	18				2	1			SOLOMON ISLANDS	SOLOMON ISLANDS			3.6
1961	8	1	5	39	53	2	1	6.6		SOLOMON ISLANDS	SOLOMON SEA	-9.9	160.5	0.9
1966	6	15	0	59	46	3	1	7.6		SOLOMON ISLANDS	SOLOMON ISLANDS	-10.4	160.8	0.1
1966	11	28				1	0			SOLOMON ISLANDS	MOHAWK BAY, SANTA CRUZ ISLANDS	-10	168	
1966	12	31	18	23	3.9	4	1	7.5		SOLOMON ISLANDS	SANTA CRUZ ISLANDS	-11.8	166.5	2.03
1966	12	31	22	15	14	4	1	7.3		SOLOMON ISLANDS	SANTA CRUZ ISLANDS	-11.3	164.8	1.52
1967	1	1	18	23	4	4	1	8.1		SOLOMON ISLANDS	SOLOMON ISLANDS	-11.8	166.5	2
1971	9	6	20			4	6		Vol	SOLOMON ISLANDS	TINAKULA, SANTA CRUZ	-10.38	165.8	
1974	1	31	23	30	5.3	4	1	7		SOLOMON ISLANDS	SOLOMON ISLANDS	-7.5	155.9	1.5
1974	2	1	3	12	33	4	1	7.1		SOLOMON ISLANDS	SOLOMON ISLANDS	-7.4	155.6	4.5
1977	4	20	23	13	10	4	1	6.8		SOLOMON ISLANDS	SOLOMON ISLANDS	-9.828	163.32	0.16
1977	4	20	23	42	51	4	1	7.6		SOLOMON ISLANDS	SOLOMON ISLANDS	-9.89	160.35	
1987	6	18	14	3	15	1	1	6		SOLOMON ISLANDS	SOLOMON ISLANDS	-10.71	162.33	0.1
1988	8	10	4	38	26	4	1	7.6		SOLOMON ISLANDS	SOLOMON ISLANDS	-10.37	160.82	0.09
1991	2	9	16	18	58	4	1	7		SOLOMON ISLANDS	SOLOMON ISLANDS	-9.929	159.14	0.1
1991	10	14	15	58	13	4	1	7.3		SOLOMON ISLANDS	SOLOMON ISLANDS	-9.09	158.44	0.2
1992	5	27	5	13	39	1	1	7.1		SOLOMON ISLANDS	SANTA CRUZ ISLANDS	-11.12	165.24	0.1
1997	4	21	12	2	26	4	1	7.7		SOLOMON ISLANDS	SANTA CRUZ IS. VANUATU	-12.58	166.68	3
2003	1	20	8	43	6	4	1	7.3		SOLOMON ISLANDS	SOLOMON ISLANDS	-10.49	160.77	2
2007	4	1	20	39	56	4	1	8.1		SOLOMON ISLANDS	SOLOMON ISLANDS	-8.46	157.04	10
2007	9	2	1	5	18	4	1	7.2		SOLOMON ISLANDS	SANTA CRUZ ISLANDS	-11.61	165.76	0.05
2010	1	3	21	48	6	4	1	6.5		SOLOMON ISLANDS	SOLOMON ISLANDS	-8.88	157.33	
2010	1	3	22	36	30	4	1	7.2		SOLOMON ISLANDS	SOLOMON ISLANDS	-8.912	157.31	3
2010	1	5	12	15	36	4	1	6.9		SOLOMON ISLANDS	SOLOMON ISLANDS	-8.886	157.52	0.03

.

European Commission

EUR 24783 EN – Joint Research Centre – Institute for the Protection and Security of the Citizen
Title: **01 APRIL 2007 SOLOMON ISLAND TSUNAMI: CASE STUDY TO VALIDATE JRC TSUNAMI CODES**
Author(s): Natalia Zamora, Giovanni Franchello, Alessandro Annunziato

Luxembourg: Publications Office of the European Union
2011 – 62 pp. – 29.7 x 21 cm
EUR – Scientific and Technical Research series – ISSN 1018-5593 (print) ISSN 1831-9424 (online)

ISBN 978-92-79-19851-9 (print)
ISBN 978-92-79-19852-6 (pdf)

doi:10.2788/859

Abstract

On April 1st 2007 a large earthquake of magnitude 8.1 occurred offshore Solomon Islands at 20:40:38 UTC. Numerical simulations of the tsunami event caused by the earthquake have been performed to compare the results obtained by the SWAN-JRC code (Annunziato, 2007), the TUNAMI (Imamura, 1996) and the HYFLUX2 (Franchello, 2008). The analysis conducted using these numerical simulations were also compared with NOAA-MOST code unit source results.

The tsunami event has been simulated considering several options for the seismological parameters as input data: Finite Fault Model (USGS, 2007), the Centroid Moment Tensor fault model and other mechanisms derived from the field survey analysis (Tanioka model).

The main aim of this study is to assess how the different fault models affect the overall results and to perform a comparison among the various codes in the wave propagation phase. Another objective of this study is to use HYFLUX2 code to calculate inundation and compare the simulation results with site field measurements.

The study has been separated into two main parts. The first one represents the collection of information about focal mechanisms: the fault analysis in chapter 4 covers one of the main aims of this research where different fault scenarios have been tested using published field data. The second part describes the different calculations that have been performed in order to analyze the response of the wave propagation models to various fault deformation models. For the inundation assessment, more detailed calculations at 300m grid siaze resolutions have been performed, using the fault model that best represent the deformation.

The calculations in the propagation assessment subsection were performed using: SWAN-JRC, HYFLUX2, TUNAMI-N2 and NOAA-MOST code. In the inundation assessment the HYFLUX2 numerical code, initialized with the Tanioka fault model was used.

The deformation comparison with field measured data shows that none of the “quick” fault mechanism was able to estimate correctly the measured value. The best model is the empirical model by Tanioka which was obtained trying to reproduce the measured value.

From the published fault mechanism the one that shows a better correlation with measurements is the simple cosinuosoidal model. Results of simulations done with 300 m grid, show a maximum wave height of 7.5 m. Though the maximum run up reported was 10 m in Tapurai site, Simbi Island, the simulation results are encouraging.

How to obtain EU publications

Our priced publications are available from EU Bookshop (http://bookshop.europa.eu), where you can place an order with the sales agent of your choice.

The Publications Office has a worldwide network of sales agents. You can obtain their contact details by sending a fax to (352) 29 29-42758.

The mission of the JRC is to provide customer-driven scientific and technical support for the conception, development, implementation and monitoring of EU policies. As a service of the European Commission, the JRC functions as a reference centre of science and technology for the Union. Close to the policy-making process, it serves the common interest of the Member States, while being independent of special interests, whether private or national.

JRC
EUROPEAN COMMISSION

LB-NA-24783-EN-C

Publications Office

ISBN 978-92-79-19851-9